

การพัฒนาพอลิเมอร์อิเล็กทรอนิกส์ไมโครชิพสำหรับการตรวจวัดตัวชี้วัดทางชีวภาพ



นางสาวกนกพร บุญทรง

สถาบันวิทยบริการ จุฬาลงกรณ์มหาวิทยาลัย

วิทยานิพนธ์นี้เป็นส่วนหนึ่งของการศึกษาตามหลักสูตรปริญญาวิทยาศาสตรดุษฎีบัณฑิต

สาขาวิชาเคมี ภาควิชาเคมี

คณะวิทยาศาสตร์ จุฬาลงกรณ์มหาวิทยาลัย

ปีการศึกษา 2550

ลิขสิทธิ์ของจุฬาลงกรณ์มหาวิทยาลัย

DEVELOPMENT OF POLYMERIC ELECTROPHORESIS MICROCHIP
FOR BIOMARKER DETECTION



Miss Kanokporn Boonsong

สถาบันวิทยบริการ
จุฬาลงกรณ์มหาวิทยาลัย

A Dissertation Submitted in Partial Fulfillment of the Requirements
for the Degree of Doctor of Philosophy Program in Chemistry

Department of Chemistry

Faculty of Science


Chulalongkorn University

Academic Year 2007

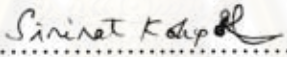
Copyright of Chulalongkorn University


Thesis Title DEVELOPMENT OF POLYMERIC ELECTROPHORESIS
 MICROCHIP FOR BIOMARKER DETECTION
By Miss. Kanokporn Boonsong
Field of Study Chemistry
Thesis Advisor Associate Professor Orawon Chailapakul, Ph.D.
Thesis Co-Advisor Luxsana Dubas, Ph.D.


Accepted by the Faculty of Science, Chulalongkorn University in Partial
Fulfillment of the Requirement for the Doctoral Degree



.....Dean of the Faculty of Science
(Professor Supot Hannongbua, Ph.D.)

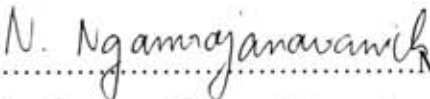
THESIS COMMITTEE


.....Chairman
(Associate Professor Sirirat Kokpol, Ph.D.)


.....Thesis Advisor
(Associate Professor Orawon Chailapakul, Ph.D.)


.....Thesis Co-advisor
(Luxsana Dubas, Ph.D.)


.....External Member
(Winai Ouangpipat, Ph.D.)


.....Member
(Associate Professor Nattaya Ngamrojnavanich, Ph.D.)

กนกพร บุญทรง : การพัฒนาพอลิเมอร์อิเล็กโทรโฟรีซิสไมโครชิพสำหรับการตรวจวัด
ตัวชี้วัดทางชีวภาพ (DEVELOPMENT OF POLYMERIC ELECTROPHORESIS
MICROCHIP FOR BIOMARKER DETECTION) อ.ที่ปรึกษา : รศ.ดร.อรรพรรณ ชัยลภากุล,
อ.ที่ปรึกษาร่วม : ดร.ลักขณา คูบาส, 116 หน้า.

งานวิจัยนี้เป็นการพัฒนาวัสดุที่ใช้สำหรับสร้างอุปกรณ์ไมโครชิพเพื่อการประยุกต์กับชีวการแพทย์ โดยได้ตรวจสอบคุณสมบัติของพอลิเมอร์ชนิดต่างๆเมื่อนำมาเตรียมเป็นไมโครชิพ ได้แก่ พอลิไดเมทิลไซลอกเซน (พีดีเอ็มเอส) และเทอโมเซทพอลิเอสเทอร์ (ทีพีอี) ไมโครชิพที่เตรียมจากพีดีเอ็มเอสใช้ตรวจวัดคาร์โบไฮเดรตและสารประกอบไทออลในตัวอย่างพลาสมา ผลการตรวจวัดบ่งชี้ว่าไมโครชิพที่เตรียมจากพีดีเอ็มเอสมีความเหมาะสมที่จะนำไปใช้ทดสอบตัวอย่างทางคลินิก ได้ศึกษาผลของการใช้พอลิเมอร์เคลือบผิวที่ละชั้น (พีอีเอ็ม) ต่อความเร็วและทิศทางการไหลของอิเล็กโทรออสโมติกฟลว์ (อีโอเอฟ) และประสิทธิภาพการแยกของพีดีเอ็มเอสไมโครชิพโดยใช้พอลิเมอร์ที่มีโครงสร้างแตกต่างกันและภาวะการทดลองแตกต่างกัน การใช้พอลิเมอร์เคลือบผิวทำให้ค่าอีโอเอฟคงที่ ทั้งนี้ขึ้นอยู่กับโครงสร้างของพอลิเมอร์ และพบว่าประสิทธิภาพการแยกดีขึ้นเมื่อเปรียบเทียบกับไมโครชิพที่เตรียมจากพีดีเอ็มเอสที่ไม่ได้ปรับสภาพ เทอโมเซทพอลิเอสเทอร์ถูกเตรียมเป็นวัสดุอีกชนิดหนึ่งสำหรับไมโครชิพอะพลาเรียอิเล็กโทรโฟรีซิสร่วมกับการตรวจวัดทางเคมีไฟฟ้า (เอ็มซีอี-อีซี) ทีพีอีไมโครชิพถูกตรวจสอบในสภาพที่ไม่ได้ปรับสภาพ ทีพีอีถูกออกซิไดส์ด้วยพลาสมา และทีพีอีที่เคลือบผิวด้วยพีอีเอ็ม ผลการทดลองพบว่าไมโครชิพที่เตรียมจากทีพีอีให้ประสิทธิภาพของการแยกสูงกว่าไมโครชิพที่เตรียมจากพีดีเอ็มเอส ถึงแม้ว่าไมโครชิพที่เตรียมจากทีพีอีสามารถเตรียมได้ง่าย จากการศึกษาค่าของอิเล็กโทรออสโมติกฟลว์ พบว่าทีพีอีไมโครชิพและทีพีอีไมโครชิพที่ถูกปรับสภาพโดยการออกซิไดส์ด้วยพลาสมาให้ค่าอิเล็กโทรออสโมติกฟลว์สูงกว่าและคงที่มากกว่าตลอดช่วงพีเอช ที่ศึกษาเมื่อเปรียบเทียบกับอิเล็กโทรออสโมติกฟลว์ของพีดีเอ็มเอสไมโครชิพ ไมโครชิพที่เตรียมจากทีพีอียังสามารถนำไปตรวจวิเคราะห์สารในเชิงปริมาณที่มีความสำคัญทางชีวภาพได้

ภาควิชา.....เคมี.....ลายมือชื่อนิสิต.....กนกพร บุญทรง
สาขาวิชา.....เคมี.....ลายมือชื่ออาจารย์ที่ปรึกษา.....
ปีการศึกษา.....2550.....ลายมือชื่ออาจารย์ที่ปรึกษาร่วม.....

4572202923 : MAJOR CHEMISTRY

KEYWORDS: MICROFLUIDICS/ MICROCHIP/ CAPILLARY ELECTROPHORESIS/
POLY(DIMETHYLSILOXANE)/ THERMOSET POLYESTER/ POLYELECTROLYTE
MULTILAYER/ SURFACE MODIFICATION/ PULSED AMPEROMETRIC DETECTION

KANOKPORN BOONSONG : DEVELOPMENT OF POLYMERIC
ELECTROPHORESIS MICROCHIP FOR BIOMARKER DETECTION
THESIS ADVISOR: ASSOC.PROF. ORAWON CHAILAPAKUL, Ph.D.,
THESIS COADVISOR: LUXSANA DUBAS, Ph.D., 116 pp.

In this work, the development of material to fabricate lab-on-a-chip devices for biomedical applications is demonstrated. The property of different type of polymers: poly(dimethylsiloxane) (PDMS) and thermoset polyester (TPE) microchips were investigated. The PDMS chips were used to detect carbohydrate and thiol compounds in plasma samples. The results indicated that PDMS microchips suitable for clinical testing. The effect of layer-by-layer polyelectrolyte multilayer (PEM) coatings on the velocity and direction of electroosmotic flow (EOF) and the separation efficiency of PDMS microchips was studied using different polymer structures and different deposition conditions. The use of polyelectrolyte coatings generated a consistent EOF depending on the polymer structure and improved separation efficiency when compared to unmodified PDMS microchips. Thermoset Polyester (TPE) was prepared as an alternative material for microchip capillary electrophoresis with electrochemical detection (MCE-EC). TPE microchips were characterized in their native, plasma-oxidized, and PEM-coated forms. TPE microchips provided higher separation efficiencies compared to PDMS microchips, even though fabrication of TPE microchips is still very simple. The EOF of native and plasma-treated TPE microchip was higher and more consistent as a function of pH than the EOF of PDMS microchip. The TPE microchip was used to quantify biologically important compounds.

Department.....Chemistry.....Student's signature.....*Kanokporn Boonsong*
Field of study.....Chemistry.....Advisor's signature.....*Orawon Chailapakul*
Academic year2007.....Co-advisor's signature.....*D. S.*

ACKNOWLEDGEMENTS

I would like to express my gratitude to all those who gave me the possibility to complete this dissertation. First of all, I would like to express my deepest gratitude and thanks to my adviser, Assoc. Prof. Dr. Orawon Chailapakul for her kind supervision, constructive advice, and helpful criticism throughout my studied. I would like to thank for her support, inspiration, patience, valuable guidance, and continuous encouragement during this work. I am deeply grateful to Dr. Luxsana Dubas, my thesis coadvisor for her guidance, support and valuable advice.

I would also like to express my deep gratitude to Assoc. Prof. Dr. Charles S Henry from Colorado State University for giving me the opportunity to collaborate with his research group and for his stimulating suggestions and encouragement helped me in all the time of research.

I am deeply indebted to Assoc. Prof. Dr. Sirirat Kokpol for giving me an honor of being the thesis chairman. I really appreciate my committee members, Assoc. Prof. Nattaya Ngamrojnavanich, and Dr. Winai Ouangpipat for their comment, technical guidelines and advice given to me for the completion of my thesis work.

I would like to acknowledge the Thailand Research Fund through the Royal Golden Jubilee Ph.D. Program (Grant number PHD/0063/2547) for the financial support during my Ph. D course.

I would like to express my extreme gratitude to all the staff of the Division of Chemistry, Department of Science, Faculty of Science and Technology, Rajamangala University of Technology Krungthep for their help and support. I am also like to thank also staffs in the Department of Chemistry, Faculty of Science, Chulalongkorn University for their helpfulness.

Thank for my lovely friends in Henry's lab and TSA@CSU for fulfilling the happiness inside and make my stay in USA very pleasant one. Thanks to all members in electrochemical research group for their friendship and always a warm atmosphere in which to work. Special thank must go to all of my friends who have cheered me up in several hard time.

Last but not the least, I would express a deep sense of gratitude to my parents for their unconditional love, moral support, encouragement, blessings, and always stood by me in times of need.

CONTENTS

	PAGE
ABSTRACT (IN THAI)	iv
ABSTRACT (IN ENGLISH)	v
ACKNOWLEDGEMENTS	vi
CONTENTS	vii
LIST OF TABLES	xi
LIST OF FIGURES	xii
LIST OF ABBREVIATIONS AND SYMBOLS	xvii
CHAPTER I INTRODUCTION	1
1.1 Introduction.....	1
1.2 Research objective	2
1.3 Scopes of research	2
CHAPTER II THEORY AND LITERATURE SURVEY	4
2.1 Fundamentals of electrochemistry.....	4
2.1.1 Voltammetry.....	6
2.1.2.1 Cyclic voltammetry.....	7
2.1.2 Amperometry	9
2.1.2.1 Pulse amperometry.....	10
2.2 Capillary electrophoresis	11
2.2.1 Background theory.....	12
2.2.2 Electroosmotic flow.....	13
2.2.3 Injection scheme.....	16
2.2.3.1 Gated injection.....	17
2.2.3.2 Pinched injection.....	19
2.2.4 Dimension of the microfluidic channels.....	21
2.2.5 Factor affecting separation efficiency.....	24
2.2.5.1 Electromigration dispersion.....	24
2.2.5.2 Joule heating.....	25
2.2.6 Separation modes.....	27

	PAGE
2.2.6.1 Capillary zone electrophoresis (CZE).....	28
2.2.6.2 Micellar electrokinetic chromatography (MEKC).....	28
2.3 Microchip capillary electrophoresis.....	28
2.4 Material for microchip capillary electrophoresis.....	29
2.5 Polyelectrolyte multilayer coatings.....	31
2.5.1 Successive multiple ionic layer (SMIL) coatings.....	32
2.6 Detection methods compatible with microchip capillary electrophoresis...	33
2.6.1 Electrochemical detection.....	34
2.6.2 Amperometric detection.....	36
2.7 Biomarkers.....	37
2.7.1 Thiol compounds.....	38
2.7.1.1 Homocysteine	38
2.7.1.2 Cysteine.....	41
2.7.1.3 Glutathione.....	42
2.7.2 Carbohydrate.....	43
CHAPTER III EXPERIMENTAL.....	44
3.1 Instruments and equipments.....	44
3.2 Apparatus for microchip capillary electrophoresis	45
3.3 Chemical and reagents	46
3.4 Preparation of solutions.....	48
3.4.1 Preparation of 20 mM TES buffer pH 7.2.....	48
3.4.2 Preparation of 20 mM MES buffer pH 6.5.....	48
3.4.3 Preparation of 20 mM boric acid buffer pH 9.4.....	49
3.4.4 Preparation of 20 mM boric acid with 20 mM SDS buffer pH 9.4...	49
3.4.5 Preparation of 25 mM potassium dihydrogenorthophosphate pH 3.0.....	49
3.4.6 Preparation of stock standard solution of dopamine.....	49
3.4.7 Preparation of stock standard solution of catechol.....	49
3.4.8 Preparation of stock standard solution of carbohydrate.....	49

	PAGE
3.4.9 Preparation of stock standard solution of thiol compounds.....	50
3.4.10 Preparation of stock standard solution of carbohydrate and thiol compounds for calibration.....	50
3.5 Microchip fabrication.....	50
3.5.1 Method for making a mold.....	50
3.5.2 Fabrication of PDMS devices.....	51
3.5.3 Fabrication of TPE devices.....	51
3.6 Successive multiple ionic layer (SMIL) coating.....	52
3.7 Electroosmotic flow measurements.....	53
3.8 Procedures of microchip CE.....	54
3.8.1 Microchip CE with amperometric detection.....	54
3.8.1.1 Microchip CE layout.....	54
3.8.1.2 Electrophoresis procedure	55
3.8.1.3 Electrochemical detection.....	56
3.8.1.4 Safety consideration.....	57
3.8.1.5 Microchip CE optimization conditions.....	57
3.8.1.6 Calibration and linear range.....	58
3.8.1.7 Limit of detection	58
3.8.1.8 Pricision.....	58
3.8.2 Plasma sample analysis.....	59
3.8.2.1 Standard thiol compounds and plasma sample preparation.....	59
CHAPTER IV RESULTS AND DISCUSSION.....	60
4.1 Microchip capillary electrophoresis/electrochemistry.....	60
4.1.1 Microchip capillary electrophoresis characterization.....	60
4.1.2 Capillary electrophoresis optimization.....	61
4.1.2.1 Influence of separation voltage.....	61
4.1.2.2 Influence of injection time.....	62

LIST OF TABLES

TABLE	PAGE
2.1 Comparison of electrophoretic and chromatographic terms.....	12
3.1 List of chemical and reagents and their suppliers.....	46
3.2 Weight of thiol compounds for preparation of stock standard solution.....	50
4.1 PAD parameters for the detection of the glucose and thiol compounds.....	73
4.2 Analytical parameters corresponding to the calibration curves for glucose and thiol compounds.....	75



สถาบันวิทยบริการ
จุฬาลงกรณ์มหาวิทยาลัย

LIST OF FIGURES

FIGURE	PAGE
2.1 Schematic diagram of general electroanalytical methods.....	5
2.2 Typical excitation signals for voltammetry.....	7
2.3 Schematic of (a) a potential wave form used in cyclic voltammetry, and (b) a cyclic voltammogram.....	8
2.4 A typical waveform employed in amperometry.....	9
2.5 Typical PAD waveform.....	11
2.6 Double layer potential. This scheme shows the electric double layer formed next to the negative charged solid surface. The EDL is due to the surface potential ψ_0 , applied to the wall of the channel.....	15
2.7 Electroosmotic velocity profile in microchannels. This is a schematic representation of the fluid flow inside a symmetric channel with constant electric potential at the walls.....	15
2.8 Flow profiles and the effect on peak shapes for electroosmotic flow and hydrodynamic flow.....	16
2.9 Examples of sample injector types. A) cross, B) double-T, C) double-L, D) double cross, E) triple-T, F) multi-T, G) stacking type, H) π -injector. Sample inlet s, waste w and BGE inlet B are indicated.....	17
2.10 Principle of gated injection. Red stream is the sample, and white stream is the mobile phase. S: Sample, SW: Sample waste, B: Buffer, W: Waste.....	18
2.11 Principles of pinched injection. Red stream is the sample, and white stream is the mobile phase. S: Sample, SW: Sample waste, B: Buffer, W: Waste.....	20
2.12 Representation of the resolution in separation science.....	23
2.13 Electromigration dispersion caused by mismatched analyte and electrolyte mobilities.....	25
2.14 Ohm's law plots showing the optimum voltages for different papillary temperature using air circulation for tempearturte control.(A) No control; (B) 25 °C; (C) 10 °C; (D) 4 °C.....	26

FIGURE	PAGE
2.15 Separation mechanism in (a) CZE and (b) MEKC.....	27
2.16 Structure of homocysteine.....	38
2.17 Structure of cysteine.....	41
2.18 Structure of glutathione.....	42
2.19 Structure of glucose.....	43
3.1 (A) Schematic of the microchip showing placement of the electrode alignment channels. Working electrode channel (50 μm deep, 50 μm wide). Decoupler electrode channel (50 μm deep x 25 μm wide, 50 μm gap to separation channel). (B) Decoupled microchip. Fluorescent image of 1 mM FITC as it passes the decoupler. No sample leakage was observed around the Pd microwire. Dotted lines indicate the outline of the channels in the PDMS.....	45
3.2 The microchip capillary electrophoresis with electrochemical detection layout.....	54
3.3 A photograph showing electrode alignment in a completed microchip.....	55
3.4 The microchip capillary electrophoresis with electrochemical detection layout.....	57
4.1 Electropherogram of the separation of dopamine and catechol. Experimental parameters: 500 μM dopamine and 500 μM catechol, TES (pH 7.2) running buffer, separation potential 1100 V, detection potential 0.8 V, pinched injection time 15 s, working electrode: 25 μm Au wire.....	61
4.2 Separation of a solution of 500 μM dopamine and 500 μM catechol as a function of separation voltage (1000 – 1400 V).....	62
4.3 Effect of separation voltage on the migration times of 100 μM homocysteine (\square), glucose (\blacktriangle), cysteine (\bullet), and glutathione (\blacksquare). Experimental conditions: pinched injection time 15 s, detection voltage 0.8 V, BGE 20 mM boric acid (pH 9.0).....	63
4.4 Electropherograms of a solution of 500 μM dopamine and 500 μM catechol separated with injection times from 15-25 s.....	64

FIGURE	PAGE
4.5 Effect of injection time on peak currents of 100 μM homocysteine (\square), glucose (\blacktriangle), cysteine (\bullet), and glutathione (\blacksquare). Experimental conditions: separation voltage 1400 V, detection voltage 0.8 V, BGE 20 mM boric acid (pH 9.0).....	65
4.6 Effect of BGE pH on the migration times of homocysteine 100 μM (\square), glucose (\triangle), cysteine (\circ), and glutathione (\blacksquare). Experimental conditions: separation voltage 1400 V, pinched injection time 15 s, detection voltage 0.8 V.....	66
4.7 (a) Effect of BGE concentration on the migration times of 100 μM homocysteine (\square), glucose (\triangle), cysteine (\circ), and glutathione (\blacksquare). (b) Effect of BGE concentration on peak currents of 100 μM homocysteine (\square), glucose (\triangle), cysteine (\circ), and glutathione (\blacksquare).....	67
4.8 Electropherograms of thiol compounds separated using boric acid (pH 9.0) running buffer containing SDS concentrations from 10 – 30 mM. Experimental conditions: separation voltage 1400 V, pinched injection time 15 s, detection voltage 0.8 V.....	69
4.9 Electropherograms of glucose separation using various cleaning potentials (E_{oxd}) between 1.1 V and 1.6 V. Experimental conditions: separation potential 1400 V, pinched injection time 15 s, BGE 20 mM boric acid with 20 mM SDS (pH 9.0).....	70
4.10 Hydrodynamic voltammograms of peak current during the electrophoretic separation of 500 μM glucose (\blacktriangle), homocysteine (\bullet), glutathione (\blacksquare), and cysteine (\circ) at various cleaning potentials (E_{oxd}) between 1.1 and 1.6 V	71
4.11 Electropherograms for the separation of glucose at various detection potentials (E_{det}) between 0.1 V and 0.9 V.....	72
4.12 Hydrodynamic voltammograms of peak current during the electrophoretic separation of 500 μM glucose(\blacktriangle), homocysteine (\bullet), glutathione (\blacksquare), and cysteine (\circ) at various detection potentials (E_{det}) between 0.1 V and 0.9 V..	73

FIGURE	PAGE
4.13 Linear relationships between peak currents and concentration for a) glucose from 0.25 – 62.5 μM , homocysteine from c) 61 – 3900 nM and d) 15.6 – 500 μM , and glutathione from e) 1- 400 pM and f) 15 – 500 nM.....	76
4.14 Electropherogram for the separation of 1 pM glucose on a PDMS microchip.....	77
4.15 Electropherogram for the separation of 2 nM homocysteine and 4 nM cystine on a PDMS microchip.....	78
4.16 Electropherogram for the separation of 3.8 nM glucose on a PDMS microchip.....	79
4.17 Electropherogram corresponding to the separation of a mixture of 2.5 mM TCEP, 100 μM homocysteine, 100 μM glucose, and 100 μM glutathione.....	81
4.18 Electropherogram of the separation of glucose and thiol compounds in human plasma. (a) Human plasma sample. (b) Human plasma sample spiked with 250 μM glucose and glutathione.	82
4.19 Polyelectrolyte structure: (A) poly(allylamine)hydrochloride, PAH (B) poly(ethyleneimine), PEI (C) polybrene, PB (D) poly(acrylic acid), PAA (E), dextran sulfate, DS.....	84
4.20 Electroosmotic flow as a function of number of layers deposited for different polyelectrolyte coatings: 3% PB/PAA, 3% PB/PAA with 0.5 M NaCl, 3% PEI/PAA, 3% PEI/PAA with 0.5 M NaCl, 3% PAH/PAA, 3% PAH/PAA with 0.5 M NaCl.....	86
4.21 Electroosmotic flow as a function of number of layers deposited for different polyelectrolyte coatings: 3% PEI/PAA, 3% PEI/PAA with 0.5 M NaCl, 3% PEI/DS, 3% PEI/DS with 0.5 M NaCl. EOF was measured with phosphate buffer (pH 7.0).....	87
4.22 Comparison of electropherograms of FTPD separations using (from top to bottom) native PDMS device and devices with six-layer coatings of either PEI/PAA, PAH/PAA, or PB/DS.....	88

FIGURE	PAGE
4.23 Number of theoretical plates (N) as a function of layer number. A) PB/DS alternating layers. B) PEI/PAA alternating layers. C) PAH/PAA alternating layers.....	90
4.24 Electropherogram of the separation of 100 μM dopamine and 100 μM catechol on a TPE microchip. Experimental conditions: separation potential 1200 V, pinched injection time 15 s, BGE 20 mM TES (pH 7.2).....	91
4.25 Day-to-day EOF stability of TPE microchips. EOF measurements are given for native TPE devices over an 18-day period(■) and for plasma-treated TPE devices over an 11 day period (●). EOF was determined using the current-monitoring method.	92
4.26 EOF measured for five microchips made at different times from different batches of TPE. Each chip was run multiple times at different pH values (4, 7, and 10) to determine the effect of pH effect on reproducibility.....	94
4.27 EOF values of untreated TPE(●) modified with a single layer of PB (anionic polyelectrolyte) (◄) or a double layer of DS (cationic polyelectrolyte) and PB (■) for pH values between 3 and 10.	96
4.28 Example electropherograms of the separation of 1 μM dopamine, 1 μM catechol, and 1 μM ascorbic acid with a TPE microchip (top) and with a PDMS microchip (bottom).....	98
4.29 Efficiencies of separation of a solution containing 1 μM dopamine, 1 μM catechol, and 1 μM ascorbic acid with identical TPE (left) and PDMS (right) microchips.....	99
4.30 Separation of a solution of 1 μM dopamine, 1 μM catechol, and 1 μM ascorbic acid with a TPE microchip using a variety of separation potentials. The optimal separation potential was determined to be 266 V/cm (1600 V).....	100
4.31 Electropherogram of the separation of 50 μM homocysteine, 50 μM glutathione, and 50 μM cysteine with a TPE microchip.....	101

ABBREVIATIONS AND SYMBOLS

i	current (A)
i_{pa}	anodic peak current (A)
i_{pc}	cathodic peak current (A)
E_p	peak potential (V)
E_{pa}	anodic peak potential (V)
E_{pc}	cathodic peak potential (V)
F	Faraday constant (96,484.6 C equiv ⁻¹)
A	area of electrode (cm ²)
D	diffusion coefficient (cm ² s ⁻¹)
ν	kinematic viscosity of the liquid (cm ² s ⁻¹)
υ	scan rate (V sec ⁻¹)
ω	angular velocity of the disk (radians per second)
C	solution concentration (mol dm ⁻³)
ppm	part per million
ppb	part per billion
mL	milliliter
μ L	microliter
g	gram
μ g	microgram
μ A	microamp
nA	nanoamp
μ m	micrometer
μ M	micromolar
nm	nanometer
i.d.	internal diameter
r^2	correlation coefficient
V	volt
TES	N-Tris(hydroxymethyl)methyl-2-aminoethanesulfonic acid
MES	2-Morpholinoethanesulfonic acid
PDMS	Poly(dimethylsiloxane)
TPE	Thermoset polyester
TCA	Trichloroacetic acid

TCEP	Tris(2-carboxy-ethyl) phosphine hydrochloride
MEKP	Methyl ethyl ketone peroxide
PEI	Poly(ethyleneimine)
PAA	Poly(acrylic acid)
PAH	Polyallylamine hydrochloride
PB	Polybrene
HMDS	Hexamethyldisilazane
SDS	Sodium dodecyl sulfate
SMIL	Successive multiple ionic layer
PEM	Polyelectrolyte multilayer
EOF	Electroosmotic flow
I_{sep}	Separation current
PAD	Pulsed amperometric detection
LOD	Limit of detection
MCE	Microchip capillary electrophoresis
EC	Electrochemical detection
Hcy	Homocysteine
Cys	Cysteine
GSH	Glutathione
EMD	Electromigration dispersion
CZE	Capillary Zone Electrophoresis
MEKC	Micellar electrokinetic chromatography
E_{det}	Detection potential
t_{det}	Detection time
t_{del}	Delay time
t_{int}	Integration time
t_{oxd}	Oxidation time
t_{red}	Reduction time
E_{oxd}	Oxidation potential
E_{red}	Reduction potential
ζ	zeta potential
EDL	electrical double layer
N	plate number
H	plate height

D	diffusion coefficient
μ	electrophoretic mobility
LIF	laser-induced fluorescence



สถาบันวิทยบริการ
จุฬาลงกรณ์มหาวิทยาลัย

CHAPTER I

INTRODUCTION

1.1 Introduction

Lab-on-a-chip technology, or micro-Total Analysis Systems (μ TAS), is a rapidly growing field in recent years. This technology has generated considerable excitement because of its potential impact on the field of chemical separations. Since the first reports of micro-Total Analysis Systems (μ TAS) [1], there has been an increase in the development of microchip-based analytical systems, because μ TAS can perform the all necessary tasks, such as sample pretreatment, separation, and detection, with a single miniature device. Lab chips can be engineered to perform the same analyses as conventional scale systems, but because of their small size, the same procedures can be conducted with reduced sample and reagent consumption, at lower overall cost, and in less time [2]. The field of microfluidics combines the fabrication methods of micro- and nanotechnology with fundamental knowledge about the behavior of fluids on the microscopic level to give rise to very powerful techniques for controlling and measuring micro- and nanoscale chemical reactions and physical and biological processes. The use of microfluidic devices to conduct biomedical research and create clinically useful technologies could potentially have a number of significant advantages. Because the volume of fluid contained within the channels is very small, usually on the order of several nanoliters, the necessary quantities of reagents and analytes are typically quite small. For assays requiring expensive reagents, this is an especially significant advantage. Also, the fabrications techniques used to construct microfluidic devices are relatively inexpensive and also are very amenable both to the construction of highly elaborate, multiplexed devices and to mass production. The use of microfluidic devices has proven potential to increase both the speed and the sensitivity of measurements. The length scales associated with lab-on-a-chip devices are of the same order of magnitude as a single cell as well as many of other fundamental biological processes, and so these devices are particularly well-suited for investigating and manipulating these very processes. Like microelectronics, microfluidic technologies enable the fabrication of highly integrated devices capable of performing several different functions on a single substrate chip.

One long term goal in the field of microfluidics is to create integrated, portable clinical diagnostic devices for home and bedside use, thereby eliminating certain time-consuming laboratory analysis procedures.

This dissertation focuses on the development and optimization of microchip capillary electrophoresis devices fabricated from poly(dimethylsiloxane) (PDMS) and other materials for the detection and measurement of carbohydrate and thiol compounds for clinical testing applications. The effects of polyelectrolyte multilayer (PEM) coatings and polymer structure on separation efficiency and electroosmotic flow (EOF) in microchip devices were studied. Furthermore, Thermoset polyester (TPE) microchips were fabricated and used for microchip capillary electrophoresis with electrochemical detection (MCE-EC). The surface stability and EOF of native and modified TPE were also studied.

1.2 Research objective

The objectives of this dissertation are three-fold.

1. To develop a fast and sensitive microchip capillary electrophoresis system with electrochemical detection for analysis of carbohydrate and thiol compounds in plasma sample.
2. To develop the surface modification method for poly(dimethylsiloxane) (PDMS) microchip.
3. To develop an alternative material for microchip capillary electrophoresis with electrochemical detection.

1.3 Scope of research

To achieve the research objectives, the following scope was set:

- The microchip capillary electrophoresis with electrochemical detection was developed for the separation and detection of thiol compounds and glucose in human blood plasma.
- The effects of polymer structure on electroosmotic flow and separation efficiency was studied using layer-by-layer polyelectrolyte coatings.

- An alternative material, Thermoset polyester, was developed for applications in microchip capillary electrophoresis with electrochemistry.

There are five chapters in this dissertation. Chapter I is the introduction. Chapter II contains the principles of electroanalytical techniques related to the detection and analysis of chemical compounds. The theoretical aspects of microchip capillary electrophoresis, potential materials for microchip CE, and polyelectrolyte multilayer coatings are also covered in this chapter. Chapter III outlines the experiments performed for this dissertation, including the chemicals, instruments, and chemical procedures used in this work. Chapter IV contains the results and discussion of experiments investigating various elements of MCE-EC methods for measuring thiol compound and glucose concentration with a PDMS-based device. The effect of different layer-by-layer polyelectrolyte coatings on the electroosmotic flow and separation efficiency of these devices was investigated. Furthermore, The characteristic of thermoset polyester was tested as an alternative material for MCE-EC devices. Finally, Chapter V is the conclusion and future perspectives.



สถาบันวิทยบริการ
จุฬาลงกรณ์มหาวิทยาลัย

CHAPTER II

THEORY AND LITERATURE SURVEY

2.1 Fundamentals of electrochemistry[3]

Electroanalytical chemistry encompasses a group of quantitative analytical methods that are based upon the redox properties of the analyte when it is made part of an electrochemical cell. Electroanalytical methods have certain general advantages over other types of procedures. First, electrochemical measurements are often specific for a particular oxidation state of the element. For example, electrochemical methods make possible for the determination of each species in a mixture of cerium (III) and cerium(IV), whereas most other analytical methods are able to reveal only the total cerium concentration. Second, electrochemical instrumentation is relatively inexpensive. The third feature of certain electrochemical methods which may be an advantage or disadvantage, is that they provide information about activities rather than concentrations of chemical species. Ordinarily, in physiological studies, activities of ions such as calcium and potassium are of greater significance than concentrations.

Up to now, there are various electroanalytical methods that have been used for wide range applications. Figure 2.1 shows the flow diagram of electroanalytical methods that are generally used. These methods are divided into bulk methods and interfacial methods which is wider usage than the former ones.

Interfacial methods are the methods in which the reactions occur at the interface between the surface of electrode and the thin layer of solution near the surfaces. On the other hand, bulk methods are the methods that reactions occur in the bulk of the solution that avoid the interfacial effects.

Static and dynamic methods are the major subgroups of the interfacial methods based upon the electrochemical cell being performed in the presence and absence of current. There are a few methods including potentiometric measurement

that is the subgroups in the static methods, however, it is quite used until now because of their speed and selectivity.

Dynamic interfacial methods, in which the currents play an important role, are divided into controlled-potential and constant current methods. The potential of the cell in controlled potential methods is controlled while the other variables are measured. The advantages of these methods are high sensitivity and wide dynamic range, portability, wide range of working electrode that can be used, low consumption of sample volumes, and low limit of detection (LOD). In the constant-current dynamic methods, the current in the cells is held constant while the data are collected.

In this research, the dynamic methods especially voltammetry and amperometry were used. The details of these methods are described as the following topics.

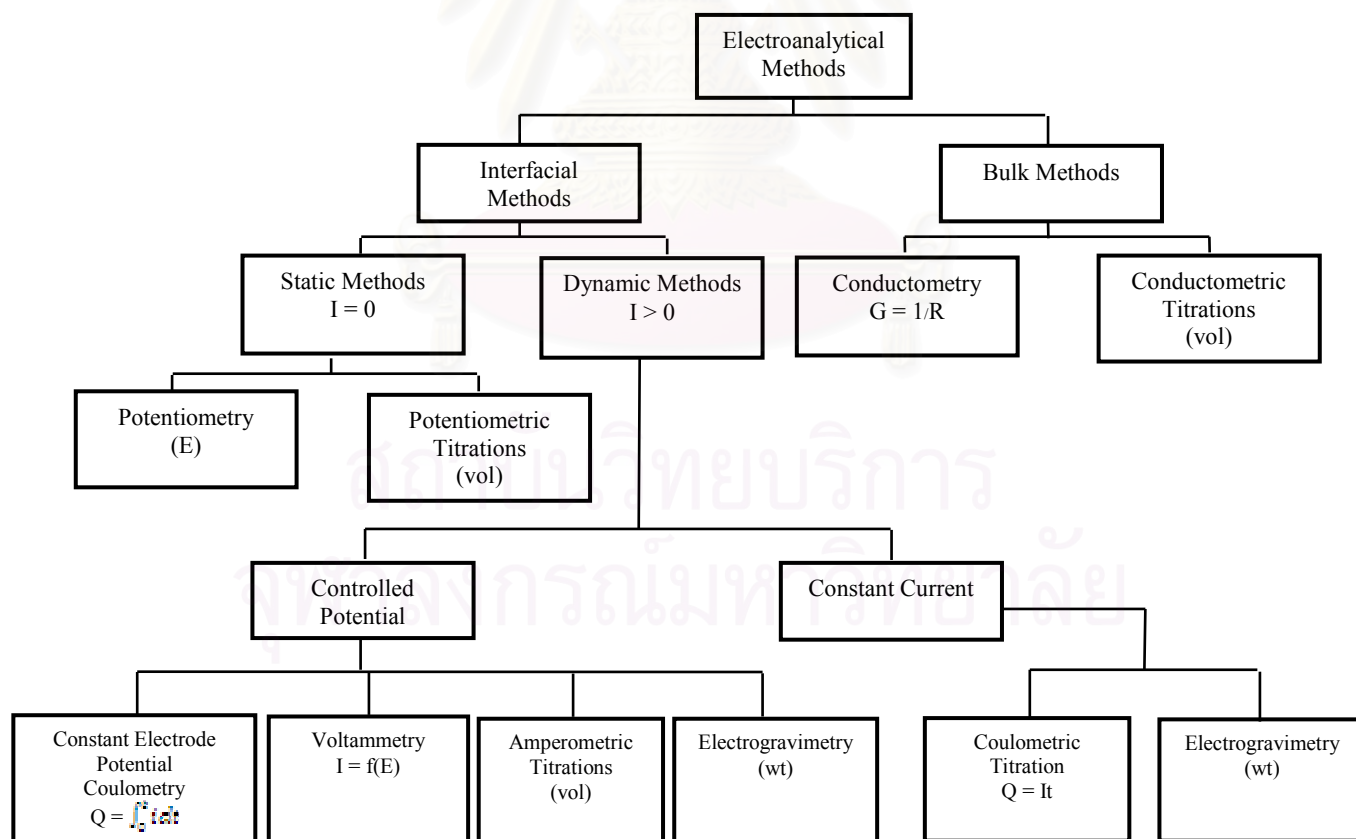


Figure 2.1 Schematic diagram of general electroanalytical methods

2.1.1 Voltammetry [4-6]

Voltammetry comprises a group of the electroanalytical methods in which information about the analyte is derived from the measurement of current as a function of applied potential. It is based on the measurement of a current that develops in an electrochemical cell under conditions of complete concentration of polarization of working electrode. In the presence of the electroactive (reducible or oxidizable) species, a current will be recorded when the applied potential becomes sufficiently negative or positive for it to electrolyze. The recording result is called a voltammogram. The potential excitation signal is imposed on an electrochemical cell containing an electrode. Three waveforms of most common excitation signals used in voltammetry are shown in Figure 2.2. The classical voltammetric excitation signal is a linear scan shown in Figure 2.2a. The potential applied to the cell of this excitation increases linearly as a function of time. The two pulse excitation signals are shown in Figure 2.2b and 2.2c. The current responses of the pulse type are measured at various times during the lifetime of these pulses.

Voltammetry is widely used for the fundamental studies of oxidation and reduction processes in various media, adsorption process on electrode surfaces, and electron transfer mechanisms at electrode surfaces. In the mid-1960s, several major modifications of classical voltammetric techniques were developed that enhanced the sensitivity and selectivity of the method.

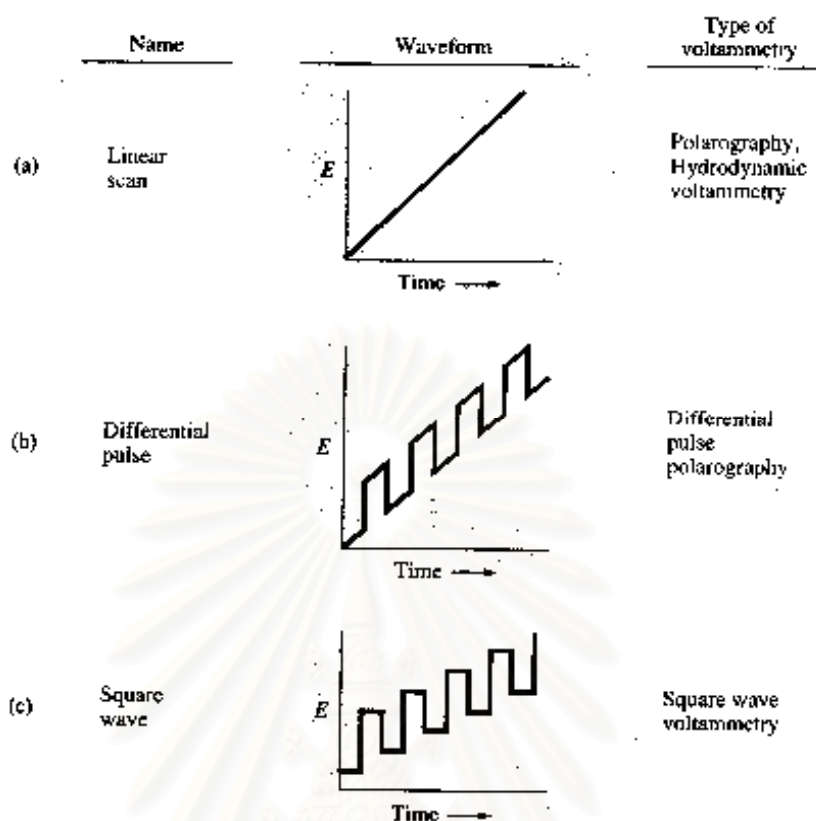


Figure 2.2 Typical excitation signals for voltammetry [5]

2.1.1.1 Cyclic voltammetry [7-9]

Cyclic voltammetry is the most widely used technique for acquiring qualitative information about electrochemical reactions. The power of cyclic voltammetry result from its ability to rapidly provide considerable information on the thermodynamics of redox processes, on the kinetics of heterogeneous electron-transfer reactions, and on coupled chemical reaction or adsorption processes. Cyclic voltammetry is often the first experiment performed in an electroanalytical study. In particular, it offers a rapid location of redox potentials of the electroactive species, and convenient evaluation of the effect of media upon the redox process.

Cyclic voltammetry consists of scanning linearly the potential of a stationary working electrode (in an unstirred solution) using a triangular potential

waveform (Figure 2.3a). The triangular waveform produces the forward and then the reverse scan. Depending on the information sought, single or multiple cycles can be used. During the potential sweep, the potentiostat measures the current resulting from applied potential. The resulting plot of current versus potential (i-E plot) is termed a cyclic voltammogram (Figure 2.3b). The significant parameters in cyclic voltammogram are the cathodic peak potential (E_{pc}), the anodic peak potential (E_{pa}), the cathodic peak current (i_{pc}), and the anodic peak current (i_{pa}). The cyclic voltammogram is a complicated, time-dependent function of a large number of physical and chemical parameters.

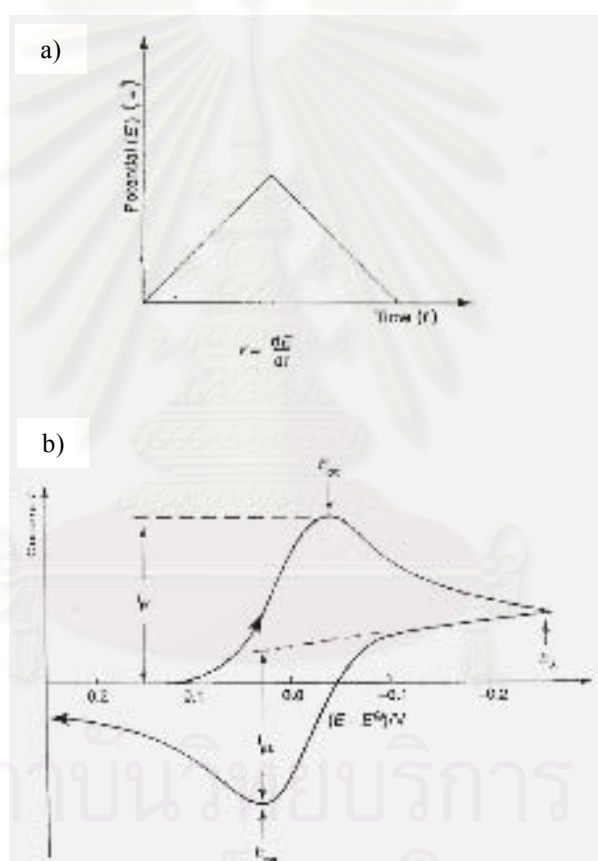


Figure 2.3 Schematic of (a) a potential wave form used in cyclic voltammetry, and (b) a cyclic voltammogram [8]

2.1.2 Amperometry

Amperometry is one of the controlled-potential electrochemical techniques. A simple potential-time waveform is shown in Figure 2.4. It is normally carried out in stirred or flowing solutions or at working electrode. The potential of a chosen working electrode with respect to a reference electrode is set at a fixed potential to detect the change in current response. At this potential, the electroactive species undergo an oxidation or reduction at the electrode [7, 8, 10-12]. The amperometric current is a function of the number of the molecules or ions that have been removed by the reaction at the electrode. Hence, the resultant amperometric signal is directly proportion to the concentration of the analyte.

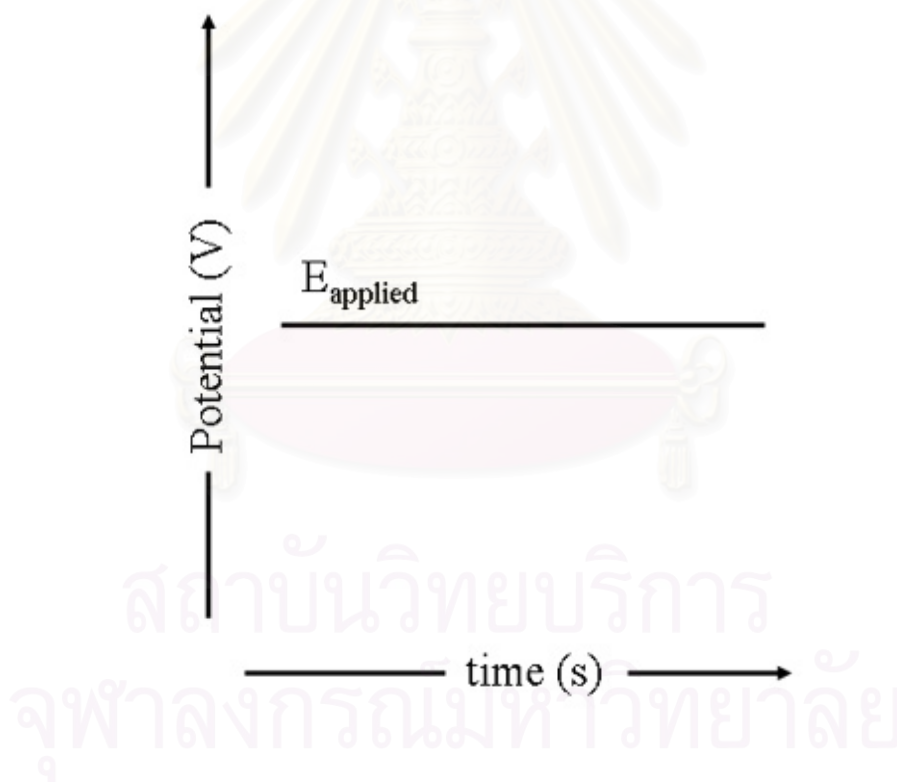


Figure 2.4 A typical waveform employed in amperometry [11]

2.1.2.1 Pulse amperometry[13-16]

Pulsed amperometric detection (PAD) is the amperometric detection under the control of a multistep potential-time waveform. The typical waveform for PAD is the triple step waveform. This waveform consists of three potential steps, which are detection, cleaning, and reactivation steps. In detection step, the oxidation reaction of the electroactive species of analyte interest is occurred. The potential applied in this step is called a detection potential (E_{det}). The time duration for the application of this potential is called a detection time (t_{det}). This time duration consists of two timing parameters, namely, delay time (t_{del}), and integration time (t_{int}). The delay time is necessary to overcome the double-layer charging currents. The current response is sampled during a short integration time period after a delay of delay time. The adsorption of the adsorbed products and/or solution impurities is occurred in the step of detection. These adsorbed species are necessary desorbed from the electrode surface before the next detection process. The desorption process is performed at the oxidation step (cleaning step). In cleaning step, the electrode potential is set at the potential value more positive than the detection potential. The timing parameter for the application of this potential is oxidation time, t_{oxd} . Besides the removal of the adsorbed molecule from the electrode surface, the oxide layer is also developed in this cleaning step. This oxide layer covering the electrode surface can be deactivated the electrode activity, Thus, the electrode activity must be regenerated by a subsequent negative potential to reduction potential, E_{red} , for a duration of reduction time, t_{red} . This last step called the reactivation step. In the last step, the oxide film is dissolved from the electrode surface and the active surface is ready for the next cycle for PAD waveform. The typical PAD waveform is shown in Figure 2.5. From the schematic diagram of PAD waveform displayed in Figure 2.5, the PAD waveform parameters can be divided into two categories; potential and timing parameters. The overall PAD waveform parameters are E_{det} , t_{det} (t_{del} and t_{int}), E_{oxd} , t_{oxd} , E_{red} , and t_{red} . Therefore, there are seven waveform parameters which the optimization must be performed.

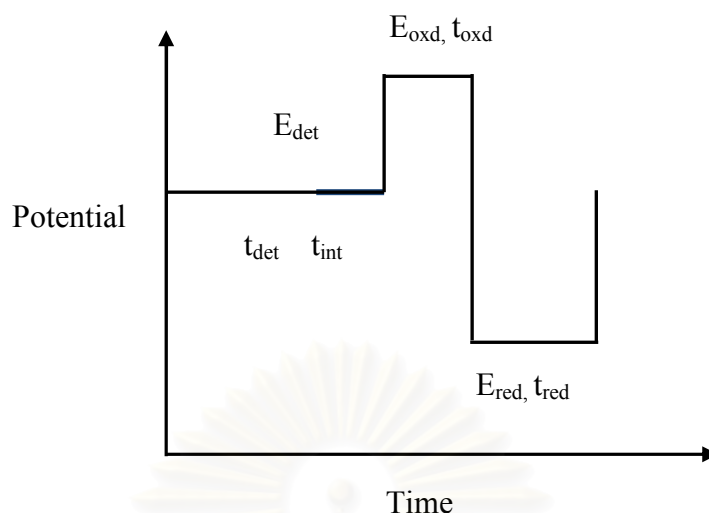


Figure 2.5 Typical PAD waveform

2.2 Capillary electrophoresis[17, 18]

The electrophoretic separation technique is based on the principle that under the influence of an applied field, different species in solution will migrate at different velocities from one another. When an external electric field is applied to a solution of charged species, each ion moves toward the electrode of opposite charge. The velocities of the migrating species depend not only on the electric field, but also on the shapes of the species and their environment. Historically, electrophoresis has been performed on a support medium such as a semisolid slab gel or in nongel support media such as paper or cellulose acetate. The support media provide the physical support and mechanical stability for the fluidic buffer system. Capillary electrophoresis is emerged as an alternative form of electrophoresis, where the capillary wall provides the mechanical stability for the carrier electrolyte. Capillary electrophoresis is the collective term which incorporates all of the electrophoretic modes that are performed within a capillary. Capillary electrophoresis is a novel separation technique, using a separation mechanism completely different to that of liquid chromatography. This means it can be used in a variety of situations in which liquid chromatography is limited.

The advantages of capillary electrophoresis are it:

- has very high efficiencies, meaning hundreds of components can be separated at the same time
- requires minute amounts of sample
- is easily automated
- can be used quantitatively
- consumes limited amounts of reagents

2.2.1 Background theory[19]

Capillary electrophoresis (CE) is similar to chromatography in many respects, and most of the words used in chromatography are also found in CE. For example resolution and efficiency are common to both techniques and are defined in a similar way. However, some of the terminology is different, as illustrated in Table 2.1. For example, in chromatography, a column is used to separate the analytes; in electrophoresis, a capillary is used. In Chromatography a pump is used to propel the sample through the column; in electrophoresis, there is no external pumping system, and the sample constituents move as a result of their mobilities in an applied potential field and the electroosmotic flow, if present.

Table 2.1 Comparison of electrophoretic and chromatographic terms[19]

Capillary electrophoresis	Chromatography
Electropherogram	Chromatogram
Applied potential	Flow rate
Carrier electrolyte or buffer	Eluent or mobile phase
Injection mode(hydrostatic or electromigration)	Injector
Migration time	Retention time
Electrophoretic mobility	Column capacity factor
Velocity	-
Electroosmotic flow	-
High-voltage power supply	Pump
Capillary	Column

2.2.2 Electroosmotic flow

The onset of an electroosmotic flow (EOF) is an important phenomenon in CE. Many materials, including glass, develop a charge at the surface when they come into contact with a protic solvent. For glass, the surface charge develops from the protonation or deprotonation of silanol groups (pKa~3.5). For polymers without any proton donating or accepting groups, traces of residual unreacted material in the bulk or charged substances adsorbed to the surface can result in a surface charge.

Electroosmosis is the process of inducing ionized liquid motion adjacent to a stationary charged surface under an applied external electric field. In microchannel systems, the liquid flows under the influence of external electric fields. An influential factor of the flow behavior is the zeta potential (ζ) because it regulates the ion mobility, which is in turn an important factor on the velocity of the analyte. The zeta potential is directly proportional to the applied field and the channel material. This flow is governed by a slightly modified the Navier-Stokes equation that accounts for the potential distribution in the diffuse-layer, which is in turn governed by the Poisson-Boltzmann equation.

$$\mu \left[\frac{\partial V}{\partial t} + (V \cdot \nabla) V \right] = -\nabla p + \mu \nabla^2 V - \rho_f E \quad (\text{Equation 2.1})$$

Potential distribution term
↓

In microscales, electroosmosis is a good alternative for controlling the flow in micro fluidic systems for biological and chemical analysis because it alleviates difficulties associated with the large pressure gradients required in the traditional pressure driven flows. It also eliminates the moving mechanical components such as valves, switches and gates.

In microchannels, the flow moves with low Reynolds numbers and laminar flow. Consequently, species mixing is a slow, diffusion-dominated

phenomenon that requires long mixing channels and large retention times to attain a homogeneous solution. When an electric field is applied across the channel, the ions in the double layer move towards the electrode of opposite polarity. This creates motion of the fluid near the walls that transfers via viscous forces into convective motion of the bulk fluid. The velocity profile is laminar and parabolic except when close to the walls of the channel.

There are two significant disadvantages of electroosmotic flow. First, it is affected by the surface properties. Second, it requires high voltages to obtain appreciable velocities.

Selecting the proper material to construct the channels is also a great challenge because it controls the formation of the electrical double layer (EDL) in which the excess of positive ions flow and induce the fluid motion. This section, where the excess of positive ions flow, is also known as the Debye length and it is equivalent to the distance from the wall where the electroosmotic potential energy is equal to the thermal energy. The EDL has two distinctive sections, as shown in Figure 2.6. The first is the Stern plane, which is the immobile layer of ions next to the solid surface. Its function is to stabilize the charge of the wall. The second section is the diffusion layer, which is characterized by the zeta potential (ζ) and governed by the Poisson-Boltzmann equation.

Poisson-Boltzmann Equation $\nabla^2\psi = \kappa^2\psi$ (Equation 2.2)

สถาบันวิทยบริการ
จุฬาลงกรณ์มหาวิทยาลัย

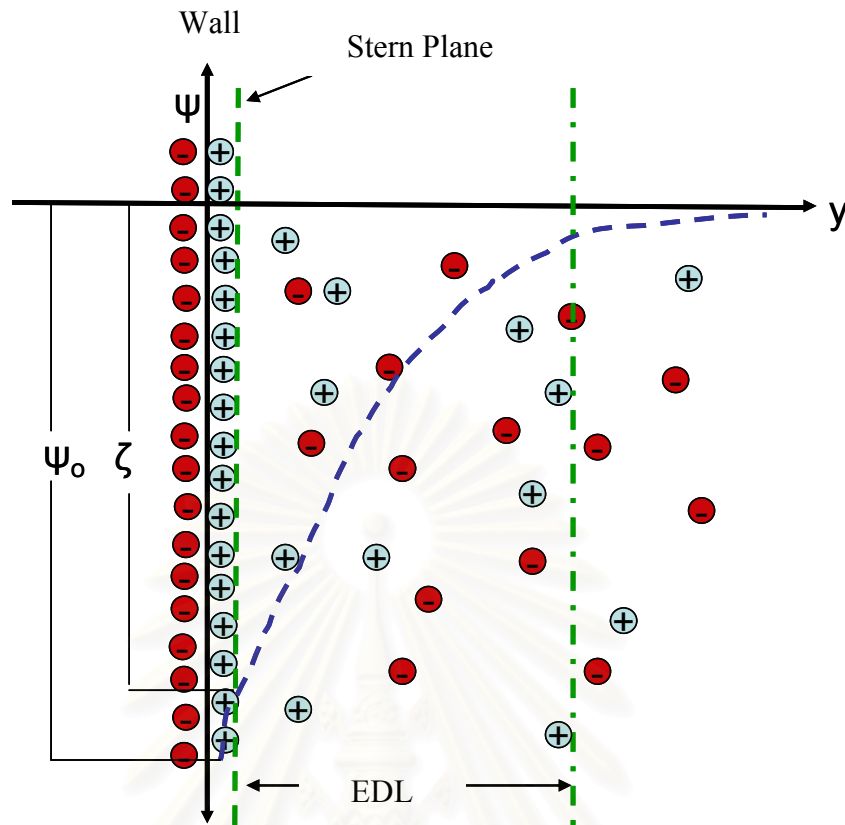


Figure 2.6 Double layer potential. This scheme shows the electric double layer formed next to the negative charged solid surface. The EDL is due to the surface potential ψ_0 , applied to the wall of the channel.

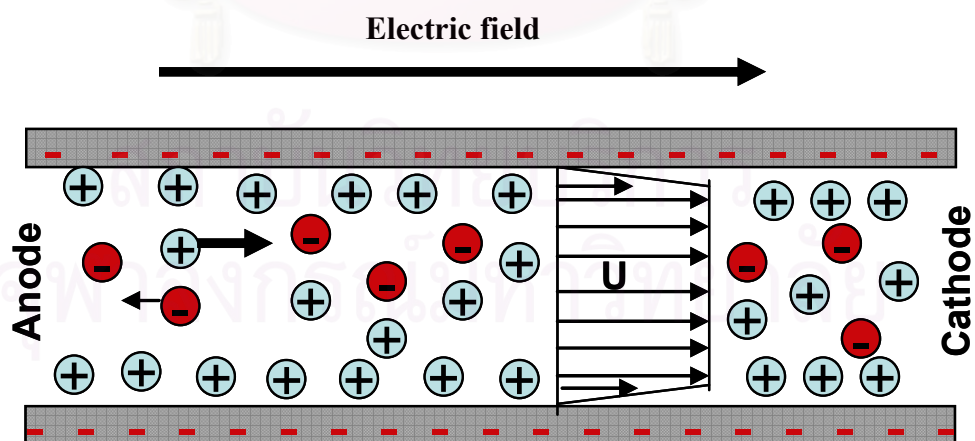


Figure 2.7 Electroosmotic velocity profile in microchannels. This is a schematic representation of the fluid flow inside a symmetric channel with constant electric potential at the walls.

The rest of the fluid is dragged along in the capillary, creating a bulk flow of liquid in it. The flow profile will not be parabolic as in hydrodynamic flow, where drag from stationary surfaces slows the liquid at the walls. Instead the flow profile is flat. Flat flow profile gives less band broadening than a parabolic flow profile from hydrodynamic flow, see Figure 2.8

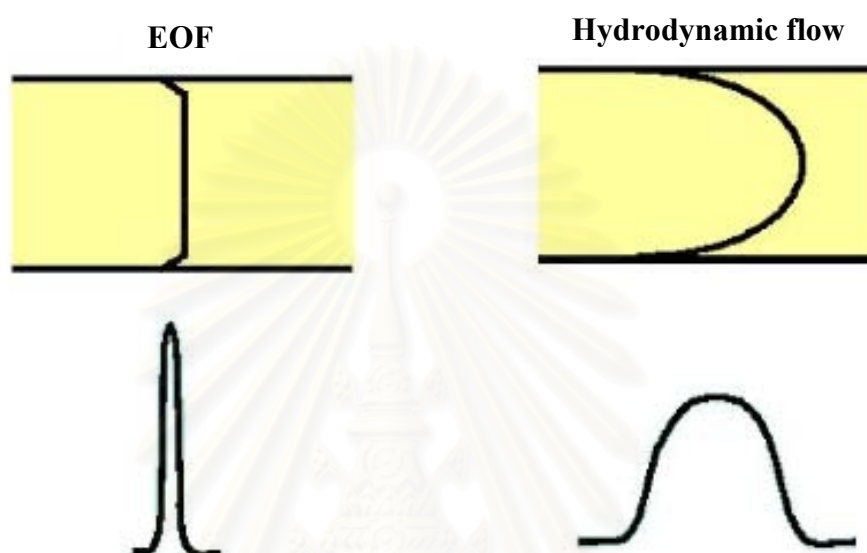


Figure 2.8 Flow profiles and the effect on peak shapes for electroosmotic flow and hydrodynamic flow.

2.2.3 Injection scheme

One of the differences between microchip CE and conventional CE is the method by which the sample plug is introduced into the capillary. In conventional instruments, one end of the capillary is immersed in the sample solution. The sample is driven into the capillary by applying a pressure pulse (hydrodynamic injection) or using EOF (electrokinetic injection). For a microchip separation, a very short sample plug (<1 mm) needs to be introduced. To permit this, microchip CE devices typically employ a column coupling configuration of channels (Figure 2.9A-H). In the cross injector design and double-T in Figure 2.9, A and B are among the earliest designs employed in microchip CE [20].

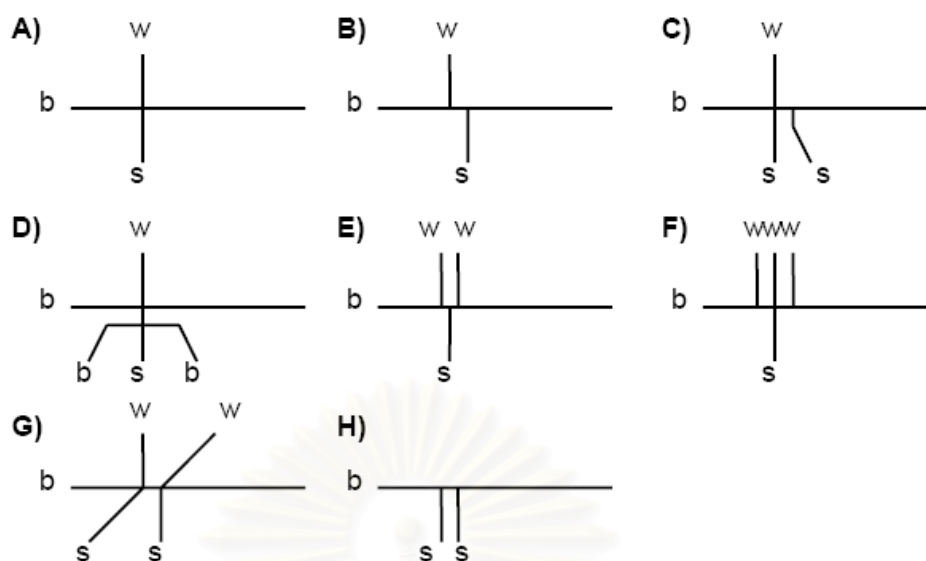


Figure 2.9 Examples of sample injector types. A) cross, B) double-T, C) double-L, D) double cross, E) triple-T, F) multi-T, G) stacking type, H) π -injector. Sample inlet s, waste w and BGE inlet B are indicated [21].

There are two main types of injection methods used in microchips: the gated injection and pinched injection described as follows.

2.2.3.1 Gated injection

Figure 2.10 illustrates the principle of the gated injection. The main waste reservoir on the end of the injection channel is set to ground at all times. In pre-injection and run mode, the settings are the same. Voltages are set so that the mobile phase will flow from the buffer reservoir (B) to the waste reservoir (W), and the sample will run from the sample reservoir (S) to the sample waste reservoir (SW). To prevent any sample from “bleeding” into the separation channel, the voltage on B is set higher than the voltage on S so that some mobile phase will always run into the SW reservoir.

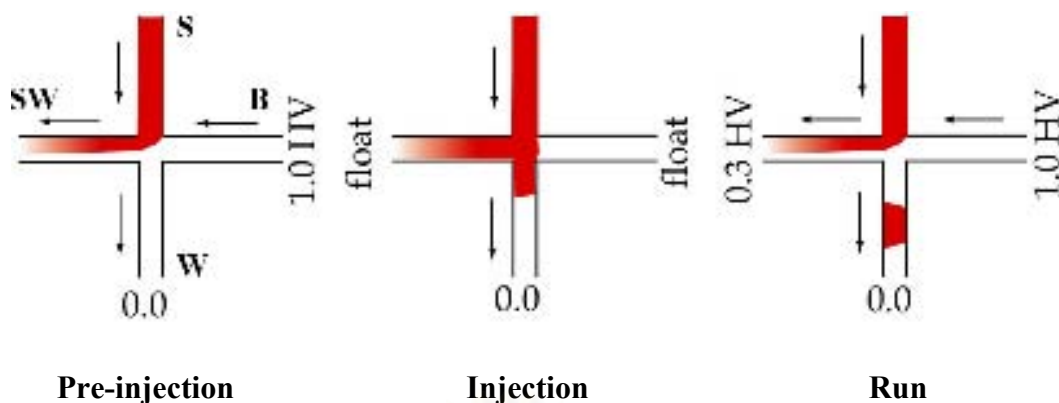


Figure 2.10 Principle of gated injection. Red stream is the sample, and white stream is the mobile phase. S: Sample, SW: Sample waste, B: Buffer, W: Waste [21].

In the injection mode, both B and SW are set to “float”, which means that no current will run through either reservoir. As a result no fluid will flow to or from either reservoir. The voltages on S and W are the same as those in the run mode, so a “plug” of sample will flow into the separation channel as long as the voltages are in the injection settings. Typically, the injection mode is switched on for 0.1-1 seconds. The longer the settings are on the injection step, the longer the plug is injected into the column.

After the desired amount of analyte has been injected into the separation channel, the voltages are changed to the run mode. The settings in the run mode are the same as those in the pre-injection mode. The sample will flow from S to SW as before, and the fresh mobile phase will flow down the separation channel from B. The injected sample plug will flow down the separation channel, where individual components will be separated and finally detected.

Gated injection is very simple to perform and it allows for injection of as long a plug as thought necessary for injection into the separation channel. That a new sample plug can be injected into the separation channel at any time is another advantage of the gated injection. This means that a new sample can

even be injected into the separation channel before the previous sample reaches the detector.

One drawback to the gated injection method is a bias in the injection. The species with the highest electrokinetic velocity are injected at a larger extent than those with lower electrokinetic velocities. This means that in regular EOF, a sample plug injected into the cation sample plug will be slightly longer than that for neutral species and the anion sample plug will be slightly shorter than for neutrals. This will lower the limit of detection somewhat for negatively charged species, but the effect is usually not large enough to be significant. If the gated injection is also used to make a calibration curve for the species, this bias will even out since the same bias will apply for the calibration and sample injection. That flows are steered by applying electrical potentials to different points on the chip is an advantage of electrokinetic injection, which does not require mechanical components. Overall, the simple cross and double-T designs are still the most commonly used types owing to their simplicity. For all experiments in this dissertation, a double-T design is used.

2.2.3.2 Pinched injection

Figure 2.11 illustrates the principles of the pinched injection. Here, the sample is placed on one of the side-arms of the cross, the mobile phase is placed in the top reservoir, and the sample waste is placed on the other side-arm. The waste reservoir needs to be filled with fresh mobile phase. In the “load position”, sample flows from S towards SW, over the cross. Mobile phase flows from both B and W to the SW to prevent bleeding of the sample into the main channel. The sample stream is “pinched” together by the two mobile phase streams.

In the “run position”, the voltages are switched so that the mobile phase will flow from B to the cross and towards all three reservoirs. Most of the flow is directed toward the separation column to drive the sample plug forward, but some mobile phase flow will also be directed towards S and SW to avoid bleeding.

The size of the sample plug is determined by the geometry of the injection cross, so that its length can never be more than the width of the channels at the injection cross. However, the sample plug can be made smaller. By increasing the buffer flow from B and W, the pinched sample stream at the junction becomes narrower, and a shorter plug is injected.

As long as the loading step in the pinched injection is given sufficient time, there is no bias in the sample injected, as in the gated injection. A drawback of using the pinched injection is that after each run, the microchip needs to be switched to the “load position” and allowed to equilibrate before a new run is possible. Another disadvantage of the pinched injection is that the “load position” has a backflow of mobile phase from the W reservoir, which will contain some analytes after a few runs. Therefore, the separation channel will fill up with analytes during this backflow. Since the sample volumes in the channels are very small, a sufficiently large volume of the reservoirs will dilute the analytes so much so that they should be undetectable when they run back through the detector from the waste reservoir. Care should be taken by regularly changing the buffer in waste reservoirs.

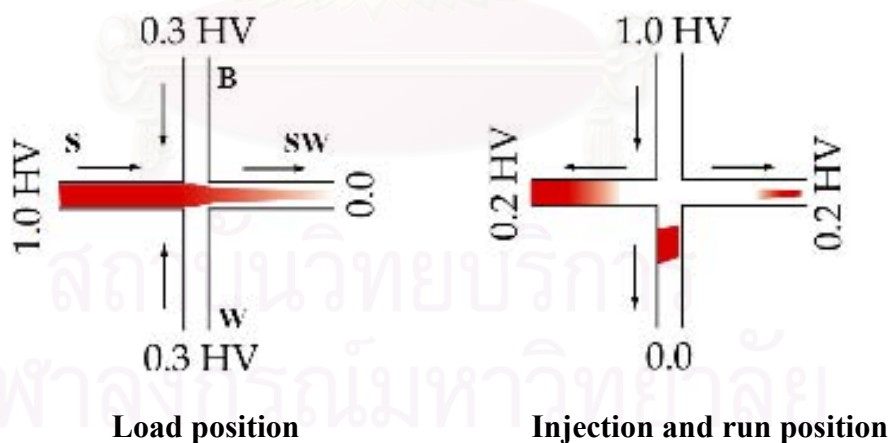


Figure 2.11 Principles of pinched injection. Red stream is the sample, and white stream is the mobile phase. S: Sample, SW: Sample waste, B: Buffer, W: Waste [21].

2.2.4 Dimension of microfluidic channels

The two main factors defining the microchip are the length of the separation channel and the length of the sample plug. In order to compare different designs, a measure to describe the performance is necessary. Following the definitions used in chromatographic separations, the terms, number of theoretical plates, plate height and resolution are used.

The plate number N is defined by the spatial variance of a zone σ^2 (m^2) after migrating a distance L (m):

$$N = \frac{L^2}{\sigma^2} \quad (\text{Equation 2.3})$$

In analogy, the plate height H (m) is given by:

$$H = \frac{L}{N} = \frac{\sigma^2}{L} \quad (\text{Equation 2.4})$$

In the ideal case, the broadening of a zone is the result of only molecular diffusion in the time interval t (s) before the analyte zone reaches the detector. The spatial variance resulting from the diffusion of an initial infinitely small zone with a diffusion coefficient D (m^2/s) is provided by the Einstein equation:

$$\sigma_{diff}^2 = 2Dt \quad (\text{Equation 2.5})$$

Combining equations 2.5, 2.12 and 2.14 yields the plate number under ideal conditions:

$$N = \frac{\mu V}{2D} \quad (\text{Equation 2.6})$$

This equation forms the basis of microchip CE. It shows that the separation efficiency is independent of the separation channel length under condition

that the diffusion solely determines the spatial variance. The only experimentally accessible parameter is the applied voltage V .

The diffusion constant and electrophoretic mobility both involve movement through the medium and can be converted into one another:

$$D = \frac{\mu RT}{zF} \quad (\text{Equation 2.7})$$

Equations 2.6 and 2.7 demonstrate that the plate number is also not affected by the mobility or diffusion constant, since they cancel each other out.

A more useful parameter to characterize the separation performance is the resolution (R_s) between two analyte peaks (see Figure 2.12) that are separated by a distance of Δx (m):

$$R_s = \frac{\Delta x}{4\sigma} = 1.18 \frac{\Delta x}{w_{1/2}^{peak1} + w_{1/2}^{peak2}} \quad (\text{Equation 2.8})$$

To calculate the resolution from experimental data, it is easier to measure the width of the peak at half height, $w_{1/2}$, instead of the variance or the width at the baseline (w_1 , w_2 in Figure 2.12).

The equations for plate number, plate height and resolution all indicate that the only way to increase the separating performance is to either increase the separation voltage or reduce the EOF. In reality, diffusion is only one of many potential sources of dispersion.

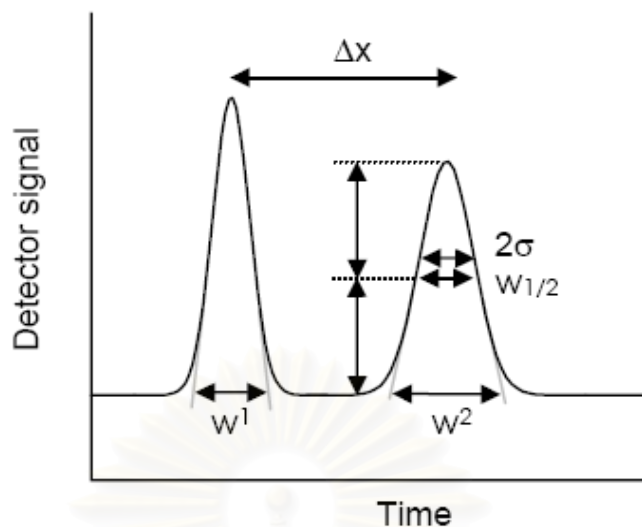


Figure 2.12 Representation of the resolution in separation science.

Also, the length of the initial sample plug and the size of the detection area are not infinitely small. When these effects are taken into account it is possible to define a set of design rules for CE microchips that will provide the best performance.

For conventional CE separations, fused silica capillaries ranging in length from a few decimeters up to a meter are used. It is possible to incorporate such a length onto a microchip by folding up the channel. However, the turns that are introduced are an additional source of zone broadening [22]. Although the dispersion can be kept to a minimum, following a couple of design rules (e.g. optimizing the turn radius and using narrow channels in the turns), long channels are seldom used. One of the reasons is that the migration time increases due the longer migration distance, while the migration velocity decreases due to the lower electrical field strength at the same voltage. This diminishes the benefits of microchip CE as a faster alternative to conventional systems. The separation channels on microchips are therefore typically shorter than 10 cm. The width and depth of the channel also affect the performance, but in a more indirect manner. A hydrostatic pressure difference will cause a hydrodynamic flow during the separation. The flow profile has a parabolic shape, which produces additional dispersion of the zones. A pressure difference is avoided by filling all fluid compartments to the same height. However, since the

channels are typically very short, the low hydrodynamic resistance can cause problems even for small pressure differences.

2.2.5 Factor affecting separation efficiency[19]

In the discussion of separation efficiency thus far, it has been assumed that one-dimensional diffusion is the major contributor to peak broadening in CE, and other factors that contribute to the diffusion process have been ignored. In reality, the total variance of a zone, once corrections have been made for zone velocity and finite detector width, is given by

$$\sigma^2 = \sigma_i^2 + \sigma_d^2 + \sigma_e^2 + \sigma_t^2 + \sigma_{eo}^2 + \sigma_o^2 + \sigma_o'^2 \quad (\text{Equation 2.9})$$

where the right-hand terms represent the contributions of injection, diffusion, electromigration, temperature profiles due to Joule heating, electroosmosis, and other effects such as interactions between the analytes and the capillary wall, respectively. Except for σ_i^2 , the variances are directly proportional to the analysis time.

The first four terms on the right hand side of equation 2.9 represent effect inherent in the principle of the method and cannot be suppressed to zero; however their influence on the separation efficiency can be controlled by instrument design and selection of appropriate working condition. Interactions between the analyte and capillary wall is a concern primarily for the analysis of biomolecules, and they may be reduced or eliminated by coating capillary wall. Other factors in equation 2.9 are injection length, diffusion, electromigration dispersion, joule heating, and solute-wall interactions. Two major factors effect in the microchip CE; electromigration dispersion and joule heating, were briefly discussed.

2.2.5.1 Electromigration dispersion[19]

Electromigration dispersion (EMD) is, together with the diffusion, the most important source of band broadening. It originates from the fact that the analyte zones change the local electrical conductivity and hence the local

electrical field strength. The migration velocity of a species is therefore a function of its concentration. As a result, the zones develop a triangular shape shown schematically in Figure 2.13. The larger the difference in mobility of the analyte ion and the BGE co-ion, the higher the analyte concentration in the sample. In general, the BGE will be optimized to minimize dispersion by selecting a co-ion with a mobility close to that of the analytes. However, for conductivity detection a large difference in mobilities is required for optimum sensitivity. Electromigration dispersion is therefore an important contributor to the peak broadening.

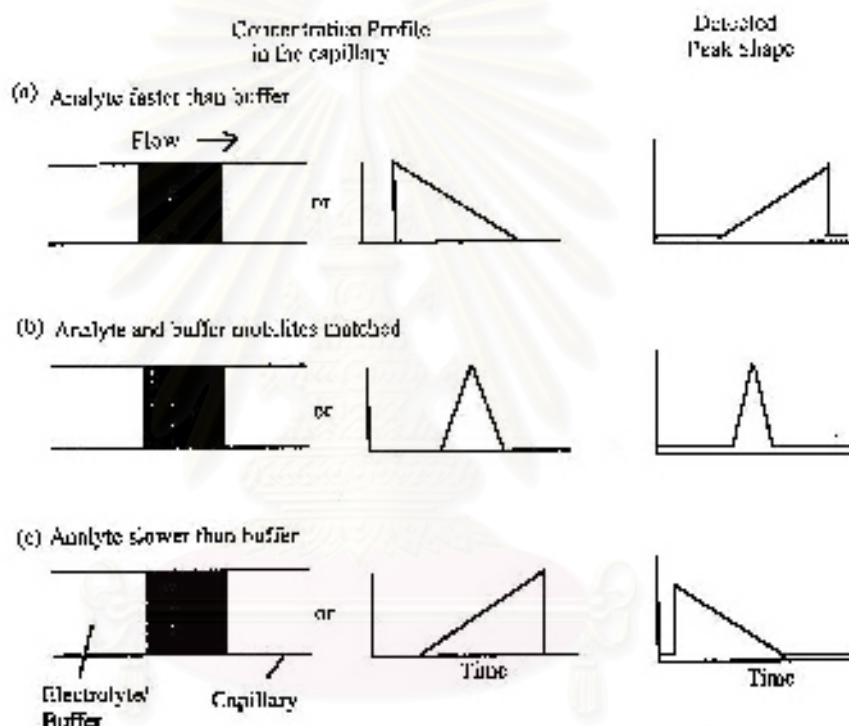


Figure 2.13 Electromigration dispersion caused by mismatched analyte and electrolyte mobilities [19].

2.2.5.2 Joule heating [19]

The high voltages applied in the microchip CE systems to minimized diffusion. However, high power inductions cause excessive band broadening because of Joule heating of the liquid inside the channel wall. Thus, a compromise is required between band broadening at lower voltage caused by diffusion and band broadening at higher voltage caused by Joule heating.

Joule of ohmic heating is the name given to the heat generation caused by collisions between solute ions and electrolyte ions as a result of the conduction of electric currents. It can cause nonuniform temperature gradients and local changes in viscosity, both of which lead to zone broadening. Without adequate heat dissipation, the heat generated by the use of high separation voltages can rapidly evaporate any electrolyte solution.

A simple, practical approach to determine the optimum voltage without exceeding the heat removal capacity of the system is to draw an Ohm's law plot, as illustrated in Figure 2.14 [23]. The capillary is filled with the BGE, voltage is applied, and the resulting current is recorded. The voltage is then varied and the current recorded at each new voltage. When the current is plotted against the applied voltage, a straight line should result. A positive deviation from linearity shows that the temperature removal capacity of the system has been exceeded.

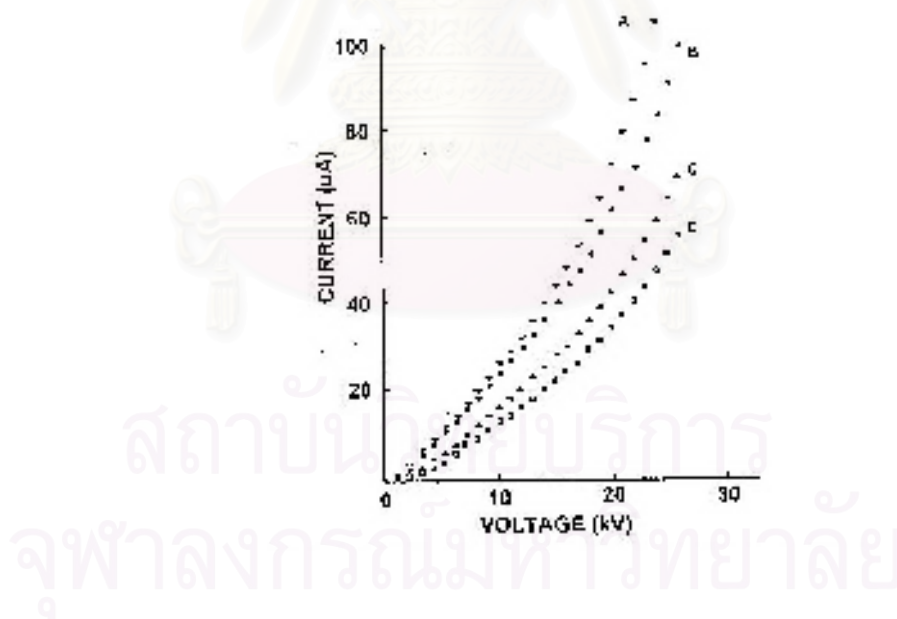


Figure 2.14 Ohm's law plots showing the optimum voltages for different capillary temperature using air circulation for temperature control. (A) No control; (B) 25 °C; (C) 10 °C; (D) 4 °C [19, 23].

2.2.6 Separation modes [19]

In capillary electrophoresis a sample, usually containing charged species, is introduced into the end of a capillary that has been filled with a solution of buffer (or electrolyte). Under the influence of an electric field, the detector end, where they are visualized. Three distinct separation mechanisms have been developed for the separation of analytes by CE. The modes of CE are classified by the different separation mechanisms allowing CE techniques to be used for a wide variety of substances. These modes include;

- Capillary Zone Electrophoresis (CZE)
- Micellar electrokinetic chromatography (MEKC)
- Capillary electrochromatography (CEC)
- Capillary gel electrophoresis (CGE)
- Capillary isoelectric focusing (CIEF)
- Capillary isotachopheresis (CITP)

The first two techniques, CZE and MEKC, used in this research were briefly discussed. Figure 2.15 shows the separation mechanism in CZE and MEKC.

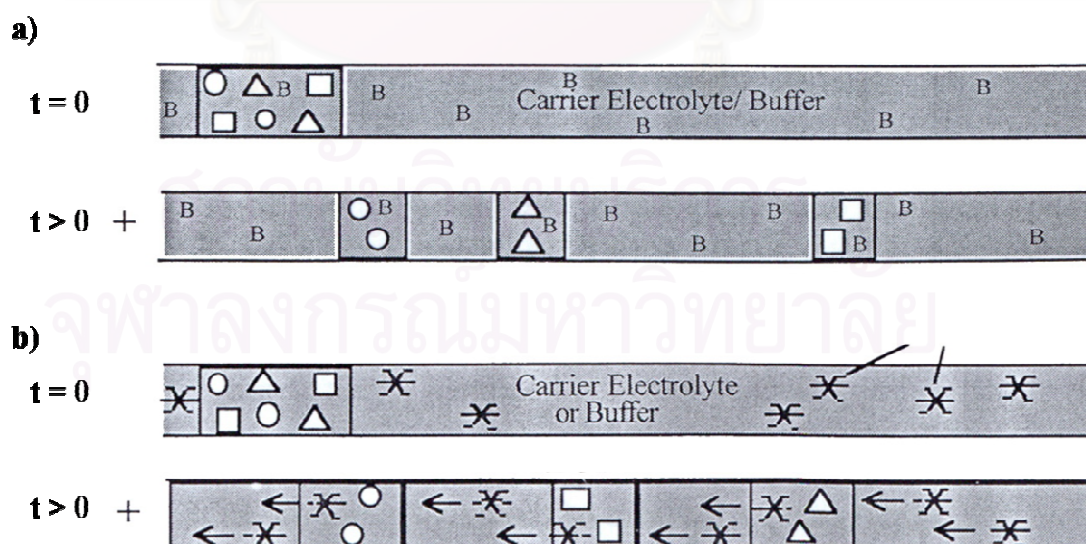


Figure 2.15 Separation mechanism in (a) CZE and (b) MEKC [19].

2.2.6.1 Capillary zone electrophoresis (CZE)

CZE is a widely used mode of electrophoresis because it is applicable to separations of cations and anions, but not neutrals, in the same run, and it is relatively simple. In CZE, the capillary is filled with a buffer of constant composition, and the source and destination vials are filled with the same buffer. The order of elution in this method is cations, neutrals and anions. Neutral compounds are not separated in CZE. Whereas ions are separated on the basis of their charge-to-size ratios. Electrophoresis mobility is depend to same extent on the shape of the ions. The method can be used to separate almost any ionized compounds that are soluble in the buffer.

2.2.6.2 Micellar electrokinetic chromatography (MEKC)

MEKC is a mode of CE similar to CZE, in which surfactants (micelles) are added to the buffer system. Micellar solutions can be used to solubilize hydrophobic compounds that would otherwise be insoluble in water. In MEKC the micelles are used to provide a reversed-phase character to the separation mechanism. The solutes are separated based on their interaction with the hydrophobic groups on the surface of micelle. The interaction is based on the partitioning of solutes between micelles and the run buffer. Although MEKC was originally developed for the separation of neutral species by capillary electrophoresis, it has also been shown to enhance resolution in the analysis of a variety of charged species.

2.3 Microchip capillary electrophoresis [24-27]

Microchip capillary electrophoresis (CE) has appeared over the decades as a result of the marriage of chemical analysis and microfabrication techniques from the integrated circuit world. The concept of microchip separation is not new, however, with the first report of a microfabricated gas chromatography column appearing in 1979 and the first example of a microfabricated liquid chromatography system appearing in 1990. Little excitement was generated over these early developments, however, because of the complexity of the operational systems and generally poor performance of the devices. Active development of microchip separation technology

did not begin until the early 1990s with the seminal work of Manz, Harrison, Verpoorte, and Widmer in microchip CE. CE proved to be an excellent match for microchip technologies because it easily manipulates volumes at the nanoliter scale, required no moving parts, and provides fast, high-resolution separations.

The theory and mechanisms of action for microchip CE are based on fundamental knowledge gained in the development of conventional CE.

2.4 Material for microchip capillary electrophoresis [24]

The first microchip CE systems were constructed on glass substrates [27, 28]. Because glass is a silicon-based compound, many well-known and well-developed microfabrication methods were directly adapted from the field of electrical engineering. In addition, glass (or quartz) has excellent optical properties, including optical transparency over a wide range of useful wavelengths. In addition, glass possesses the same surface chemistry as the fused silica capillaries used for conventional CE. Many of the developments in conventional CE can be directly applied to the design of glass microchips. Despite the advantages of glass substrates, there are also significant disadvantages. First, glass fabrication processes yield only one device, and so manufacturing costs are relatively high. Second, glass is fragile and easily broken if not handled with extreme care. Third, high-quality glass is expensive. As a result of these disadvantages, a significant amount of attention has focused on the fabrication of microchips on polymer substrates. Polymer substrates are less expensive and easier to fabricate than glass substrates. Polymer substrates are fabricated either through molding procedures or through direct write protocols employing ultraviolet lasers, electron beams, or X-rays. Either of these fabrication methods provides high throughput and uses lower-cost materials. The major limitation of polymer substrates for microchip CE is the poorly understood and poorly controlled surface chemistry of these materials. Thus, understanding and controlling the surface properties of polymer devices is an important goal.

Poly(dimethylsiloxane) (PDMS) is a polymer which is often used in microfluidic applications. It has many advantages over other materials commonly

used in microfluidics such as glass or silicon. PDMS is flexible, optically transparent to wavelengths > 230 nm, impermeable to water, and non-toxic to cells. It is, however, permeable to gases. It is also inexpensive and an excellent material for soft lithographical techniques. PDMS is composed of repeating $-\text{OSi}(\text{CH}_3)_2-$ units. Its surface is hydrophobic in its unprocessed state due to the methyl groups. This property is a considerable drawback in microfluidic applications, because it renders the substrate surface difficult to wet with aqueous solvents and prone to trapping air bubbles. Hydrophobic surfaces are susceptible to nonspecific binding, especially to proteins, which may cause serious problems in biological applications. Treating the PDMS structure with an oxygen plasma renders its surfaces hydrophilic and eliminates these difficulties associated with hydrophobicity. The mechanism behind the change in susceptibility to water is due to an oxidation of the surface, producing silanol groups (Si-OH) at the surface. An oxidized PDMS surface will stay hydrophilic if kept in contact with water, but if exposed to air for ~ 30 minutes, hydrophobic groups will once again come to dominate the substrate surface's behavior. The capacity to produce hydrophilic silanol surface groups also enables irreversible bonding to silicon-based materials, such as glass or other PDMS structures. One problem associated with the elastic properties of PDMS is the risk of elastic deformation. Because of the material's elastic nature, it very commonly deforms slightly over time. Also, should the aspect ratio of a PDMS structure stray from unity, there is a definite risk of structural collapse.

Polymeric materials have become increasingly used with MCE due to their low cost and ease of fabrication. While PDMS arguably has become the most widely used material for MCE-EC due to the simplicity of microelectrode incorporation, devices constructed from the material suffer from low separation efficiency, low surface stability, and a tendency for analytes sorption. Other polymers, such as poly(methylmethacrylate) (PMMA) and polycarbonate (PC) have higher separation efficiencies, but electrode incorporation into these materials requires more elaborate fabrication techniques. In this report, Thermoset Polyester (TPE) was studied as a possible alternative material for MCE-EC. TPE microchips were characterized in their native, plasma-oxidized, and polyelectrolyte multilayer-coated (PEM-coated) forms. TPE provides higher separation efficiencies compared to PDMS microchips, and still only requires simple fabrication techniques. In this work, separation

efficiencies as high as 295,000 N/m were observed with TPE MCE-EC devices. Furthermore, electroosmotic flow was higher and more consistent as a function of pH for both native and plasma-treated TPE than for PDMS. Finally, TPE is also amenable to surface modification with simple polyelectrolyte multilayer coatings, which offer another means of controlling surface chemistry and surface charge.

Thermoset polyester (TPE) has shown promise as an alternative microchip material, because it represents a merger of ease of fabrication and cost effectiveness, typical of PDMS, with higher separation efficiencies and increased stability, typical of PMMA and PC [29]. A process for fabricating TPE microfluidic devices has been previously described by Fiorini *et al.* [29, 30]. Because fabrication techniques are similar to those for PDMS, little or no modification to existing soft lithography techniques is needed [31, 32].

2.5 Polyelectrolyte multilayer coatings

Microchip capillary electrophoresis (MCE) has, in recent years, had a major impact on the field of chemical separations. Since the first reports of micro-Total analysis systems (μ TAS) [1], the development of microchip-based analytical systems has increased because μ TAS can be engineered to perform the same analyses as conventional scale systems, but with reduced sample and reagent consumption, lower overall cost, and faster analysis times [2]. During early work on MCE, capillary channels were typically fabricated onto glass substrates [33-35]. Although glass has several advantages over polymeric substrates for microchip-based separations, including chemical stability and high separation efficiency, it also has disadvantages such as expensive materials and increased fabrication costs and time. In light of these problems, many groups have attempted to develop microchips on polymer substrates [2, 29, 36]. Polymeric microchips have difficulties of their own, such as poorly defined, highly variable surface chemistry and the potential for sorption of moderately hydrophobic analytes. As a result, many groups have published strategies to control the surface chemistry and surface charge of polymeric microfluidic devices [37-44].

Controlling the surface charge of the capillary wall is very important in both conventional and MCE, because surface charge helps dictate electroosmotic flow

(EOF) [45, 46]. Thus polymer surface chemistry dictates analyte adsorption and peak tailing. Hydrophobic surfaces result in more extensive tailing than hydrophilic surfaces [47, 48]. One polymer in particular, poly(dimethylsiloxane) (PDMS), has received a great deal of attention due to the ease of fabrication, which can be performed outside a cleanroom, the ease of constructing complex geometries, and the relatively inexpensive material costs per chip [49]. In addition, pumps and other functional elements can be easily integrated into PDMS devices [50]. Unfortunately, there are very few proven methods for controlling the surface chemistry and EOF of PDMS substrates, and so the separation efficiencies of microchips made from this material are low [49, 51-55].

2.5.1 Successive multiple ionic layer (SMIL) coatings

Successive Multiple Ionic Layer (SMIL) (also referred to as polyelectrolyte multilayer) coatings have been introduced as semi-permanent coatings for conventional [45, 56, 57] and microchip capillary electrophoresis [54, 58-60]. Polyelectrolyte multilayers (PEMs) are uniformly thin films formed by layer-by-layer deposition of charged polymers, or polyelectrolytes, on a surface and was first developed by Decher et al [61, 62]. The mechanisms of formation and charge distribution in PEMs have been probed by electrokinetics [45, 54, 62] and radiochemical techniques [63, 64]. Alternating adsorption of cationic and anionic polyelectrolytes leads to stable coatings that are simple to deposit, can have many potential chemistries, and are robust and reproducible [63-65].

There have been several reports on the use of polyelectrolytes to stabilize EOF and/or to control surface adsorption in CE applications. Maichel *et al.* and Potocek *et al.* reported that poly(diallyldimethylammonium chloride) (PDADMAC) could be used as a replaceable pseudostationary phase in electrokinetic chromatography [66, 67]. In this work, PDADMAC served as both a capillary wall coating and a stationary phase for electrochromatography. In a separate report, Wang and Dubin used PDADMAC to minimize protein adsorption [68]. Chiu *et al.* used polyarginine (PA) as a capillary coating for conventional electrophoretic separations. Separation efficiencies of more than 2 million theoretical plates per meter were attained with this coating [69]. Katayama *et al.* used polybrene (PB) and dextran

sulfate (DS) in multiple ionic-layer coatings to control EOF as a function of pH [56]. Cordova *et al.* investigated the properties of four polycationic polymers as noncovalent coatings to address the problem of protein adsorption in conventional CE and observed substantial reduction of adsorption and significant improvement in separation efficiency and peak shape [70]. Graul and Schlenoff characterized adsorbed PEMs composed of PDADMA and poly(styrenesulfonate) (PSS) for application in capillary zone electrophoresis [45]. All of these reports, however, focused on conventional CE. Very few published examples address PEM coatings for microchip CE devices. Barker *et al.* used PEM coatings composed of polystyrene (PS) and poly(ethylene terephthalate) glycol (PETG) to control microchip EOF [71, 72]. Liu *et al.* previously used polybrene (PB) and dextran sulfate (DS) to control EOF as a function of pH in PDMS microchips [54]. None of the aforementioned examples, however, investigated the effects of PEM coatings on separation efficiency. Furthermore, no systematic studies of the effect of polymer structure on EOF and separation efficiency in microchip devices have been performed.

This dissertation reports on several different PEM coatings for PDMS microchips that improve flow control and separation efficiency relative to unmodified PDMS. The goal of this study was to determine what effect, if any, polyelectrolyte structure and deposition conditions have on separation performance. In these experiments, three cationic polymers, polybrene (PB), poly(ethyleneimine) (PEI), and poly(allylamine) hydrochloride (PAH), were used in conjunction with two anionic polymers, dextran sulfate (DS), and poly(acrylic acid) (PAA). These polymers were chosen to cover a range of chemical functionality in an effort to determine the effect of polymer functional groups on device performance.

2.6 Detection methods compatible with microchip capillary electrophoresis

As MCE devices grow in popularity, more compatible detection methods are needed to increase the number of detectable analytes, particularly for point-of-measurement applications. Absorbance [73, 74], mass spectrometry [75, 76], laser-induced fluorescence (LIF) [77-79], electrochemical (EC) techniques [80, 81] and other detection methods [82-84] have all been successfully coupled with microchip CE. Most reported microchip CE experiments relied on laser-induced fluorescence

(LIF) for detection [85, 86]. Mass spectrometry (MS) also received considerable attention to meet the needs of proteomic analysis. Unfortunately, both LIF and MS require sophisticated and expensive instrumentation. LIF typically requires either pre- or post-capillary sample derivatization to attach fluorophores, so the method is limited to fluorescent analytes and their derivatives [87, 88]. Commercially available MS systems are not inherently portable. Furthermore, they are more costly and less sensitive than LIF systems. Recently, electrochemical detection (EC) has attracted considerable interest for applications in electrophoretic microchip systems [32, 89-101]. This method offers great promise, because it is highly sensitive, inherently miniaturizable in terms of both detection and control instrumentation, low-cost, low-power, and highly compatible with microfabrication technology.

2.6.1 Electrochemical detection

Electrochemical detection (EC) instrumentation is particularly attractive for small molecule analysis, because it is less complex and less expensive than many other detection systems, such as laser-induced fluorescence [77, 78] and mass spectrometry [75, 76]. In addition, its selectivity can be altered from general, through the use of conductivity measurements [102, 103] to very specific, through the use of potential selection measurements [104, 105]. EC has demonstrated potential for many applications and offers mass sensitivity levels similar to those of fluorescence detection while not requiring a fluorophore-labeled sample [106-108].

One concern with EC methods is the appropriate choice of substrate material and the material's effect on separation performance. Glass substrates offer the best separation performance among microchip materials, but the high temperatures used to bond glass substrates can damage or destroy electrodes. In contrast, polymeric substrates provide lower separation performance, but are more amenable to the incorporation of electrodes [104, 107]. In addition, polymeric microchips are less expensive to make. Polymeric substrates, such as poly(dimethylsiloxane) (PDMS), poly(methyl-methacrylate) (PMMA), and polycarbonate (PC), have been studied for application as substrate materials for MCE devices [109-111]. A range of fabrication methods can be applied to polymers, including soft lithography [112], casting [113], laser ablation [114], injection

molding[115] and hot embossing [116]. These processes have shown to be easier, faster, and simpler than etching channels into glass [27]. Polymeric microchips do not require the same high temperatures for bonding as glass does, thereby preventing electrode damage. Unfortunately, for the most part, polymeric CE microchips have demonstrated poor separation efficiency [117-119]. While PDMS microchips are inexpensively and easily fabricated with soft lithography techniques, their separation efficiencies are low and their surface charge is unstable [112, 120, 121]. Several methods for chemically modifying the PDMS surface have been demonstrated in an effort to address some of these issues, and the attempts have met with varying degrees of success [122-124]. Both PMMA and PC have shown higher separation efficiencies, better EOF stability, and less analyte absorption into the bulk material, but fabricating and sealing these materials are more challenging than using soft lithography to make PDMS chips [109, 117].

The difference in applied voltage between the electrophoretic separation and the detection steps has been the main challenge in coupling CE and EC. However, this drawback does not apply at the micro scale. The following three strategies have been employed for EC: end-channel, in-channel, and off-channel.

In end-channel EC, the electrode is placed just outside the separation channel, so the electrode must be aligned. Separation voltage has minimal influence on the potential applied to the electrochemical detector, because most of the voltage drop occurs across the channel.

For in-channel EC, an isolated the electrode is placed inside the separation channel, so an isolated potentiostat is necessary to keep the working electrode at the proper voltage.

Recently, Henry's group reported a simple design in which a microwire was used as the in-channel working electrode for MCE-EC [31, 125, 126]. This method removes the need to fabricate microelectrodes and simplifies electrode alignment [31, 126]. The microwire is aligned perpendicular to the separation channel using a channel patterned into the microchip. Furthermore, because the electrode is solid metal, it is extremely stable and robust. Finally, because a large area of the wire

is exposed to solution, collection efficiencies are increased, and thus, detection limits are lowered. The detection limits for catecholamines, however, were on the order of 100 nM and thus too high for many important applications. One way to improve EC sensitivity is to incorporate a current decoupler into the microchip [127-131]. Current decouplers isolate the separation current from the detection current and thus have been shown to significantly reduce noise and improve the sensitivity of both conventional and microchip CE-EC systems [127, 129-133]. There are two forms of microchip decouplers, laser-etched decouplers and Pt or Pd cathodes. Pd [127, 130] and, to lesser extent, Pt [129] are used as decouplers, because they efficiently absorb the H₂ gas formed at the cathode and thus prevent the bubbles from interfering with the electrophoretic separation [134]. Lacher *et al.* [130] published a procedure using a Pd thin film microelectrode decoupler. They found 500 μm to be the optimum decoupler electrode size and 250 μm to be the optimal spacing between the decoupler and working electrodes. The resulting device's detection limit was 500 nM, partly due to the effects of the Pd decoupler. Microfabrication of two different electrode materials onto a single substrate to serve as a decoupler and a working electrode improves sensitivity, but also increases the microchip's overall cost and fabrication complexity [127, 129, 130, 135].

2.6.2 Amperometric detection

Amperometry is the most widely reported EC detection method for chip-based separations [136-144]. A constant potential is applied to the working electrode, and the resulting current, which is proportional to the concentration of analytes oxidized or reduced, is measured at the electrode surface. A band platinum detection electrode can be fabricated just outside the exit of the separation channel in an orientation parallel to the direction of flow using a photolithographic process [145]. Wang's group described a planar, screen-printed carbon line electrode for a microchip CE system [146]. The detection electrode was mounted perpendicular to the direction of flow, roughly 50 μm away from the capillary outlet. A flow-onto thick-film amperometric detector was reversibly mounted perpendicular to the channel outlet, allowing for fast and easy replacement. The resulting system successfully detected nitroaromatic explosives, phenols, nerve agents, etc. [106]. One major limitation of amperometric detection for CE is the need for very precise alignment between the

separation channel and the working electrode [147]. Another attractive route is to place the detector near the channel exit using electroless deposition and sputtering techniques. Electroless deposition is a simple, low-cost method that obviates the need for photolithographic electrode fabrication or careful channel/electrode alignment.

Alternatively the analyte fluid can be channeled through a ring detection electrode. Hilmi and Luong [148] used electroless deposition to prepare on-chip gold film electrodes at the capillary outlet. The detector's performance was characterized using a mixture of nitroaromatic explosive compounds.

2.7 Biomarkers

Biomarkers are defined as cellular, biochemical, molecular, or genetic alterations by which a normal or abnormal biological process can be recognized or monitored. Biomarkers are measured in biological media, such as human tissues, cells, or fluids. Biomarker research has the potential to impact a wide range of health concerns, including early detection of diseases, drug discovery, and improved accuracy of monitoring medical interventions. In order for biomarker to be clinically useful, biomarker assays must have high predictive accuracy and reproducibility, be easily measurable and minimally invasive, and be acceptable to patients and physicians [149]. The focus of biomarker research is shifting from methods that can analyze one marker at a time to so-called profiling methods, which allow for the simultaneous measurement of a collection of markers. It is believed that marker profiles will allow for more statistically stringent differentiation and thus, a better classification of patient groups (for example, those with cancer and those without). This should improve early detection of diseases while also reducing the number of false-positive and false-negative results. Furthermore, better classification of patients will diminish the number of subjects needed for clinical trials. Most importantly, it is hoped that focused diagnoses will lead to better therapies and earlier intervention [150].

It should be noted that a biomarker need not be causally or mechanistically involved in a disease's pathology. Once discovered, however, biomarkers can be used

for many purposes, including diagnosis and monitoring of treatment and disease recurrence. The challenge, then, is how to discover and validate biomarkers efficiently [151]. To meet this challenge, an analytical technique must be able to separate, detect, and quantify as many components of a biomixture as possible. Furthermore, biomarker assay methods must accommodate normal variations in the physicochemical properties of biological samples. An analytic technique must generate reproducible results, and it must be economical in terms time, effort, and expense. Body fluids, such as serum, urine, and cerebrospinal fluids, are the biological samples most commonly analyzed for biomarkers. Bodily fluid analysis provides a number of advantages over tissue-based analysis. Fluids are typically more accessible, and fluid sampling usually involves less pain for patients. Of course, there are certain drawbacks associated with fluid analysis. First, in order to detect tissue-specific biomarkers in body fluids, the target protein must be secreted. Second, the secreted biomarker must be uniquely identified among the multitude of secreted proteins from various cell types and organs [152].

2.7.1 Thiol compounds

Aminothiols are physiologically relevant biological agents and metabolites. This work will focus on the detection of homocysteine, cysteine, and glutathione.

2.7.1.1 Homocysteine

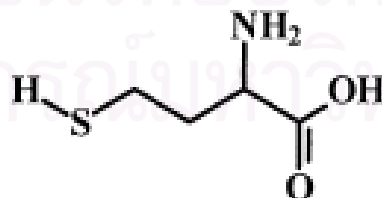


Figure 2.16 Structure of homocysteine

Homocysteine (Hcy) is a blood borne amino acid. Epidemiological studies have demonstrated that high concentrations of homocysteine in blood plasma

are related to increased risk of coronary heart disease, stroke, and peripheral vascular disease. Other evidence suggests that homocysteine may promote atherosclerosis by damaging the inner lining of arteries and promoting blood clots. At the present, however, a direct causal link has not yet been established [153, 154].

Diet and genetic factors strongly affect plasma homocysteine levels. The dietary components with the greatest influence are folic acid and vitamins B6 and B12. Folic acid and other B vitamins help degrade homocysteine within the body. Several studies have found that higher blood levels of B vitamins are at least somewhat related to lower concentrations of homocysteine. Other recent evidence showed that low blood levels of folic acid are linked to increased risks of fatal coronary heart disease and stroke. Recent findings also suggest that laboratory testing of plasma homocysteine levels can improve patient risk assessment. This strategy may be particularly useful for patients with a personal or family history of cardiovascular disease that lack the well-established risk factors (i.e. smoking, high cholesterol, high blood pressure, etc.).

Clinically, homocysteine is measured using a simple blood test. It can be measured at any time of day, and patients do not have to prepare for the blood test in any special way. A healthy homocysteine level is lower than 12 $\mu\text{mol/L}$. A level in excess of 12 $\mu\text{mol/L}$ is considered high. While no studies have shown that lowering homocysteine levels reduces the risks of strokes, heart attacks, and other cardiovascular events, lowering a high homocysteine level removes a proven risk factor for heart disease.

The largest fraction of homocysteine is protein-bound *in vivo*, because the amino acid forms covalent disulfide bonds with thiol-containing protein residues (i.e. cysteine). In plasma, 70–80% of total homocysteine is protein-bound, and 20–30% exists as either homocysteine dimers or mixed-disulfides. Reduced homocysteine is present in only trace amounts. Generally, plasma homocysteine levels are reported in terms of total homocysteine (tHcy), which includes all forms of homocysteine. In healthy individuals, the tHcy concentration ranges from 5 to 15 μM . Plasma tHcy concentrations above the normal range (16–30 μM (moderate), 30–100 μM (intermediate), > 100 μM (severe)) are referred to as hyperhomocysteinemia.

Because current laboratory techniques for measuring tHcy are not sufficiently sensitive or selective, clinical tests are unable to provide a mass-balance account of all forms of homocysteine *in vivo* during hyperhomocysteinemia. Thus, there is a need for a sufficiently sensitive and selective method for measuring all forms of homocysteine in blood plasma.

Several analytical techniques have been applied to measure tHcy in human plasma. These methods include liquid chromatography (LC) with fluorescence, ultraviolet (UV), or electrochemical (EC) detection, immunoassay, gas chromatography-mass spectroscopy (GC-MS), and electrospray-tandem mass spectrometry [155-160]. More recently, capillary electrophoresis with laser-induced fluorescence (CE-LIF) and CE-UV have been investigated [161-166]. CE has many potential advantages for this type of analysis. It is nondestructive, generates very little solvent waste, and is compatible with small-volume samples [167]. Perhaps most importantly, CE can be miniaturized into microchip format for high-throughput or point-of-care analysis. CE with UV detection is not sufficiently sensitive to detect endogenous homocysteine in plasma. The limits of detection (LODs) obtained in our laboratories were approximately 50 μM , which is well above healthy physiological plasma concentrations (5–15 μM tHcy). CE with LIF detection is much more sensitive, but it is necessary to derivatize the thiol with a fluorophore prior to analysis. The derivatization process not only is time-consuming and laborious, but also dilutes the sample and affects assay sensitivity. CE-EC has been shown to be a sensitive and selective technique for identifying a large number of compounds, including thiols [168-171]. One advantage of CE-EC is that it can be miniaturized into “lab-on-a-chip” format for eventual use in a clinical diagnostic setting [169, 172].

In this dissertation, we report the use of a CE-EC microchip equipped with a gold electrode to measure homocysteine concentrations in human blood plasma.

2.7.1.2 Cysteine

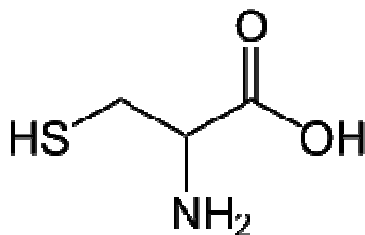


Figure 2.17 Structure of cysteine

Cysteine is a sulphur-containing amino acid, so it acts an important component of the body's protective antioxidant systems. Antioxidants are responsible for "mopping up" damaging substances called free radicals, which are produced both during normal metabolic processes and as a result of external insults from chemicals or radiation. Free radicals are thought to be linked to the aging process and chronic diseases, such as heart disease and arthritis. Cysteine is rarely taken as a dietary supplement. Instead, N-acetyl cysteine, a cysteine derivative, is the most frequently consumed form of this amino acid. Cysteine may also help strengthen the protective lining of the stomach and intestines. Cysteine's ability to boost the body's antioxidant defenses, particularly those of the liver, makes it an important detoxifying agent. N-acetyl cysteine is the medical treatment for paracetamol overdose, and has been studied in animals as a possible treatment for heavy metal poisoning from metals such as arsenic, cadmium, copper, gold, lead, mercury, and silver. Cysteine may be beneficial in cases of certain forms of respiratory disease, because it possesses both antioxidant and mucolytic (breaking up mucus) activities.

2.7.1.3 Glutathione

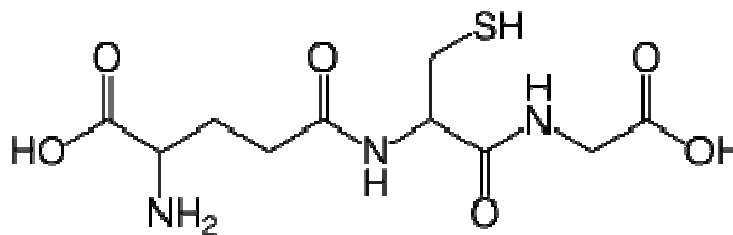


Figure 2.18 Structure of glutathione

Glutathione is a tripeptide composed of the three amino acids cysteine, glutamic acid, and glycine. Glutathione is found in every part of the body, especially the lungs, intestinal tract, and liver. The body produces and stores the largest amounts of GSH in the liver, where it is used to detoxify harmful compounds so that they can be removed from the body through the bile. The liver also directly supplies GSH to red and white blood cells in the circulation, thereby helping these cells stay healthy and maximizing their disease-fighting capabilities. Glutathione also appears to have anti-aging effects on the body. GSH levels decline with age, and a lack of glutathione has been shown to leave the body more vulnerable to damage from free radicals, thus speeding up cellular oxidation. A glutathione deficiency can have a devastating effect on the nervous system and can cause symptoms such as lack of balance and coordination, tremors, and other mental disorders. Any illness (even a bad cold), chronic disorders such as asthma and rheumatoid arthritis, injury, or heavy exposure to pollutants can cause a GSH deficiency. This is because the body uses GSH to support white blood cells and to rid the body of toxins.

2.7.2 Carbohydrates

Glucose is by far the most common carbohydrate in living systems and can be classified as a monosaccharide, an aldose, a hexose, or a reducing sugar. It is also known as dextrose, because it is dextrorotatory, which means that a pure solution rotates plane-polarized light to the right. Glucose is also commonly called blood sugar, because it circulates in the blood at a concentration of 65-110 mg/mL. Glucose is initially synthesized in plants from carbon dioxide in the air and sunlight as an energy source. Glucose is further converted to starch for storage. A blood glucose test measures the amount of glucose in one's blood. Glucose is typically ingested in the form of carbohydrate-containing foods, and it is the body's main energy source. Insulin is a hormone that helps your body's cells uptake and utilize glucose. Insulin is produced in the pancreas and released into the blood when the blood glucose levels rise.

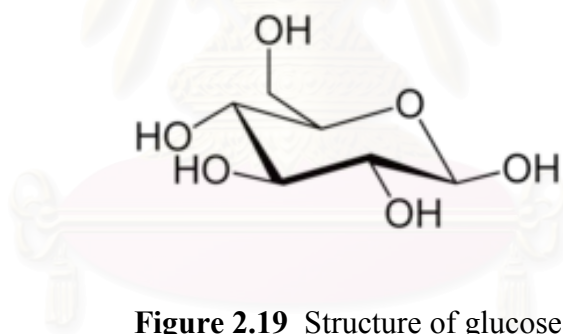


Figure 2.19 Structure of glucose

สถาบันวิทยบริการ
จุฬาลงกรณ์มหาวิทยาลัย

CHAPTER III

EXPERIMENTAL

This chapter has provided the information of instruments and equipments, apparatus, chemicals and reagents, and sample preparation employed in this work.

3.1 Instruments and equipments

The following were the list of instruments utilized in this work.

- 3.1.1 Analytical balance (AT 200, Mettler or TC 254, Denver Instrument Company) was used for weighing chemicals in the preparation of standard and reagent solution.
- 3.1.2 pH meter (755, Metrohm) was used to measure the pH of prepared buffer solutions.
- 3.1.3 Milli-Q water system (Millipore ZMQS 5 VOOY, Millipore, USA)
- 3.1.4 Homemade high-voltage power supply
- 3.1.5 Autolab Potentiostat (PG-30, Methrom) or Potentiostat, CHI812 (CH Instrument or CHI660b) was used to record the electrochemical response of analytes.
- 3.1.6 UV light source (Intella-ray 400) was used to expose the near UV light source in the photolithography process.
- 3.1.7 Air plasma cleaner (PDG-32G, Harrick plasma cleaner/sterilizer) was used to seal 2 pieces of PDMS together.
- 3.1.8 Sonicator (USA)
- 3.1.9 Auto pipette and tips were obtained from Eppendorf, Germany
- 3.1.10 Silicon wafer, 4 in. silicon wafers (Silicon, Boise, ID, USA)
- 3.1.11 Microscope (SZ-PT, Olympus, Japan)
- 3.1.12 Centrifuge, CENTAURA 2, (Sanyo)

3.2 Apparatus for microchip capillary electrophoresis

The details of the integrated CE-EC PDMS microchip system were described previously [32]. Briefly, the homemade high voltage power supply had an adjustable voltage range between 0 and +4000 V [173]. The microchip had the double-T injector (50 μ M deep, 50 μ M wide, 5.1 cm long separation channel), the working electrode channel (50 μ M deep x 50 μ M wide) and decoupler electrode channel (50 μ M deep x 50 μ M wide, 50 μ M gap to separation channel). The double-T injector had a volume of 250 pL.

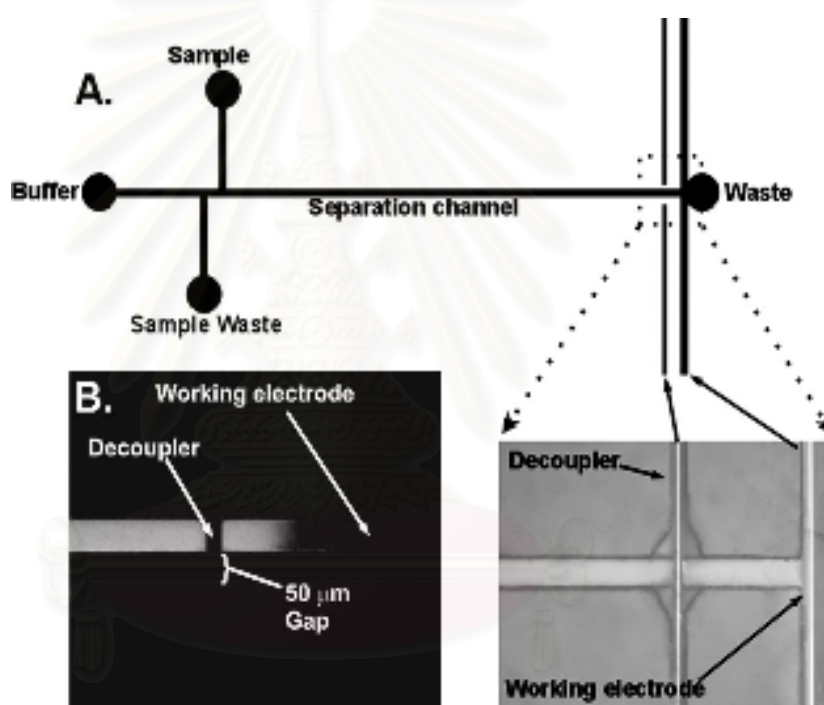


Figure 3.1 (A) Schematic of the microchip (50 μ m deep, 50 μ m wide, 5.1 cm long separation channel) showing placement of the electrode alignment channels. Working electrode channel (50 μ m deep, 50 μ m wide). Decoupler electrode channel (50 μ m deep x 25 μ m wide, 50 μ m gap to separation channel). Double-T injector (50 μ m x 50 μ m x 100 μ m) has a volume of 250 pL. Lower right is a photograph showing electrode alignment in a completed microchip. Left electrode is Pd microwire while the right electrode is the Pt working electrode. (B) Decoupled microchip.

Fluorescent image of 1 mM FITC as it passes the decoupler. No sample leakage was observed around the Pd microwire. Dotted lines indicate the outline of the channels in the PDMS [32].

3.3 Chemicals and reagents

All chemicals were of analytical grade or better and were used without further purification. Deionized-distilled water obtained from a Milli-Q-system was used for the preparation of chemical and reagent solutions. List of chemicals and their suppliers was summarized in Table 3.1

Table 3.1 List of chemical and reagents and their suppliers

Chemicals/Reagents	Formular	Suppliers	Country
Dopamine hydrochloride	$C_6H_{11}NO_2HCl$	Sigma	USA
Catechol	$C_6H_6O_2$	Sigma	USA
Homocysteine	$C_4H_9NO_2S$	Sigma	England
Cysteine	$C_3H_7NO_2S$	Sigma	USA
L-Cystine	$C_6H_{12}N_2O_4S_2$	Sigma	USA
Glutathione	$C_{10}H_{17}N_3O_6S$	Sigma	USA
N-acetyl-L-cysteine	$C_5H_9NO_3S$	Sigma	USA
Dextose	$C_6H_{12}O_6$	Fisher	USA
N-Tris(hydroxymethyl)methyl-2-aminoethanesulfonic acid (TES)	$C_6H_{15}NO_6S$	Sigma	USA
2-morpholinoethanesulfonic acid monohydrate (MES)	$C_6H_{13}NO_4S \cdot H_2O$	Sigma	USA
Boric acid	H_3BO_3	Sigma	USA
Trichloroacetic acid (TCA)	CCl_3COOH	Merck	Germany
5-sulfosalicylic acid dihydrate	$C_7H_6O_6S \cdot 2H_2O$	Sigma	USA
Ascorbic Acid	$C_6H_8O_6$	Sigma	USA

Table 3.1 List of chemical and reagents and their suppliers (Cont.)

Chemicals/Reagents	Formular	Suppliers	Country
Methanol	CH ₃ OH	Merck	Germany
Tris(2-carboxy-ethyl) phosphine hydrochloride (TCEP)	C ₉ H ₁₅ O ₆ P·HCl	Sigma	USA
Sodium hydroxide	NaOH	Fisher	USA
Hydrochloric acid	HCl	Merck	USA
Potassium Dihydrogen Orthophosphate	KH ₂ PO ₄	BDH	England
Phosphoric acid	H ₃ PO ₄	Merck	USA
SU-8 2035 photoresist	-	Micro Chem.	USA
Propylene glycol methyl ether acetate	C ₆ H ₁₂ O ₃	Aldrich	USA
4-in. silicon wafer	-	Silicon Inc.	USA
Silicone elastomer base	-	Dow Corning Corporation	USA
Silicone elastomer curing agent	-	Dow Corning	USA
TPE mixing resin	-	TAP Clear-Lite Casting Resin	USA
Styrene	C ₆ H ₅ CH=CH ₂	Sigma	USA
UV photoinitiator (2,2- dimethoxyphenylacetophenone)	C ₁₆ H ₁₆ O ₃	Sigma	USA
Methyl Ethyl Ketone Peroxide (MEKP)	C ₄ H ₁₀ O ₄	Sigma	USA
poly(ethyleneimine), (PEI)	(-CH ₂ CH ₂ NH-) _n	Polysciences, Inc.	USA
poly(acrylic acid), (PAA)	-	Polysciences, Inc.	USA
polyallylamine hydrochloride, (PAH)	[-CH ₂ CH(CH ₂ NH ₂ HCl)-] _n	Polysciences, Inc.	USA

Table 3.1 List of chemical and reagents and their suppliers (Cont.)

Chemicals/Reagents	Formular	Suppliers	Country
dextran sulfate, (DS)	$(C_6H_9O_5SO_3Na)_{n+1}$	Polysciences, Inc.	USA
Polybrene, (PB)		Polysciences, Inc.	USA
Hexamethyldisilazane (HMDS)	$C_6H_{19}NSi_2$	Sigma	USA
Sodium dodecyl sulfate (SDS)	$C_{12}H_{25}O_4S Na$	Sigma	USA
Gold 99.9%, diameter 25 μ M	Au	Good fellow	England
Palladium 99.9%, diameter 25 μ M	Pd	Good fellow	England

3.4 Preparation of solutions

Included in the following parts are the preparation procedures for the supporting electrolyte and the standard solutions employed in this work.

3.4.1 Preparation of 20 mM TES buffer pH 7.2

TES (1.146 g) was dissolved in deionized water. The resulting solution was adjusted to the required pH with either 0.1 M sodium hydroxide or 0.1 M hydrochloric acid and diluted to 250 mL total volume with deionized water in a volumetric flask.

3.4.2 Preparation of 20 mM MES buffer pH 6.5

MES (0.4265 g) was dissolved in deionized water. The resulting solution was adjusted to the required pH with either 0.1 M sodium hydroxide or 0.1 M phosphoric acid, and was diluted to 250 mL total volume with deionized water in a volumetric flask.

3.4.3 Preparation of 20 mM boric acid buffer pH 9.4

Boric acid 0.3092 g was dissolved and diluted with deionized water and then adjust with 0.1 M sodium hydroxide to the required pH and finally adjust the volume with deionized water into 250 mL volumetric flask.

3.4.4 Preparation of 20 mM boric acid with 20 mM SDS buffer pH 9.4

Boric acid (0.3092 g) and SDS (1.1419 g) were diluted with deionized water and the resulting mixture was stirred until the all components had dissolved. The solution was adjusted to pH 9.4 and diluted to 250 mL total volume with deionized water in a volumetric flask.

3.4.5 Preparation of 25 mM potassium dihydrogenorthophosphate pH 3.0

Potassium Dihydrogenorthophosphate (0.8506 g) was dissolved in deionized water in 250 mL volumetric flask. The solution was adjusted to pH 3.0 with 0.1 M hydrochloric acid.

3.4.6 Preparation of stock standard solution of dopamine

The 10 mM dopamine standard solution was prepared by dissolving dopamine hydrochloride (0.0190 g) in 10 mL of 0.1 M hydrochloric acid.

3.4.7 Preparation of stock standard solution of catechol

The 10 mM catechol standard solution was prepared by dissolving pyrocatechol (0.0110 g) in 10 mL of 0.1 M hydrochloric acid.

3.4.8 Preparation of stock standard solution of carbohydrate

Dextrose (0.0180 g) was dissolved in 10 mL of electrolyte solution using a 10 mL volumetric flask.

3.4.9 Preparation of stock standard solution of thiol compounds

The stock standard solution of thiol compounds was prepared by dissolving the appropriate amounts of the thiol compounds in 10 mL of 25 mM potassium dihydrogen orthophosphate buffer pH 3.0. The weight of each compound is given in Table 3.2.

Table 3.2 Weight of thiol compounds for preparation of stock standard solution

Thiol compounds	Weight (g)
homocysteine	0.0135
cysteine	0.0121
glutathione	0.0307
L-cystine	0.0238
N-acetyl-cysteine	0.0632

3.4.10 Preparation of carbohydrate and thiol compounds for calibration

Standard solutions of carbohydrate and thiol compounds with various concentrations were prepared for calibration purposes. The appropriate amounts of the 10 mM stock standard solutions were dissolved in 20 mM boric acid buffer solution in 1000 μ L microcentrifuge tube.

3.5 Microchip fabrication

3.5.1 Method for making a mold

Silicon masters were fabricated in accordance with previously published techniques [2]. Briefly, SU-8 2035, a negative photoresist, was spin coated onto a 100 mm silicon wafer (100.Silicon, Boise, ID, USA) to a thickness of 50 μ m. A digitally printed mask was used to define channel structures. After exposure and development, patterned silicon masters were treated with hexamethyldisilazane

(HMDS) by vapor deposition to aid in the removal of both the TPE and the PDMS. Vapor deposition was performed by placing the wafer and a small vial containing 500 mL of HMDS into a crystallization dish. The dish was then covered with foil and placed in a 657°C oven for 4–6 hours. PDMS walls and posts were used to define the molding area and to create reservoirs in the TPE devices.

3.5.2 Fabrication of PDMS devices

All experiments were performed using poly(dimethylsiloxane) (PDMS) microchips fabricated in accordance with established protocols [54, 174-176]. Briefly, a silica wafer was cleaned with a dilute solution of HF in water (1:10). The wafer was spin coated with SU-8 2035 negative photoresist, and a master mold was fabricated using a digitally printed mask. Once the master was completed, replica molding was used to create channels in PDMS. In this procedure, a degassed 10:1 mixture of Sylgard 184 elastomer and curing agent was poured onto both the mold master and a blank silica wafer and allowed to cure at 65°C for 2 hr. The cured PDMS was removed from the molds, and reservoirs were punched using a standard 6mm hole punch [174]. The surfaces of the two pieces of PDMS were cleaned with methanol and placed in an air plasma cleaner (Harrick) for 45 s at 18 W. The two pieces of PDMS were then immediately brought into conformal contact to form an irreversible seal. The assembled chip was preconditioned before use each day by rinsing it for 30 min with 1 M NaOH.

3.5.3 Fabrication of TPE devices

TPE was prepared by mixing resin (TAP Clear-Lite Casting Resin) with additional styrene, UV photoinitiator (2,2-dimethoxyphenylacetophenone), and MEKP catalyst, in accordance with published protocols [29]. Approximately 0.2 g of photoinitiator was dissolved in 0.5 g of styrene before being added to 20 g of resin. Six drops of MEKP catalyst were then added, and the mixture was stirred and degassed in a vacuum desiccator. After degassing, the TPE resin was poured onto the prepared master mold and either transparency film or a glass microscope slide was used to cover the TPE. The cover material was allowed to make contact with the TPE

mixture in order to ensure a flat top surface during UV curing. The glass cover slides were treated with HMDS to facilitate their removal from the cured TPE. TPE was partially cured by UV radiation with a UV flood lamp (364 nm) (Inteli-ray 400) at 50% power for 100 s. The TPE was then carefully separated from the mold while still slightly soft, and the PDMS posts were removed to expose the reservoirs. Microwire electrodes were placed in the designated electrode channels located at the end of the separation channel in accordance with previously published work with PDMS microchips [31, 32]. Care was taken while inserting the microwires, because TPE is easily scratched, torn, or otherwise damaged when not fully cured. Next, a blank, flat piece of TPE was prepared in the same manner with a UV exposure of 100 s. The two pieces were then placed together to form the microchannels. A final set of four 30-second UV exposures separated by 90-second cooling periods was applied to bond the two pieces together and to complete TPE curing. The chip was placed on a hot plate at 65°C for 30 min and then transferred to a 120°C hot plate for 90 min for final curing. Some microchips were subjected to plasma oxidation to study the effects on EOF. Plasma oxidation was performed for 20 min (Harrick plasma cleaner/sterilizer PDG-32G, Ithaca, NY, USA) at a 10.5 W power setting. The success rate for microchip fabrication was generally greater than 75%. Figure 1 shows a schematic of the microchip design and an enlarged picture of the detection electrodes in a fully assembled TPE microchip.

3.6 Successive multiple ionic layer (SMIL) coatings or polyelectrolyte multilayer (PEM) coatings

Capillaries were coated with polyelectrolyte multilayer coatings (PEMs) in accordance with the procedures reported by Dai *et al.* [177]. One of the following cationic polyelectrolytes was used: polybrene (PB), poly(ethyleneimine) (PEI), or poly(allylamine) hydrochloride (PAH). The anionic polyelectrolyte was either (poly(acrylic acid) (PAA) or dextran sulfate (DS)). In brief, the channel was rinsed with 1.0 M NaOH for 30 min and then filled for 5 min with the cationic polyelectrolyte solution. After rinsing the channel with water for 1 min, the channel was coated with the negatively charged polymer for 5 min and then rinsed with water for 1 min. These steps, with the exception of the initial NaOH rinse, were repeated

forming alternating layers of anionic and cationic polymers until the desired layer thickness was reached. All polyelectrolyte solutions were 3% polyelectrolyte (w/v) in either deionized water or 0.5 M aqueous NaCl. Rinsing was performed by applying vacuum pressure from a water aspirator or laboratory syringe at the channel waste outlet.

3.7 Electroosmotic flow measurements

The current monitoring method developed by Huang *et al.* was used to measure EOF [178, 179]. The polarity of the power supply was chosen such that EOF operated through a straight channel connecting two reservoirs (reservoirs 1 and 2). The channel and reservoir 2 were filled with 20 mM phosphate buffer, while reservoir 1 was filled with 18 mM phosphate buffer. When voltage was applied, some of the 18 mM phosphate buffer in reservoir 1 migrated into the channel and displaced an equal volume of 20 mM phosphate buffer. Consequently, the electrical resistance of the fluid in the channel changed, and these changes could be measured by recording the separation current, I_{sep} , during the experiment. A 1.0 k Ω resistor was inserted between the electrode in reservoir 2 and electrical ground. The choice of a 1.0 k Ω resistor meant that a 1- μ A current change produced a 1-mV drop in potential across the resistor. A multimeter (Fluke, Model 189) was used to monitor the voltage drop across the resistor. The time required for the current to plateau was measured and was indicative of the lower-concentration buffer filling the entire separation channel. Reservoir 1 was then filled with concentrated buffer, the potential was reapplied, and the time to reach a current plateau was measured. Six to eight consecutive measurements were obtained for each experiment. The time required for the current to reach this plateau was used as the neutral marker, and the EOF was calculated from the following equation:

$$\mu_{EOF} = L^2 / (Vt) \quad (\text{Equation 3.1})$$

where L is the length of the separation channel (4.4 cm), V is the total applied voltage (900 V), and t is the time (in seconds) required to reach the new current

plateau. This is a modification of the traditional mobility equation [54] that takes into account that the total and effective channel lengths are identical.

3.8 Procedures of microchip CE

3.8.1 Microchip CE with amperometric detection

3.8.1.1 Microchip CE layout

The microchip CE system used in this work is depicted in figures 3.2 and 3.3. Each system was comprised of a PDMS microchip, a microfluidic flow system, a high voltage power supply, and an electrochemical detector.



Figure 3.2 The microchip capillary electrophoresis with electrochemical detection layout.

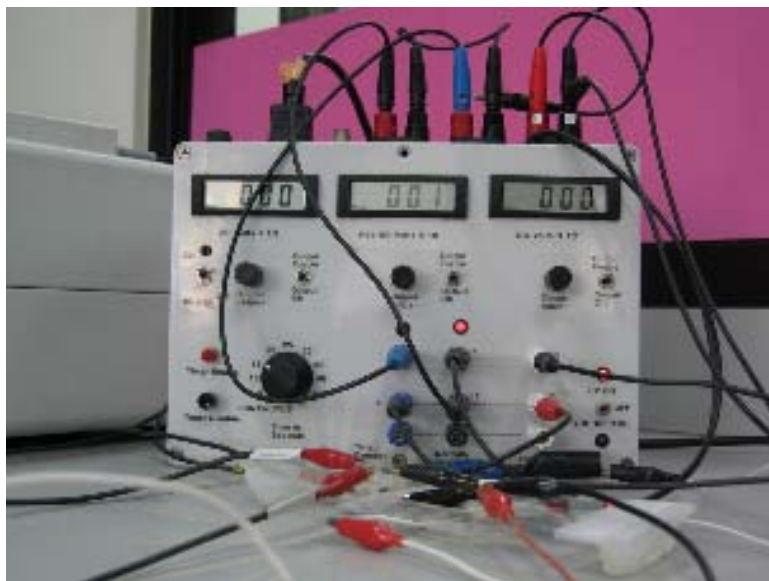


Figure 3.3 The microchip capillary electrophoresis with electrochemical detection layout.

3.8.1.2 Electrophoresis procedure

Pinched injection through a double-T injector was employed in these experiments [31, 180, 181]. The injection volume was 250 pL. The channels were pretreated with sodium hydroxide for at least 30 min in order to give the channel walls a net negative charge. The channels and reservoirs were filled with buffer solution. Before analysis, the sample and sample waste reservoirs were filled with sample solution. The microchip was designed with the two electrode channels spanning the separation channel in order to incorporate the decoupler and a working electrode [174]. A Pd microwire cathode was placed in the first electrode channel (25 μm wide) (Figure 3.4). The working electrode was placed downstream in the second electrode channel (Figure 3.4). The distance between the two electrodes was fixed at 250 μm based on previous work by Lacher *et al.* The fully-assembled microchips were allowed to equilibrate for 24 h before use in experiments. This was done to allow the EOF of plasma-sealed chips to decrease to a stable level. The typical lifetime of these devices is 1–2 weeks, but a new microchip was used every day of experimentation. For separations, 800–1500 V was applied across the buffer reservoirs while the Pd microwire decoupler was kept at ground. The sample and waste reservoirs were held at 450 V for push back.

3.8.1.3 Electrochemical detection

Amperometric detection and pulsed amperometric detection PAD were used to measure electrochemically-active analytes in accordance with a previously published chip design [31, 174]. Amperometry was used to detect dopamine, catechol, and ascorbic acid. PAD was used to detect carbohydrates and thiols. Both amperometry and PAD were conducted using a commercially available potentiostat (CHI812 or CHI660b, CH Instruments or PG-30, Methrom). For amperometry, a constant potential of 0.8 V was applied to the working electrode. The PAD waveform had a cleaning/oxidation potential of 1.6 V for 0.05 s, a reduction/regeneration potential of 20.5 V for 0.025 s, and a detection potential of 0.6 V for 0.15 s.

Amperometry and PAD experiments were run in a two-electrode configuration with a Pt wire (1.6 mm diameter) serving as the counter electrode in all cases. A gold microwire (25 μ m) was placed in the microfluidic devices and used as the working electrode. Initial cleaning and conditioning of the Pd decoupler was performed by running cyclic voltammetry (CV) from 21.0 to 1.0 V at 0.1 V/s for 50 cycles. Initial cleaning of the working electrode was performed by running CV from 21.0 to 1.0 V at 0.1 V/s until six sweep segments overlapped with each other. While conducting amperometry, the working electrode was cleaned every 15 runs via 20 sweep segments of CV run from 21.0 to 1.0 V at 0.1 V/s whilst buffer was flowed over the electrode [174].

สถาบันวิทยบริการ
จุฬาลงกรณ์มหาวิทยาลัย

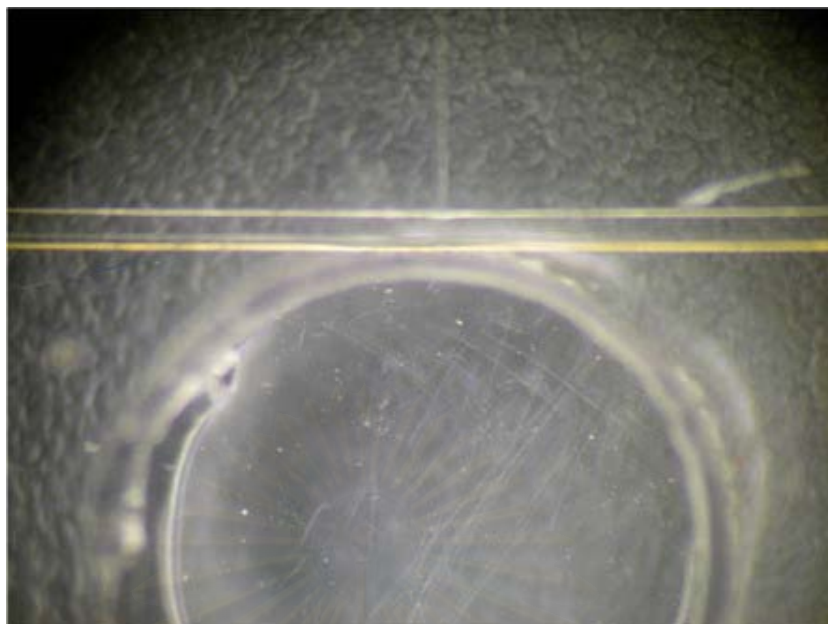


Figure 3.4 A photograph showing electrode alignment in a completed microchip.

3.8.1.4 Safety consideration

The high voltage power supply and associated open electrical connections should be handled with extreme care to prevent electrical shock. Metal ions can be toxic, irritating, and/or dangerous for the environment and should be handled in a fume hood. Accidental skin or eye contact and accidental inhalation or ingestion should be avoided. The stock solutions must be stored in small, sealed glass containers and isolated from any reducing reagents. These metals are toxic and potentially carcinogenic and/or mutagenic, and so special care must be taken to dispose of waste solution.

3.8.1.5 Microchip CE optimization conditions

The experimental conditions for microchip CE with electrochemical detection were optimized. The operational parameters, including separation voltage, injection time, pH of BGE, concentration of BGE, SDS concentration, and PAD waveform, were considered. Optimization was performed by changing a single variable while holding all other variables constant until the optimal

result was achieved. The current response, migration time, resolution, and separation efficiency were the optimized outputs.

3.8.1.6 Calibration and linear range

10 mM stock solutions of each analyte were freshly prepared and then samples were diluted to final concentrations ranging from 1 pM to 500 μ M. In these experiments, each concentration of analyte was measured five times. The results were used to plot a calibration curve and to determine the linear detection range.

3.8.1.7 Limit of detection

The limit of detection was investigated by testing analyte solutions five times each at the optimal potential. The system detection limit (SDL) was defined as the lowest concentration of an analyte, when processed through an entire analytical method, produces a signal that is statistically distinct from the signal arising from field blanks.

3.8.1.8 Precision

The precision was studied by injecting twenty replicates of each analyte solution. Precision was assessed in terms of the relative standard deviation (%RSD) using the following formula:

$$\% \text{ RSD} = \frac{\text{standard deviation}}{\text{Mean}} \times 100$$

3.8.2 Plasma sample analysis

The thiol concentrations of plasma samples are known to decrease exponentially over time when the samples are kept at room temperature [182]. Unfortunately, routine storage of frozen plasma samples does not prevent thiol concentrations from dropping to near 0 within a few weeks. In contrast, if plasma is deproteinized within 1 hour of blood collection, the thiols in the frozen deproteinized supernatant remain stable for months.

3.8.2.1 Standard thiol compounds and plasma sample preparation

Each thiol stock solution was removed from storage at -20°C and allowed to warm to room temperature (approx. 20 min). The standard solutions were diluted to the desired concentrations in 20 mM boric acid buffer pH 9.0 with 20 mM SDS and 2.5 mM TCEP. An excess of TCEP was used to ensure complete reduction of the thiols. Human plasma samples were obtained from the Prasat Neurological Institute. Samples were deprotonized by addition of an equal volume of 20 % solution of trichloroacetic acid (TCA) in the buffer that was used to prepare the relevant standard solutions. This mixture was incubated at 4°C for 30 min and the centrifuged. The resulting supernatant was collected and its glucose and thiol compound concentrations were assayed using the MCE-EC systems. All plasma samples were either analyzed within 2 hours of being drawn or were frozen at -20°C for future studies.

สถาบันวิทยบริการ
จุฬาลงกรณ์มหาวิทยาลัย

CHAPTER IV

RESULTS AND DISCUSSION

In this chapter, details will be separated into three parts. The first part contains the results and discussion from PDMS microchip experiments in which the concentrations of carbohydrate and thiol compounds in human plasma samples were measured via MCE-EC. The second part focuses on the modification of PDMS microchips with polyelectrolyte coatings to improve flow control and separation efficiency. The last part investigates microchips fabricated from TPE rather than PDMS. A similar set of experiments was conducted with these TPE microchips in which the concentrations of carbohydrate and thiol compounds in human plasma were measured, and the results were compared to those from the PDMS microchip experiments.

4.1 PDMS microchip capillary electrophoresis/electrochemistry

4.1.1 Microchip capillary electrophoresis characterization

The amperometric detection was used during characterization of microchip CE systems. Dopamine and catechol were chosen as standard analytes to demonstrate the microchip CE system's performance.

A solution of 500 μM dopamine and 500 μM catechol was separated on a PDMS microchip (Figure 4.1). The separation was performed using 20 mM TES (pH 7.2) as the background electrolyte (BGE) at the separation potential of 1100 V with a 15 s injection. Baseline resolution of two compounds was observed. The migration times for dopamine and catechol were 32 and 57 s, respectively. This first example demonstrated the basic performance of prepared PDMS microchip systems.

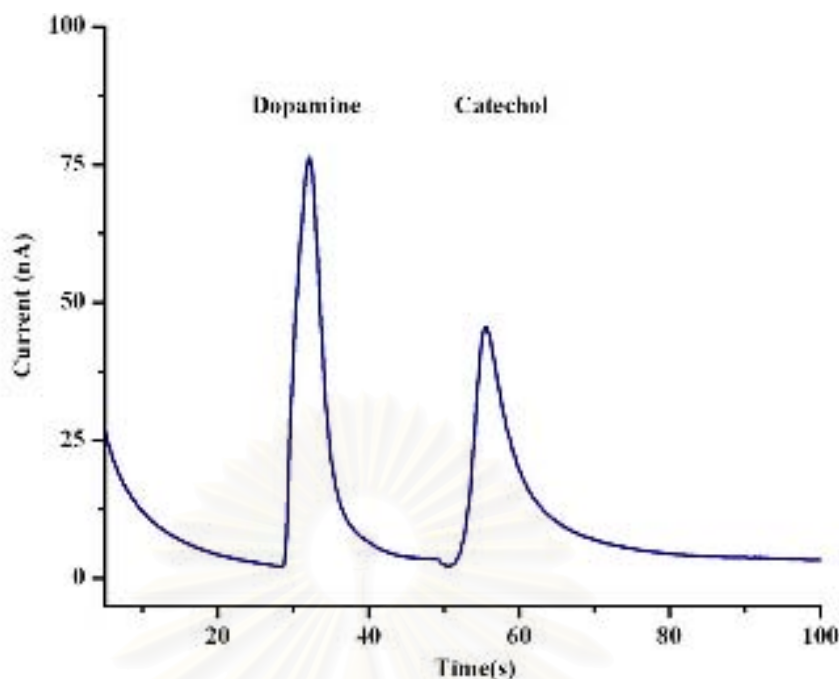


Figure 4.1 Electropherogram of the separation of dopamine and catechol. Experimental parameters: 500 μM dopamine and 500 μM catechol, TES (pH 7.2) running buffer, separation potential 1100 V, detection potential 0.8 V, pinched injection time 15 s, working electrode: 25 μm Au wire.

4.1.2 Capillary electrophoresis optimization

4.1.2.1 Influence of separation voltage

The separation voltage affects the electric field strength, which, in turn, affects the EOF and the migration velocities of the charged particles within the capillary and ultimately determines the migration time of the analytes. The electrochemical response was based on the coupling of the electric field for separation and the electrochemical detector, so optimizing separation voltage was needed to improve detection sensitivity. In addition, higher separation voltages result in higher joule heating. The same solution of dopamine and catechol was again separated on a PDMS microchip using 20 mM TES (pH 7.2) running buffer at a variety of separation potentials (Figure 4.2). As the separation potential was increased, the migration times decreased.

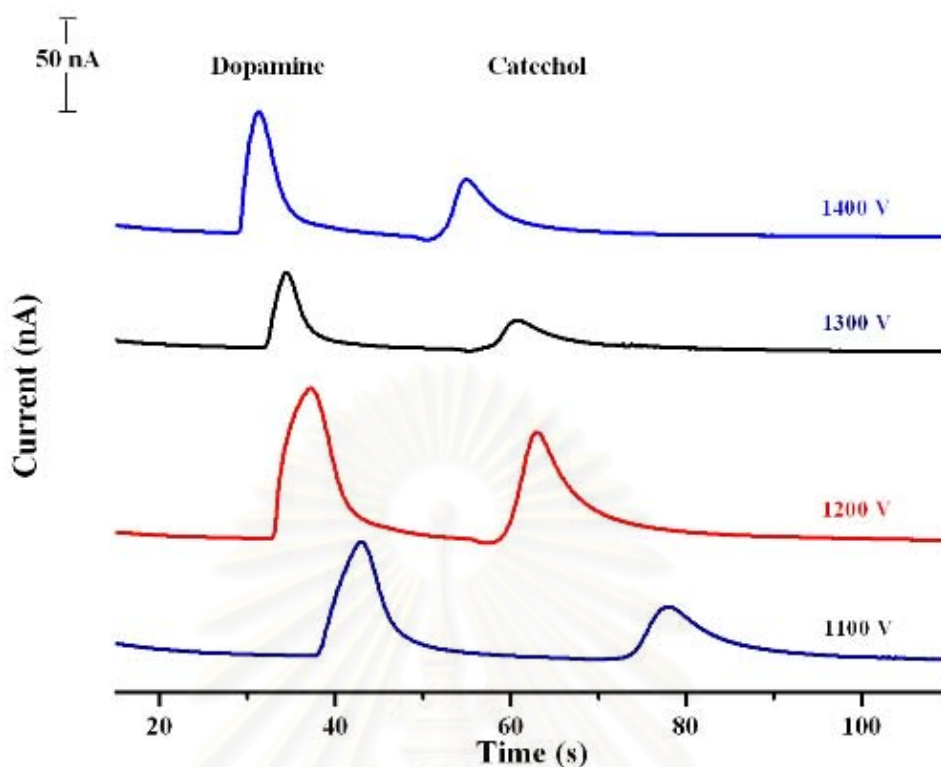


Figure 4.2 Separation of a solution of 500 μM dopamine and 500 μM catechol as a function of separation voltage (1000 – 1400 V). Experimental conditions: pinched injection time 15 s, detection voltage 0.8 V, BGE 20 mM TES (pH 7.2).

The effect of separation voltage on the migration time of the analytes is shown in Figure 4.3. The effect of the potential applied to the separation channel was studied in the 1000 – 1600 V range (Figure 4.3). Higher separation voltage yielded shorter migration times but also increased the baseline noise (e.g. 1.8 ± 0.6 nA at 1500 V for homocysteine) and the formation of bubbles (due to Joule heating). Therefore, 1400 V was selected as the optimum separation voltage at which the separation of carbohydrate and thiol compounds was achieved in less than 80 s with a baseline noise of 0.5 ± 0.1 nA (peak-to-peak).

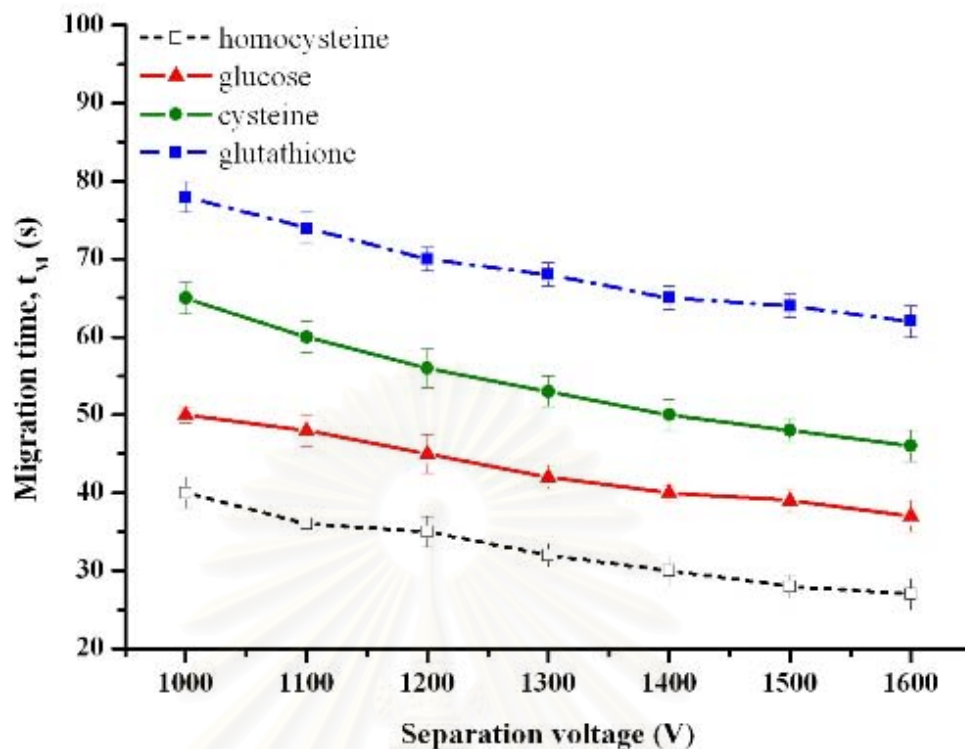


Figure 4.3 Effect of separation voltage on the migration times of 100 μM homocysteine (\square), glucose (\blacktriangle), cysteine (\bullet), and glutathione (\blacksquare). Experimental conditions: pinched injection time 15 s, detection voltage 0.8 V, BGE 20 mM boric acid (pH 9.0).

4.1.2.2 Influence of injection time

After determining the appropriate electrical biasing conditions, the length of time required for sample injection was investigated. The injection time affects the sample volume, and also affects the peak current and peak shape. Injection time was varied between 15 and 25 s, and the aforementioned mixture of dopamine and catechol was separated using the optimal conditions for analysis (BGE 20 mM TES (pH 7.2), separation potential of 1400 V, detection voltage of 0.8 V). The mixture of carbohydrate and thiol compounds was separated using the optimal conditions for analysis (BGE 20 mM boric acid (pH 9.0), separation potential 1400 V, detection voltage 0.8 V). The injection time affects the sample volume, also affects the peak current and peak shape. A significant increase in the peak current was observed in the 10 – 15 s range. This can be explained that the

double-T injector (see Figure 3.1) is filled in only less than 10 s. If injection time was more than 15 s, the response was increased slightly. For that reason, 15 s was selected as the optimal injection time.

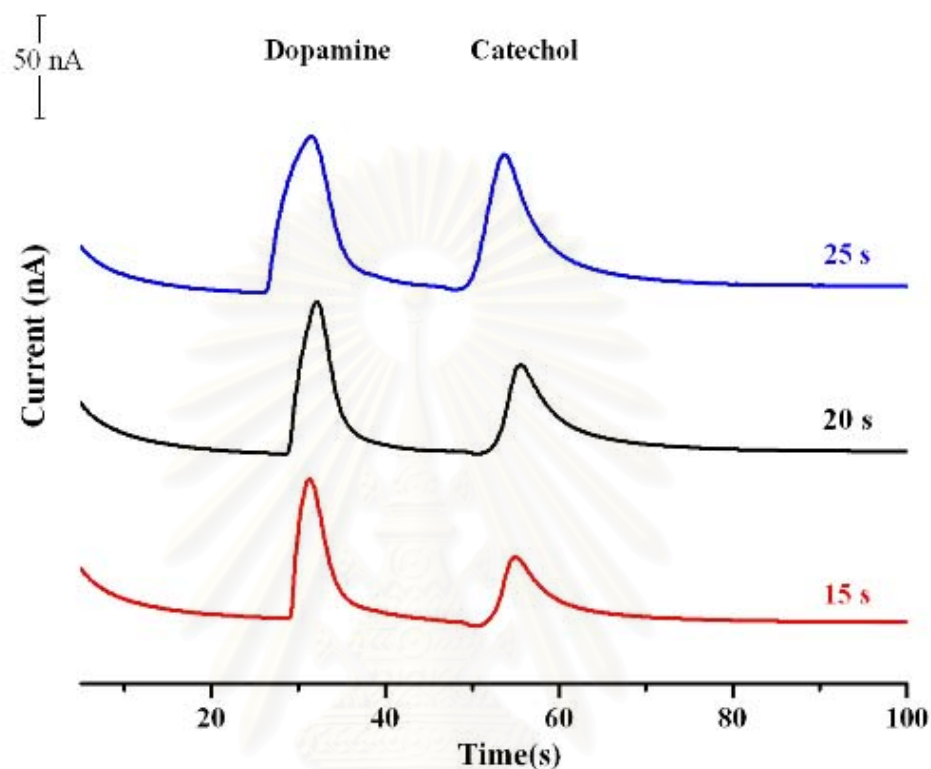


Figure 4.4 Electropherograms of a solution of 500 μM dopamine and 500 μM catechol separated with injection times from 15-25 s. Experimental conditions: separation voltage 1400 V, detection voltage 0.8 V, BGE 20 mM TES (pH 7.2).

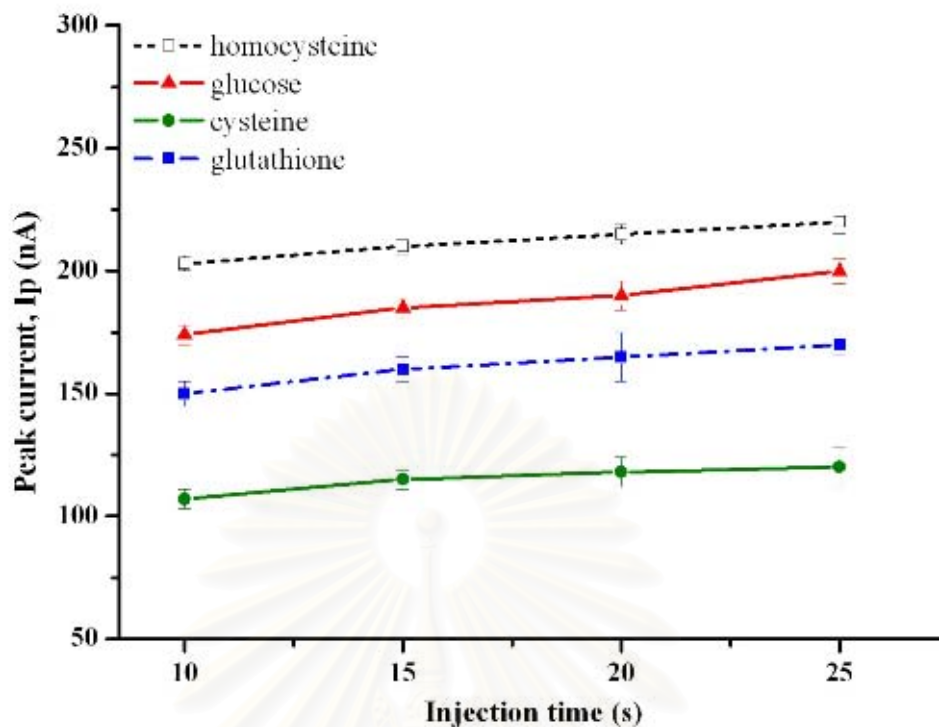


Figure 4.5 Effect of injection time on peak currents of 100 μM homocysteine (\square), glucose (\blacktriangle), cysteine (\bullet), and glutathione (\blacksquare). Experimental conditions: separation voltage 1400 V, detection voltage 0.8 V, BGE 20 mM boric acid (pH 9.0).

4.1.2.3 Influence of background electrolyte pH

One of the most important variables in CE is the pH of the BGE, because pH affects the migration time, the separation of the analytes, and the EOF. The effect of running buffer pH on the migration times of glucose and thiol compounds was investigated between pH 7.5 and 9.5 using 20 mM boric acid solution as the BGE. Almost all the glucose and thiol compounds were separated over the entire pH range tested (Figure 4.6). More specifically, it was reported the pKa values of the selected thiol compounds were around 2.5 (deprotonation of the carboxyl group) and 9.0 (deprotonation of the amino group). This implies that at $\text{pH} > 9.0$, both the carboxyl group and amino groups were dissociated allowing the separation by the electric field. Longer migration times were observed at higher pH values. Therefore, in order to maximize the separation of the analytes, pH 9.0 was selected as the optimal value and used for all subsequent experiments.

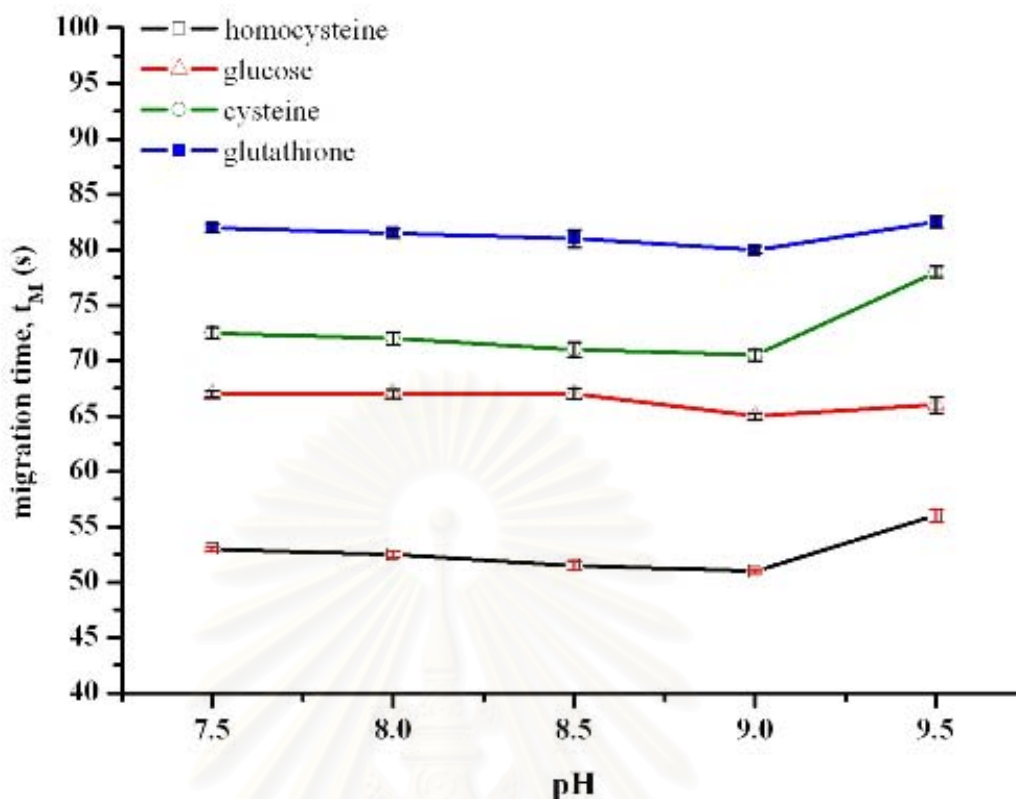


Figure 4.6 Effect of BGE pH on the migration times of homocysteine 100 μM (\square), glucose (\triangle), cysteine (\circ), and glutathione (\blacksquare). Experimental conditions: separation voltage 1400 V, pinched injection time 15 s, detection voltage 0.8 V.

4.1.2.4 Influence of background electrolyte concentration

In order to study the effect of BGE (boric acid) concentration on the separation of and detector response to glucose and the thiol compounds, BGEs containing 10, 20, and 30 mM boric acid (pH 9.0) were prepared. Higher buffer concentrations resulted in longer migration times with no change in migration order (Figure 4.7a). Buffer concentration had negligible effects on the migration time of the analytes. The peak current of glucose and thiol compounds increased when buffer concentrations were increased from 10 to 20 mM, but peak current decreased with further increases in buffer concentration (Figures 4.7b). Separation efficiency and analysis time were considered, and 20 mM boric acid was selected as the optimal BGE concentration.

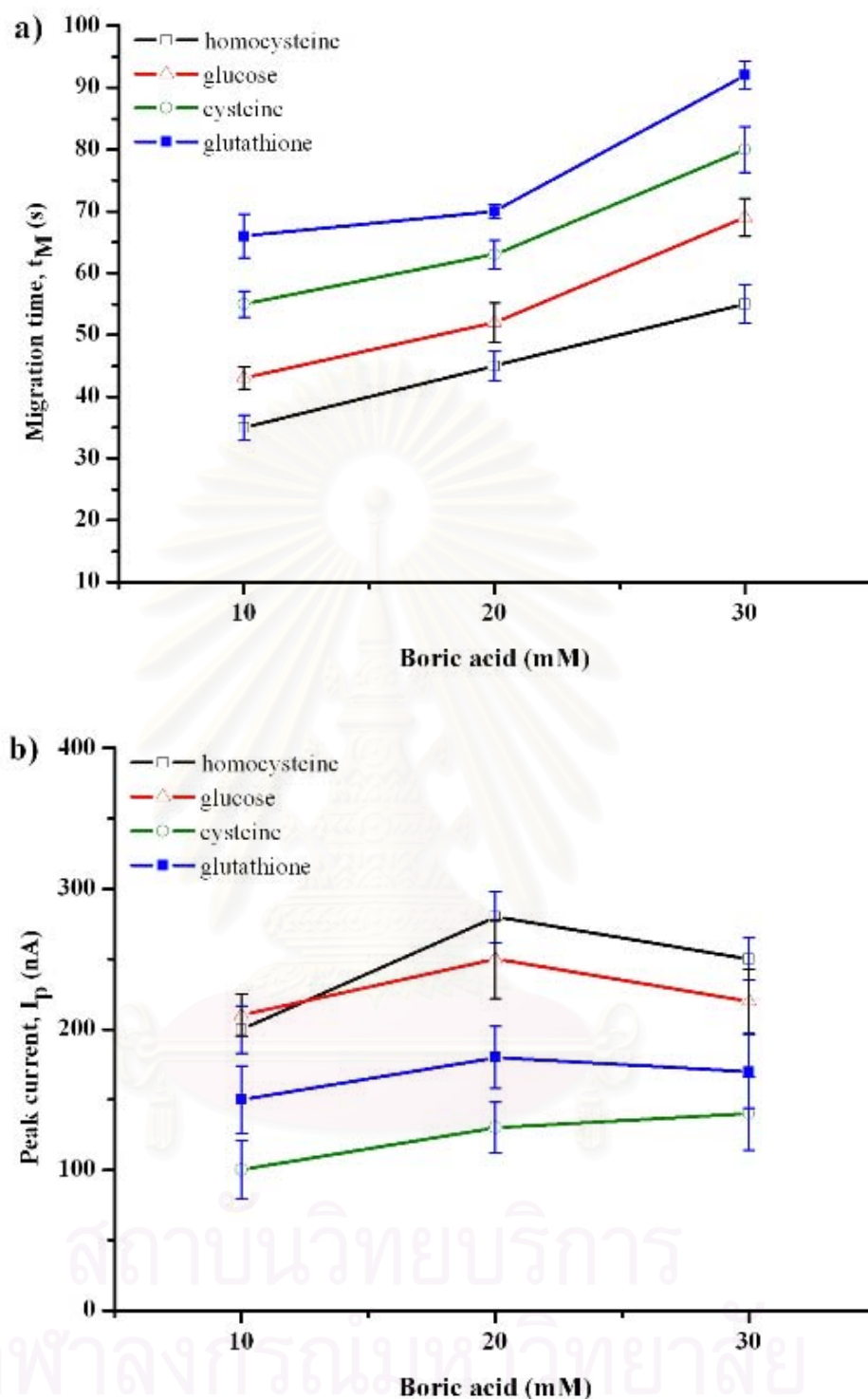


Figure 4.7 (a) Effect of BGE concentration (boric acid pH 9.0) on the migration times of 100 μ M homocysteine (□), glucose (△), cysteine (○), and glutathione (■). Experimental conditions: separation voltage 1400 V, pinched injection time 15 s, detection voltage 0.8 V. (b) Effect of BGE concentration on peak currents of 100 μ M homocysteine (□), glucose

(Δ), cysteine (\circ), and glutathione (\blacksquare). Experimental conditions: separation voltage 1400 v, pinched injection time 15 s, detection voltage 0.8 V.

4.1.2.5 Influence of SDS concentration

Using 20 mM boric acid (pH 9.0) running buffer, the effect of SDS concentration on the separation of thiol compounds was investigated (Figure 4.8). Different behavior was observed when the concentration of surfactant was varied from 10–30 mM. When SDS concentration was increased from 10 mM to 20 mM, an increase in the analysis time was observed. This behavior was attributed to both the increase in buffer ionic strength and the increased interaction between the analytes and detergent micelles accompanying higher SDS concentrations. At 30 mM SDS, the three thiol compounds were separated, but tailing of the homocysteine peak was observed. Thus, 20 mM SDS was chosen as the optimal condition with regards to analyte resolution.

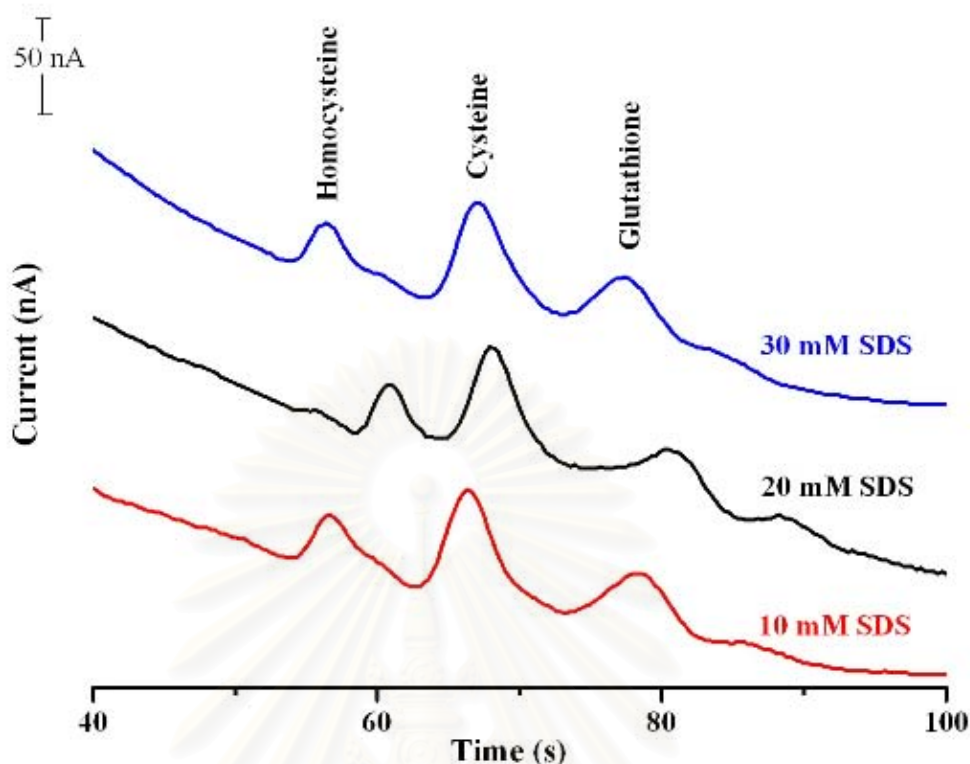


Figure 4.8 Electropherograms of thiol compounds separated using boric acid (pH 9.0) running buffer containing SDS concentrations from 10 – 30 mM. Experimental conditions: separation voltage 1400 V, pinched injection time 15 s, detection voltage 0.8 V.

4.1.2.6 Influence of the PAD wave form

The amperometric detection of carbohydrates and thiol compounds at the gold electrode at constant electrode potential was not adequate, because adsorbed reaction products and/or oxide films accumulated at the electrode surface. Pulsed amperometric detection (PAD), in which a three-potential waveform is applied to the working electrode, can overcome this problem by ensuring each detection step is performed on a fresh electrode surface. Since these potentials directly affect the sensitivity, detection limit, and stability, the effect of the PAD waveform on the response of the analytes, measured in terms of the peak current, was investigated. The effect of detection potential on the peak current (hydrodynamic voltammograms) during glucose detection was examined (Figures 4.10 and 4.12).

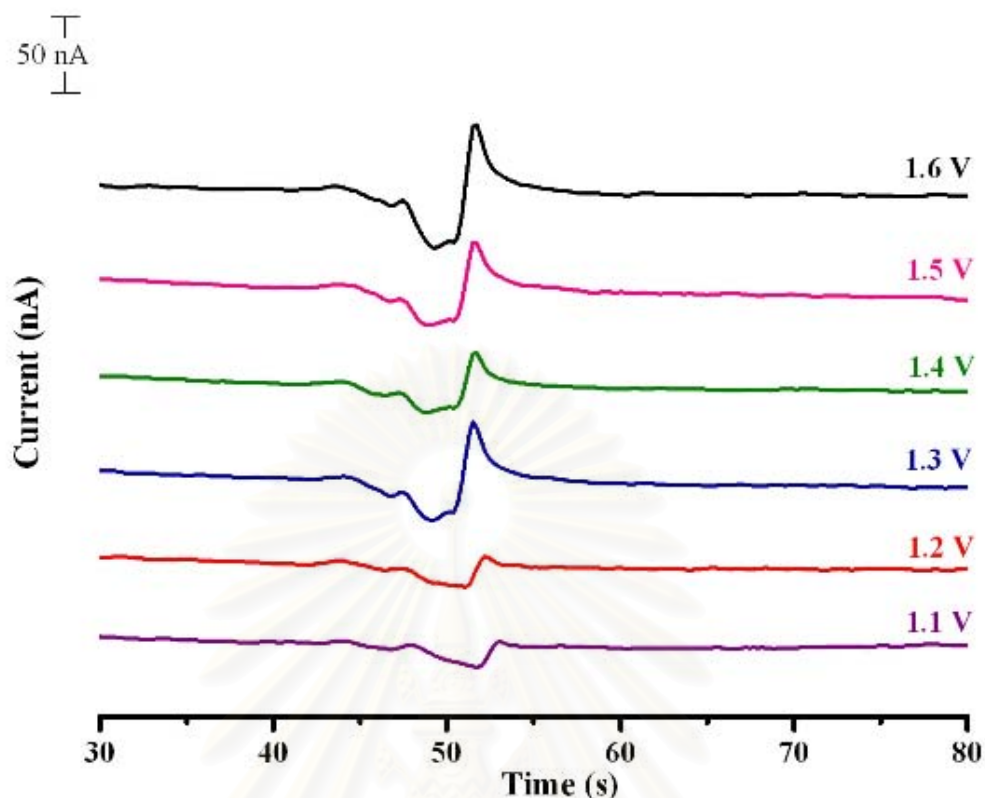


Figure 4.9 Electropherograms of glucose separation using various cleaning potentials (E_{oxd}) between 1.1 V and 1.6 V. Experimental conditions: separation potential 1400 V, pinched injection time 15 s, BGE 20 mM boric acid with 20 mM SDS (pH 9.0).

The effects of the potential used to clean the electrode (oxidation potential) and the potential used to reconstruct the surface (reduction potential) were also studied via hydrodynamic voltammetry. Based on these experiments, 1.6 was selected as the cleaning potential, and -0.5 V was selected as the reconstruction potential. At these potentials, the maximum signal magnitude and stability were obtained (Figures 4.9 and 4.11).

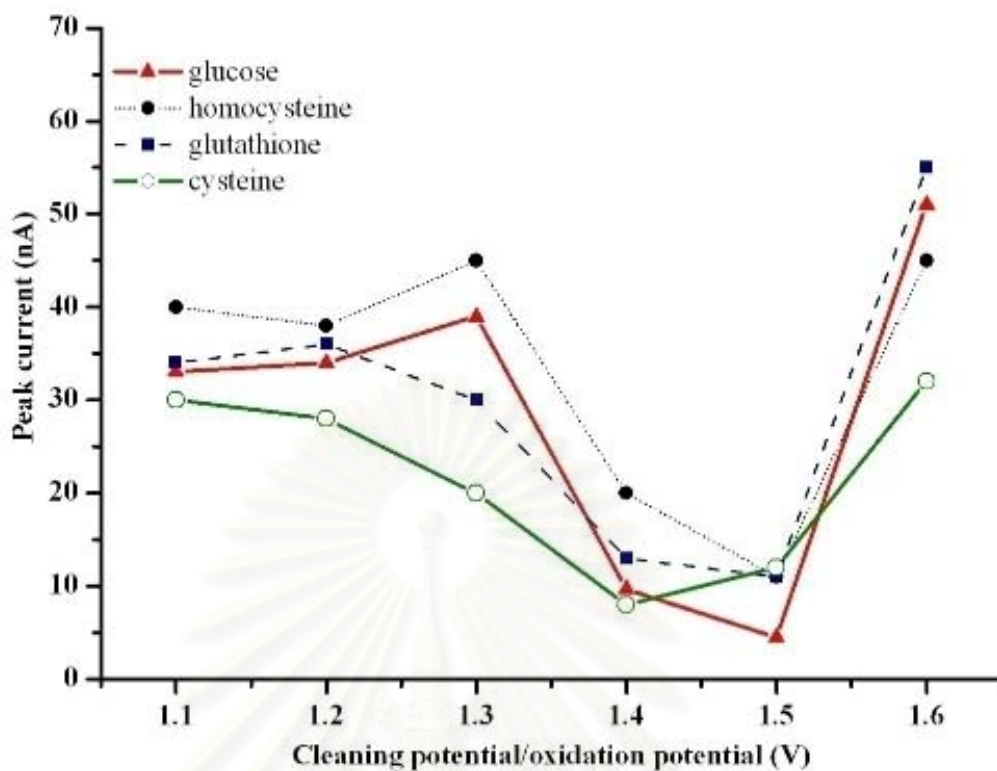


Figure 4.10 Hydrodynamic voltammograms of peak current during the electrophoretic separation of 500 μM glucose (\blacktriangle), homocysteine (\bullet), glutathione (\blacksquare), and cysteine (\circ) at various cleaning potentials (E_{oxd}) between 1.1 V and 1.6 V. (Same experimental conditions as Figure 4.7)

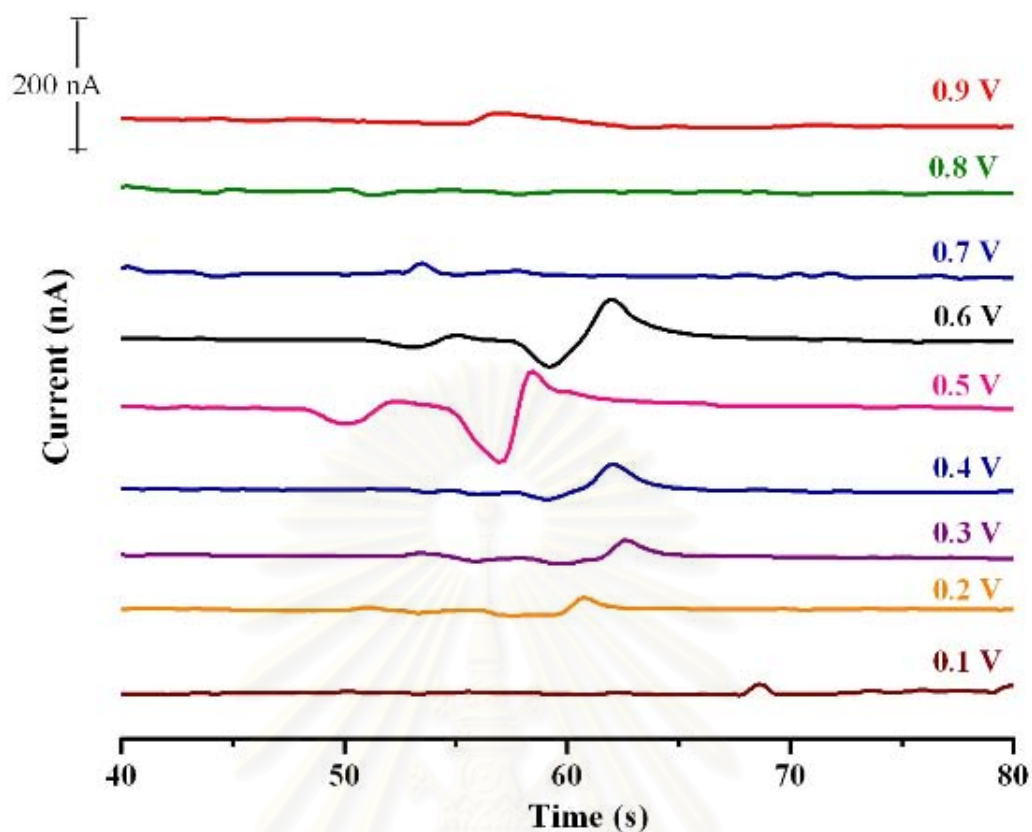


Figure 4.11 Electropherograms for the separation of glucose at various detection potentials (E_{det}) between 0.1 V and 0.9 V. Experimental conditions: separation potential 1400 V, pinched injection time 15 s, BGE 20 mM boric acid with 20 mM SDS (pH 9.0).

สถาบันวิทยบริการ
จุฬาลงกรณ์มหาวิทยาลัย

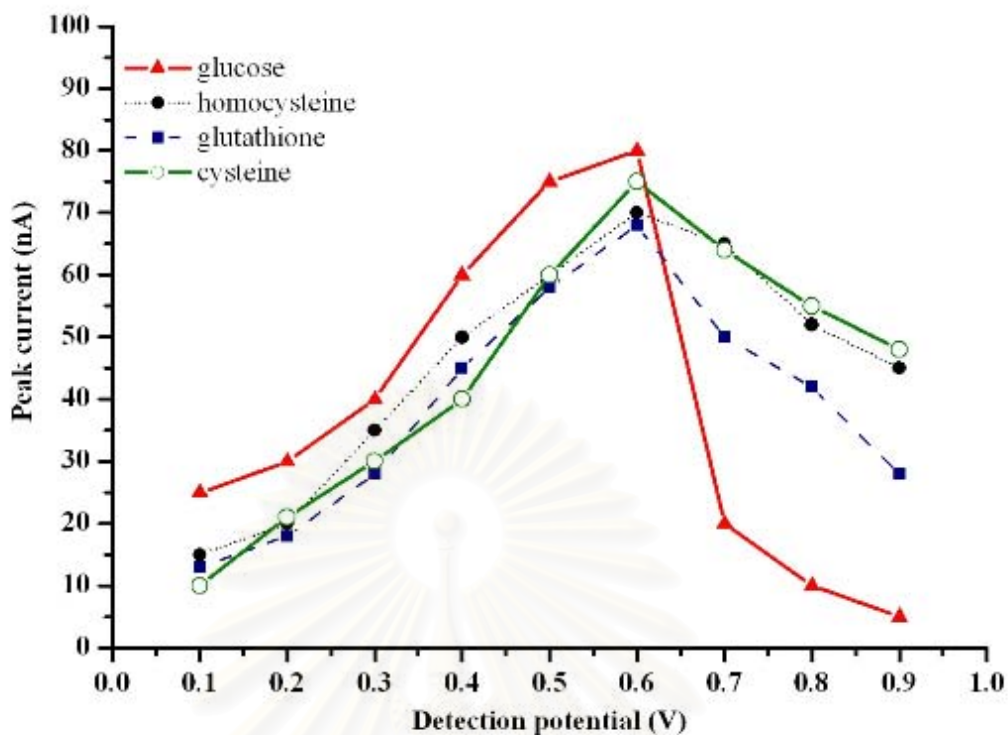


Figure 4.12 Hydrodynamic voltammograms of peak current during the electrophoretic separation of 500 μM glucose(\blacktriangle), homocysteine (\bullet), glutathione (\blacksquare), and cysteine (\circ) at various detection potentials (E_{det}) between 0.1 V and 0.9 V. (Same experimental conditions as Figure 4.9.)

Table 4.1 PAD parameters for the detection of glucose and thiol compounds

	Potential applied (V)	Time (ms)
Oxidation	+ 1.6	0.05
Reduction	-0.5	0.025
Detection	0.6	0.15

Experimental conditions: separation potential 1400 V, pinched injection time 15 s, BGE 20 mM boric acid with 20 mM SDS (pH 9.0).

4.1.2.7 Linear range and detection limit

Using the optimal conditions for separation (BGE 20 mM boric acid (pH 9.0), separation potential 1400 V, and injection time 15 s) and the optimized PAD waveform (Table 4.1), glucose and thiol compounds were separated and detected within 80 s (Figure 4.17). Under these conditions, linear relationships between concentration and peak current were observed for homocysteine, glucose, and glutathione. The LODs were also measured for glucose (3.8 nM), homocysteine (2 nM), cysteine (2 nM), and glutathione (1 pM). The analytical parameters (regression equation, corresponding correlation coefficient, linear range, LOD, and sensitivity) for each compound are summarized in Table 4.2.



Table 4.2 Analytical parameters corresponding to the calibration curves for glucose and thiol compounds

	glucose	homocysteine	cysteine	glutathione
Regression equation	$y = 0.087x + 3.461$	$y = 0.012x + 85.38$ $y = 0.704x + 264.9$	$y = 0.030x + 15.53$	$y = 0.090x + 1.801$ $y = 0.092x + 25.9$
R ²	0.993	0.996 0.995	0.982	0.996 0.986
Linear range	0.25 μM - 62.5 μM	61 nM - 3900 nM 15.6 μM - 500 μM	4 μM - 500 μM	1 pM - 400 pM 15 nM - 500 nM
Detection limit	3.8 nM	2 nM	2 nM	1 pM
Sensitivity	0.087 nA • μM	0.012 nA • nM 0.704 nA • nM	0.030 nA • μM	0.090 nA • nM 0.092 nA • nM

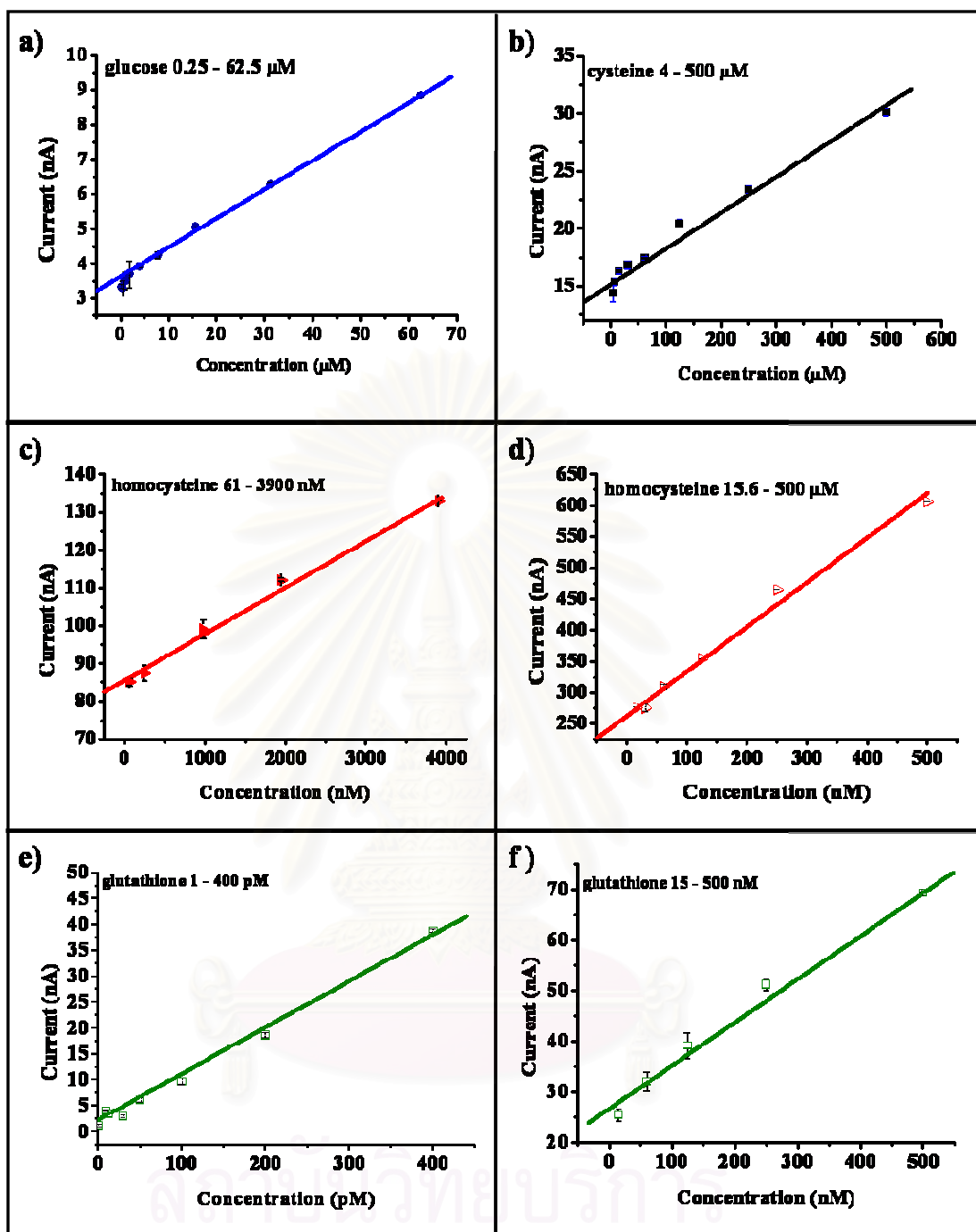


Figure 4.13 Linear relationships between peak currents and concentration for a) glucose from 0.25 – 62.5 μM , homocysteine from c) 61 – 3900 nM and d) 15.6 – 500 μM , and glutathione from e) 1- 400 pM and f) 15 – 500 nM. Experimental conditions: separation potential 1400 V, pinched injection time 15 s, BGE 20 mM boric acid with 20 mM SDS (pH 9.0).

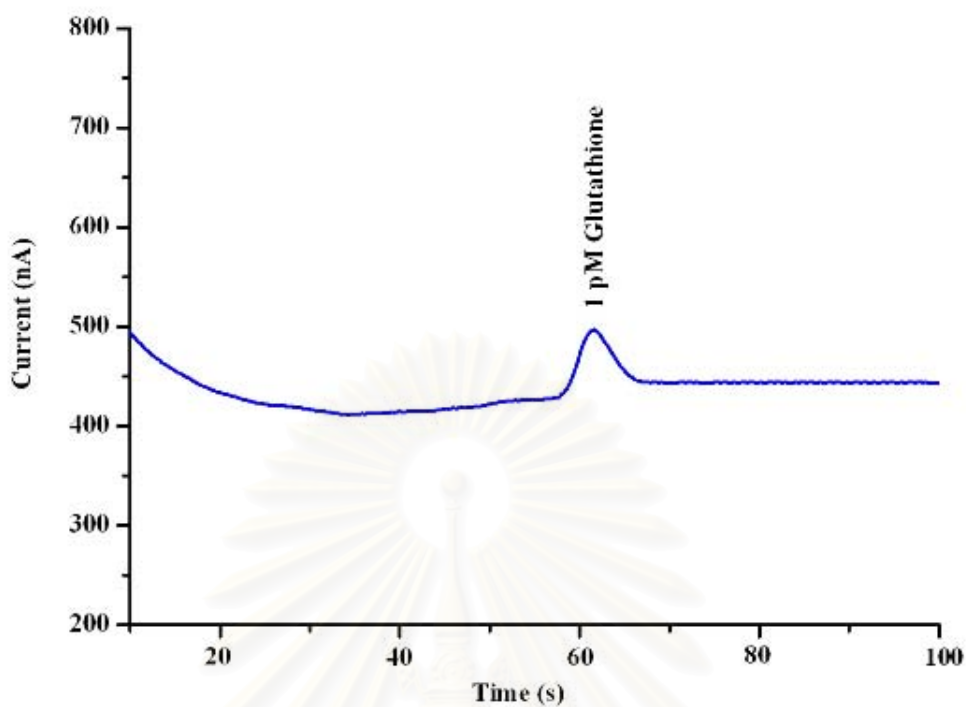


Figure 4.14 Electropherogram for the separation of 1 pM glutathione on a PDMS microchip. Experimental conditions: separation potential 1400 V, pinched injection time 15 s, BGE 20 mM boric acid with 20 mM SDS (pH 9.0).

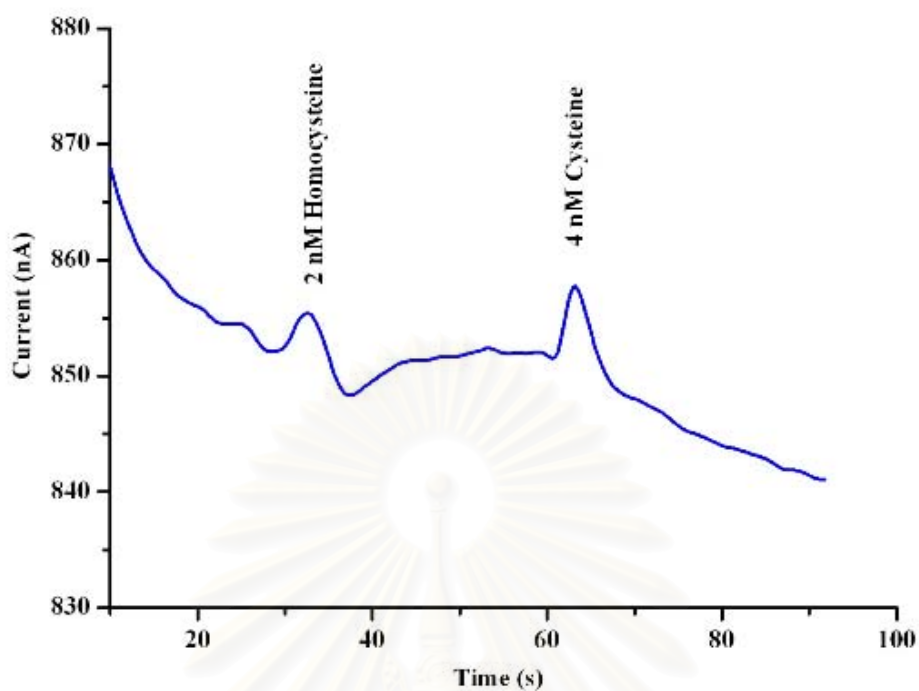


Figure 4.15 Electropherogram for the separation of 2 nM homocysteine and 4 nM cystine on a PDMS microchip. Experimental conditions: separation potential 1400 V, pinched injection time 15 s; BGE 20 mM boric acid with 20 mM SDS (pH 9.0).

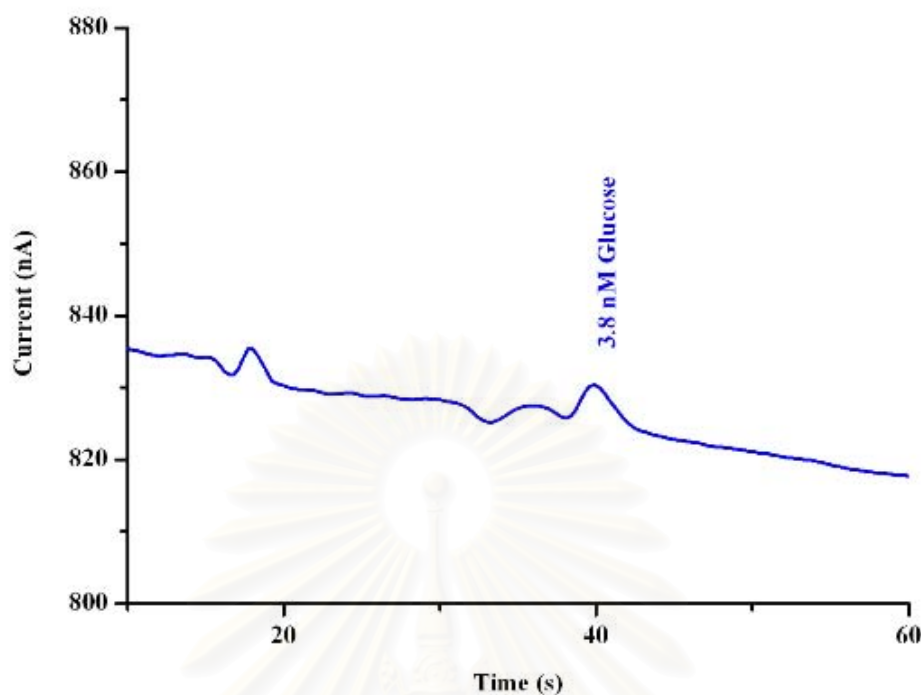


Figure 4.16 Electropherogram for the separation of 3.8 nM glucose on a PDMS microchip. Experimental conditions: separation potential 1400 V, pinched injection time 15 s, BGE 20 mM boric acid with 20 mM SDS (pH 9.0).

4.1.2.8 Precision and accuracy

The precision of this MEC-EC method was evaluated by comparing the responses (I_p and t_M) of 20 consecutive separations of a mixture of glucose and thiol compounds (100 μM each) under the selected optimal conditions. The RSDs of the responses and migration times were less than 6 and 2%, respectively (data not shown).

4.1.2.9 Application

4.1.2.9.1 Determination of glucose and thiol compounds in plasma samples

As mentioned in the introduction, most thiols are present in human plasma as oxidized species, and thus, accurate measurement of thiol concentration in plasma requires disulfide bond reduction. In this work, TCEP was employed as the necessary reducing agent. The concentration of TCEP was modified to optimized reduction potential (data not show). The established optimal conditions (BGE containing 2.5 mM TCEP and 20 mM SDS in 20 mM boric acid buffer (pH 9.0), separation potential 1400 V, pinched injection time 15 s) were adopted for the analysis of thiols in human plasma. An electropherogram of the separation of blank plasma spiked with 100 μ M glucose and selected thiol compounds under the optimal conditions is given in Figure 4.17.

The applicability of the developed MEC-EC method to real human plasma samples was tested. A representative electropherogram is show in Figure 4.18a. The sample was subsequently spiked with 250 μ M glucose and glutathione to confirm the identities of the glucose and glutathione peaks (Figure 4.18b). Good resolution of glucose and glutathione was achieved.

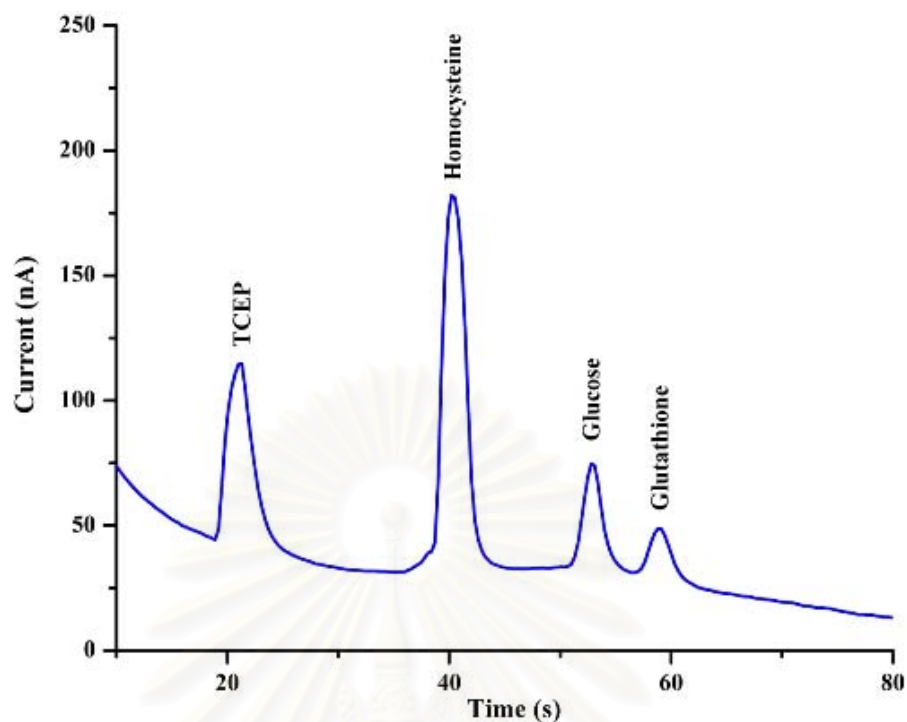


Figure 4.17 Electropherogram corresponding to the separation of a mixture of 2.5 mM TCEP, 100 μ M homocysteine, 100 μ M glucose, and 100 μ M glutathione. Experimental conditions: separation potential 1400 V, pinched injection time 15 s, BGE 20 mM boric acid (pH 9.0) with 20 mM SDS and 2.5 mM TCEP.

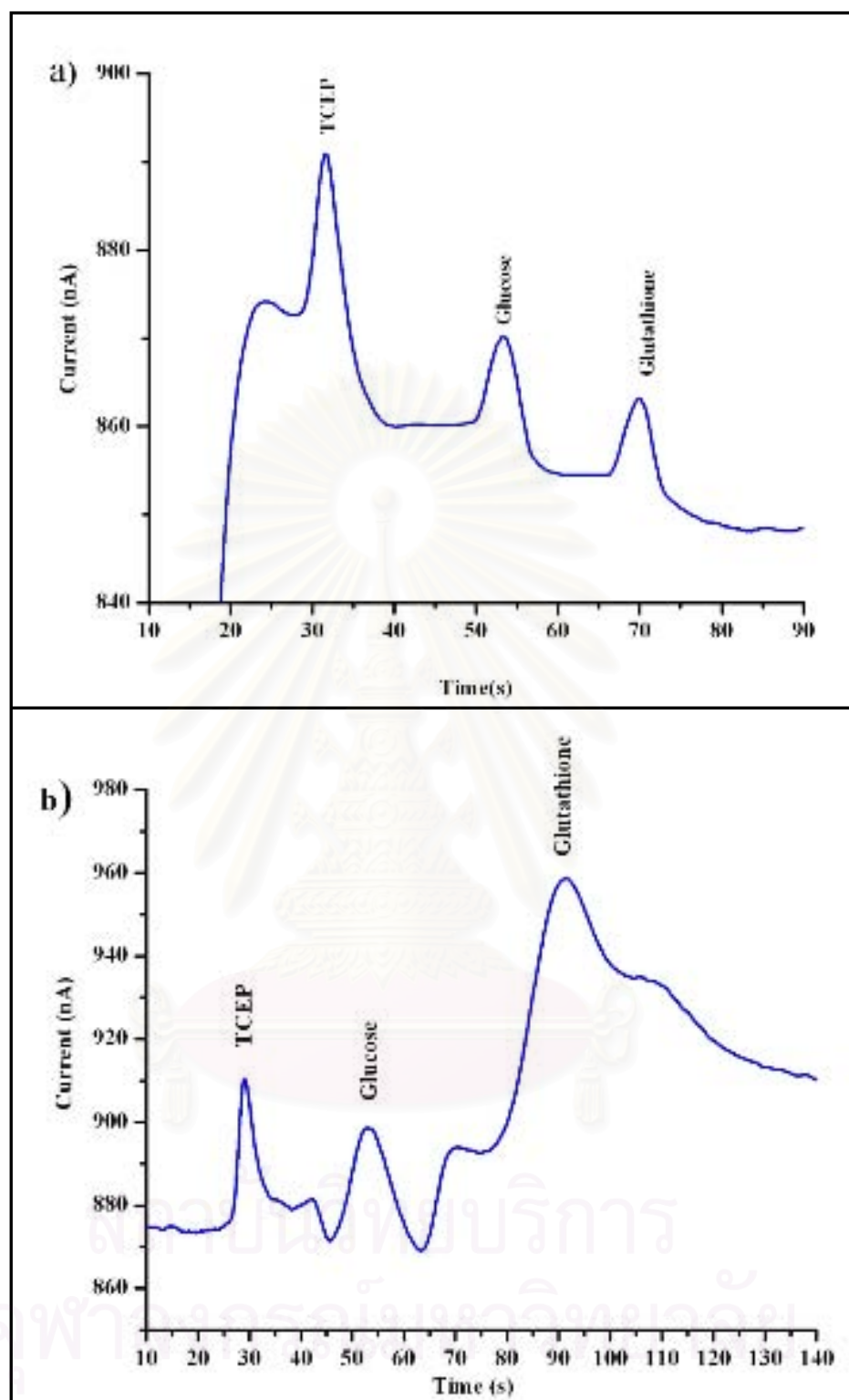


Figure 4.18 Electropherogram of the separation of glucose and thiol compounds in human plasma. (a) Human plasma sample. (b) Human plasma sample spiked with 250 μ M glucose and glutathione. Experimental conditions: separation potential 1400 V, pinched injection time 15 s, BGE 20 mM boric acid (pH 9.0) with 20 mM SDS and 2.5 mM TCEP.

4.2 Polyelectrolyte coatings for PDMS microchip electrophoresis

The effect of layer-by-layer polyelectrolyte multilayer (PEM) coatings on the velocity and direction of electroosmotic flow (EOF) and on the separation efficiency of poly(dimethylsiloxane) (PDMS) microchips was studied using different polymer structures and deposition conditions. EOF was measured as a function of polymer structure and number of layers. In one set of experiments, the same anionic polymer was used while the cationic polymer was varied. In another set of experiments, the same cationic polymer was used while the anionic polymer was varied. In cases, the direction of EOF reversed with each additional layer of polymer deposited. The EOF magnitude, however, did not vary significantly with the number of layers or the polyelectrolyte composition. Next, different PEM coatings were compared in terms of the separation efficiencies of the corresponding PDMS microchips. For native, uncoated PDMS microchips, the average separation efficiency was 4105 ± 1540 theoretical plates. The addition of two layers of polyelectrolyte increased the separation efficiency anywhere from 2- to 5-fold, depending on the polymer used. A maximum separation efficiency of $12,880 \pm 1050$ theoretical plates was achieved for a six total layer coating of polybrene (cationic) and dextran sulfate polymers. The use of polyelectrolyte coatings generated consistent EOF irrespective of the polymer structure and improved separation efficiency compared to unmodified PDMS microchips.

4.2.1 Polymer coatings

Surface modification with PEMs is attractive because of the wide variety of chemistries available for controlling surface properties. In this study, five different polymers, including primary (PAH), secondary (PEI), tertiary (PEI), and quaternary (PB) amines, and both strong (DS, sulfate) and weak (PAA, carboxylic acid) anions (see Figure 4.19), were studied in an effort to understand how differences in polymer chemistry impact overall separation performance.

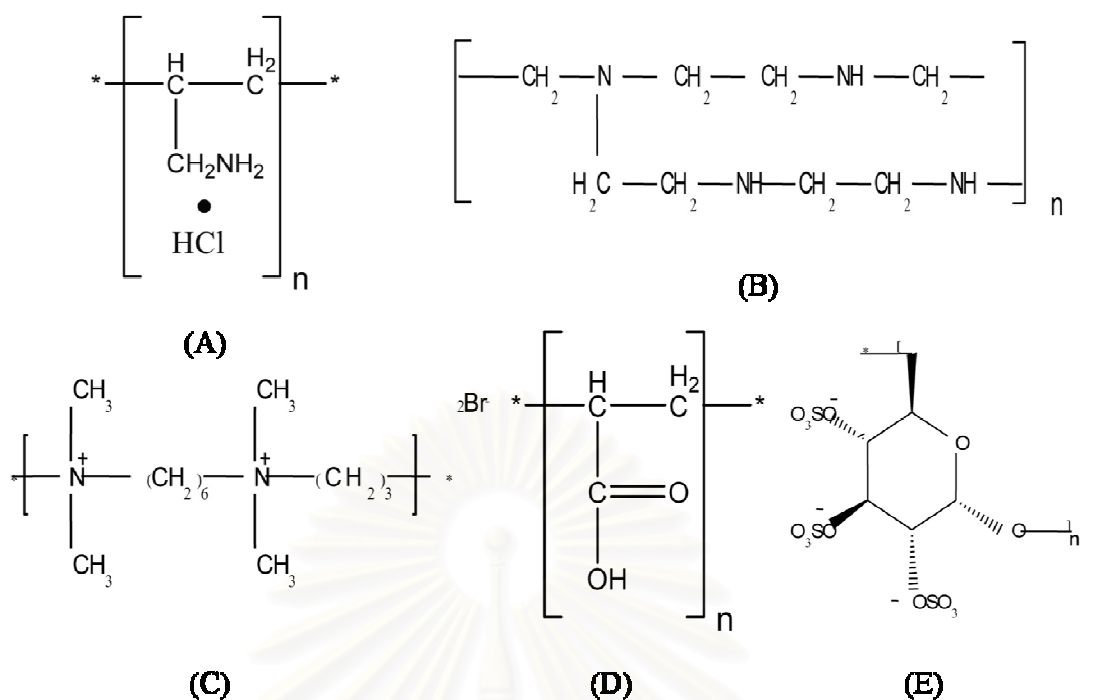


Figure 4.19 Polyelectrolyte structures: (A) poly(allylamine)hydrochloride, PAH (B) poly(ethyleneimine), PEI (C) polybrene, PB (D) poly(acrylic acid), PAA (E), dextran sulfate, DS.

4.2.2 Effect of polymer coatings

The effect of polymer chemistry on surface charge and EOF reproducibility was investigated first. Two set of experiments were performed, one in which the anionic polymer was held constant while the cationic polymer was varied and another in which the cationic polymer was held constant while the anionic polymer was varied. In the former set, EOF was measured as a function of number of layers, up to 10 layers, for PEMs containing one of the cationic polyelectrolytes, polybrene (PB), poly(ethyleneimine) (PEI), or poly(allylamine hydrochloride) (PAH), and the anionic polyelectrolyte poly(acrylic acid) (PAA) (Figure 4.20). In the latter set, EOF was similarly measured as a function of number of PEM layers, up to 10 layers, for both anionic polyelectrolytes and with PEI as the cationic polymer (Figure 4.21). For odd numbers of layers, the topmost layer was cationic, while for even numbers of layers, the topmost layer was anionic, and the reversal of EOF was observed with the addition of each subsequent layer, as anticipated. When a positively charged polyelectrolyte was the topmost layer adsorbed, EOF was the

opposite of the desired direction, and when a negatively charged polyelectrolyte was the topmost layer adsorbed EOF was in the normal direction (Figures 4.18 and 4.19). Notably, the magnitude of the EOF values, while variable for low numbers of layers, became relatively constant for higher numbers of layers. For example, the standard deviation for all single layer data was $2.9 \times 10^{-5} \text{ cm}^2\text{V}^{-1}\text{s}^{-1}$ was significantly larger than those of the five layer ($1.44 \times 10^{-5} \text{ cm}^2\text{V}^{-1}\text{s}^{-1}$) and the ten layer ($1.11 \times 10^{-5} \text{ cm}^2\text{V}^{-1}\text{s}^{-1}$) data. This trend was consistent between the two sets of experiments and among films deposited in either the absence or the presence of NaCl. The variability in EOF observed in films composed from a low number of layers was most likely attributable to variations in film structure and to incomplete surface coverage. As the films were thickened, the overall consistency of the films improved, and the surface charge became more consistent. This data also suggested that a maximum surface charge density exists when these polymers are deposited on PDMS, and this conclusion was consistent with observations of similar PEM films on other substrates [63, 71].

The application of NaCl during the polyelectrolyte coating step is known to increase film thickness [45, 183]. Nevertheless, no statistically significant difference in EOF was observed between polyelectrolyte coatings formed in the presence (0.5 M NaCl) or the absence of salt. The adsorption of polyelectrolytes onto a surface of opposite charge is an ion exchange phenomenon in which small salt counter ions are replaced by the polymeric ions, thereby maintaining negation of the surface charge. As previously reported [184], deposition with low-concentration salt solutions increases the efficiency of polyelectrolytes binding to the surface charge. In the present example, the presence of salt in the deposition solution led to a slight reduction in the average EOF ($3.40 \times 10^{-5} \pm 1.32 \times 10^{-5} \text{ cm}^2\text{V}^{-1}\text{s}^{-1}$) compared to those of films deposited without salt, but the difference was not statistically significant. The slight reduction in EOF was most likely the result of the salt partially offsetting the charged groups of the PEM layer [184]. Because the presence or absence of salt had an insignificant effect on EOF, all additional coating experiments were performed in the absence of NaCl.

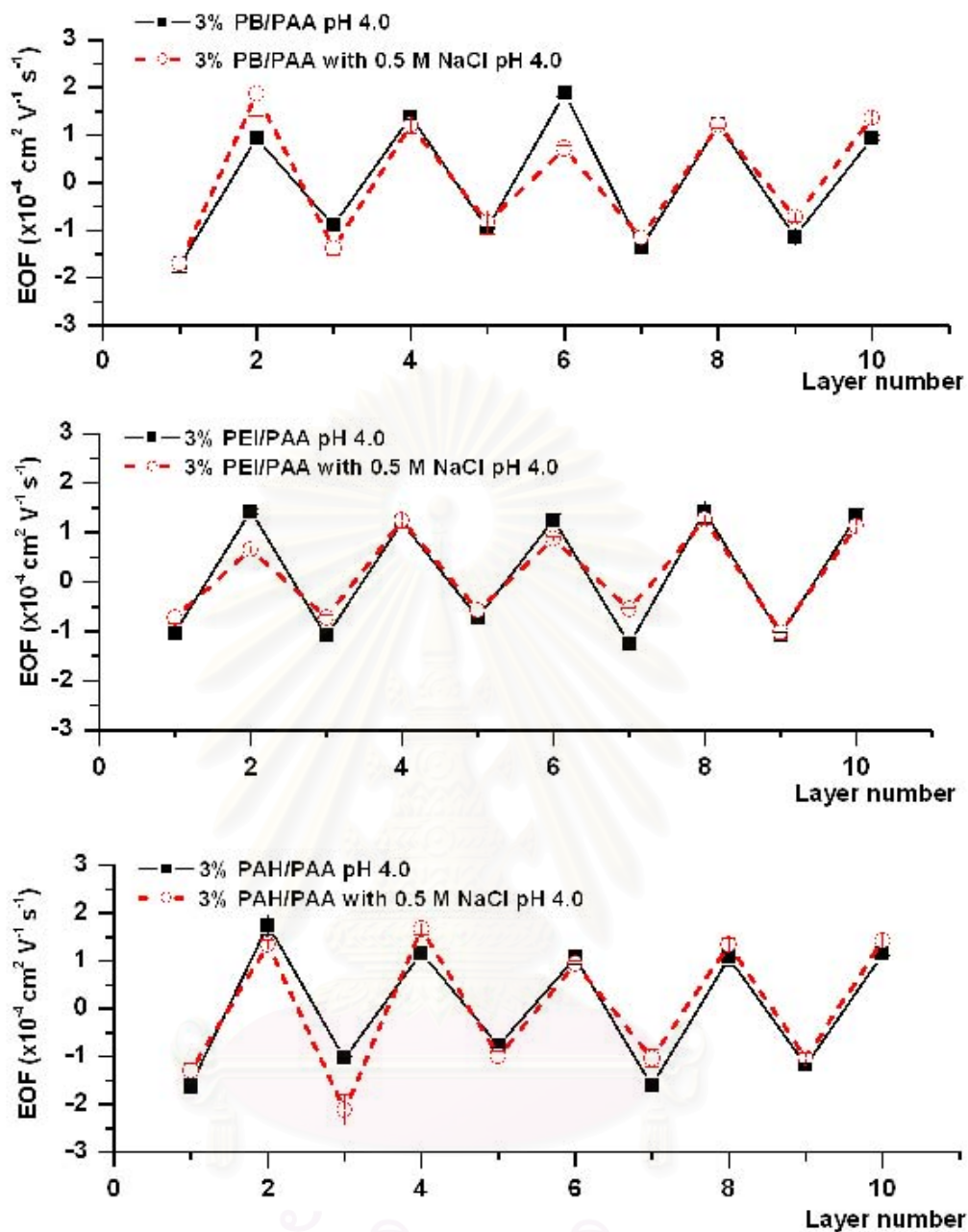


Figure 4.20 Electroosmotic flow as a function of number of layers deposited for different polyelectrolyte coatings: 3% PB/PAA, 3% PB/PAA with 0.5 M NaCl, 3% PEI/PAA, 3% PEI/PAA with 0.5 M NaCl, 3% PAH/PAA, 3% PAH/PAA with 0.5 M NaCl. EOF was measured with phosphate buffer (pH 7.0).

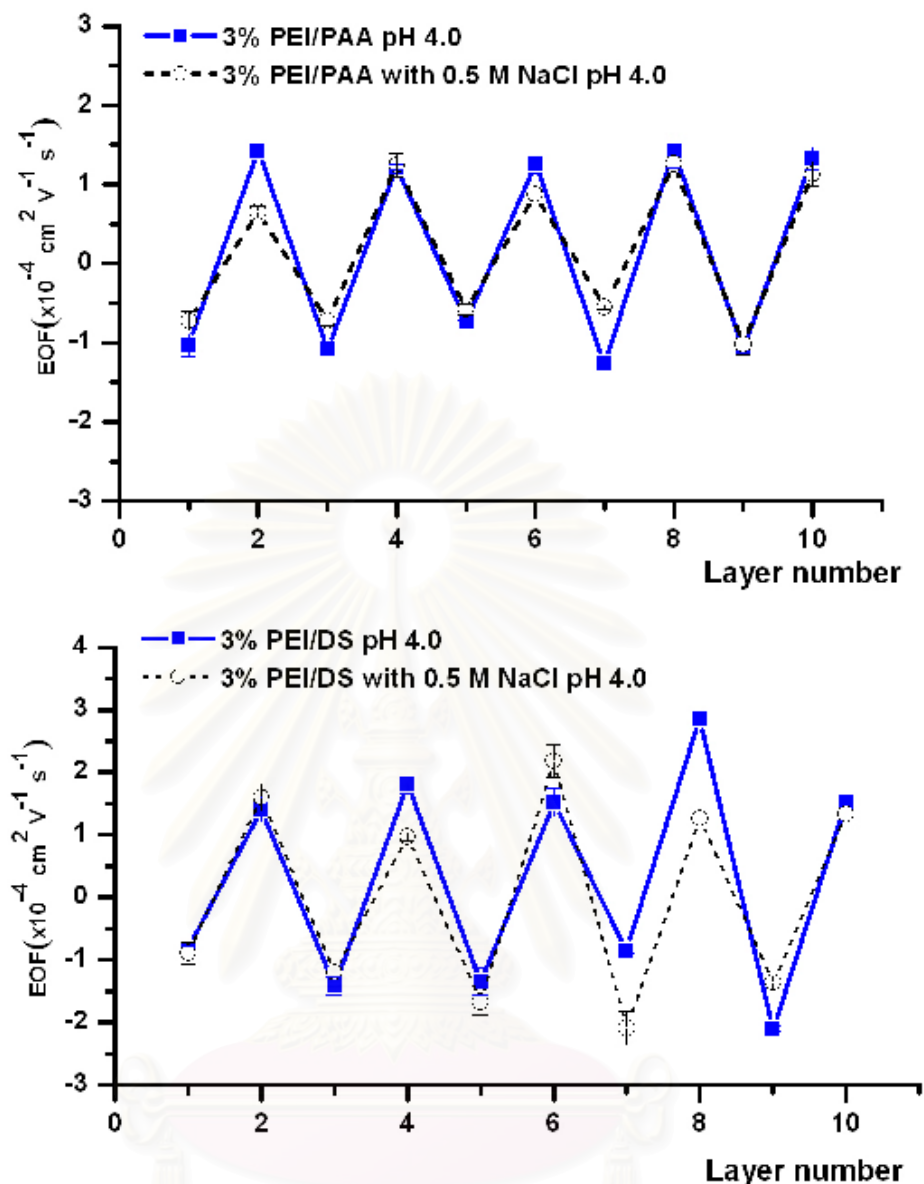


Figure 4.21 Electroosmotic flow as a function of number of layers deposited for different polyelectrolyte coatings: 3% PEI/PAA, 3% PEI/PAA with 0.5 M NaCl, 3% PEI/DS, 3% PEI/DS with 0.5 M NaCl. EOF was measured with phosphate buffer (pH 7.0).

4.2.3 Effect of polymer-coated PDMS on separation efficiency

In addition to measuring EOF, separation efficiency was also measured as functions of film composition and thickness using LIF detection. In all cases, the addition of PEMs significantly improved separation efficiency. Separation efficiency was assessed by separating sample solutions containing FTPD using a native PDMS device and a set of devices each modified with a six-layer coating of one of the PEMs tested (Figure 4.22).

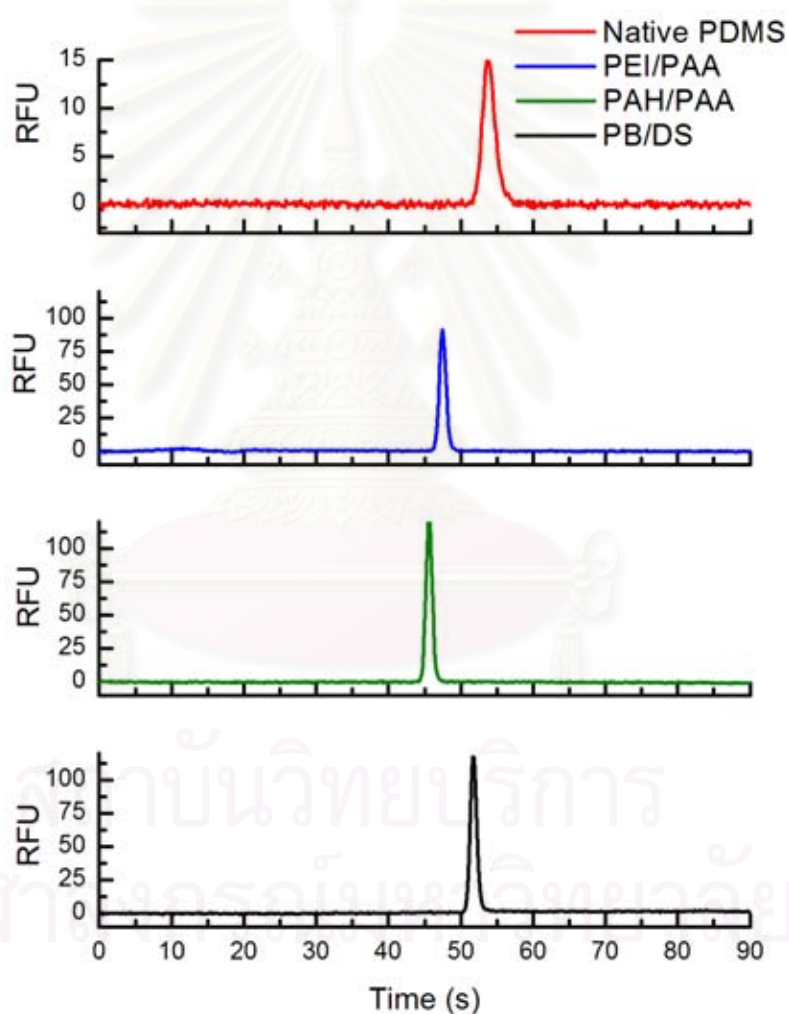


Figure 4.22 Comparison of electropherograms of FTPD separations using (from top to bottom) native PDMS device and devices with six-layer coatings of either PEI/PAA, PAH/PAA, or PB/DS.

4.2.4 Effect of different polymer coatings on separation efficiency

Separation efficiency was measured as a function of even numbers of polyelectrolyte layers (up to six layers) for three different coating combinations, PB/DS, PEI/PAA, and PAH/PAA (Figure 4.23). For each polyelectrolyte combination, there was a specific number of layers for which the number of theoretical plates (N) reached a maximum value. For PB/DS, six layers maximized separation efficiency ($N = 12,883$ plates), for PEI/PAA, six layers maximized separation efficiency ($N = 11,402$ plates), and for PAH/PAA four layers maximized separation efficiency ($N = 11,912$ plates). These values represented 2- to 6-fold improvements in maximal separation efficiency compared to that of the uncoated PDMS system. PB/DS demonstrated the highest separation efficiency, while PAH/PAA reached maximum separation efficiency with only four layers. The observed improvement in separation efficiency was most likely attributable to the increased hydrophilicity of channel walls, thereby decreasing analyte-wall interactions.

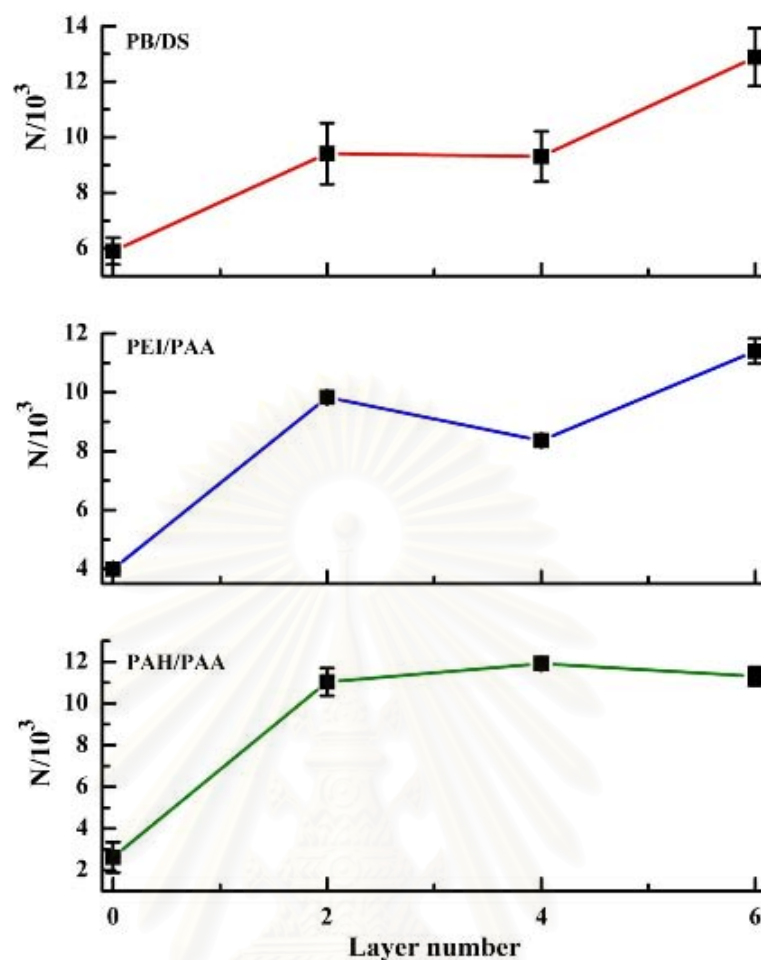


Figure 4.23 Number of theoretical plates (N) as a function of layer number. A) PB/DS alternating layers. B) PEI/PAA alternating layers. C) PAH/PAA alternating layers.

4.3 Thermoset polyester microchip electrophoresis/electrochemistry

4.3.1 Electrochemical characteristics of microchip devices

As previously mentioned in section 4.1.1, the microchip CE (MCE) systems designed were characterized using amperometric detection techniques. Dopamine and catechol were chosen as standard analytes to demonstrate the microchip CE systems' performance. TPE-based microchip CE devices were constructed and used to separate a solution of 100 μM dopamine and 100 μM catechol (Figure 4.24). The migration times of dopamine and catechol were 36 and 48 s,

respectively. Separation was performed using 20 mM TES (pH 7.2) as the background electrolyte (BGE), and the separation potential was set to 1100 V with a 15 s injection. Baseline resolution of two compounds was observed, and Figure 4.22, was a typical example of the performance of the TPE microchip CE systems.

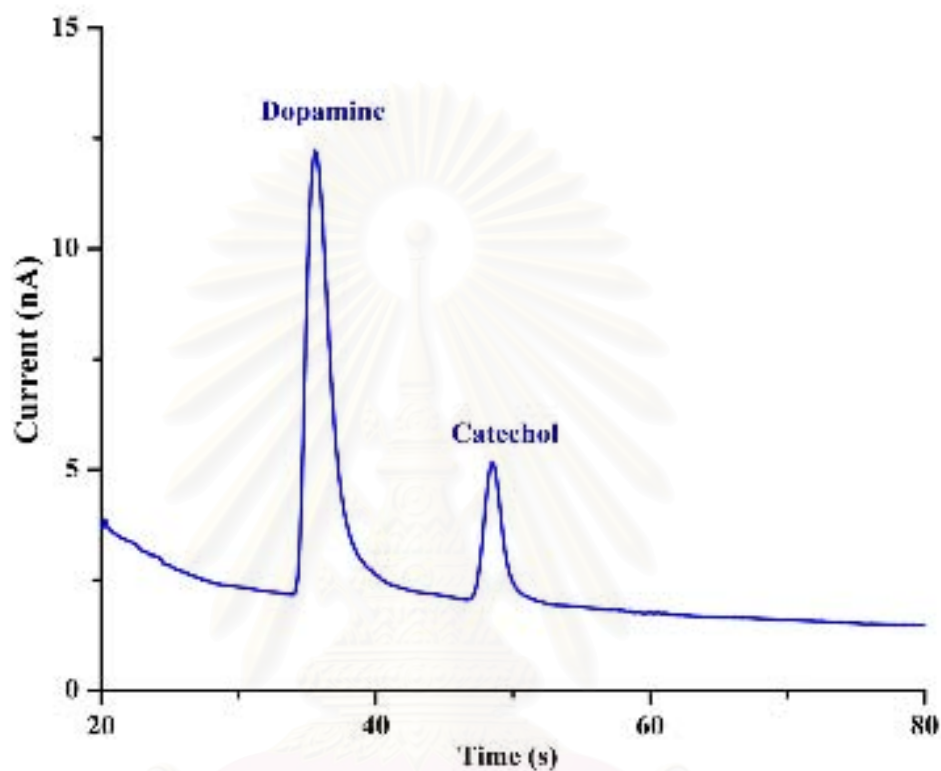


Figure 4.24 Electropherogram of the separation of 100 μ M dopamine and 100 μ M catechol on a TPE microchip. Experimental conditions: separation potential 1200 V, pinched injection time 15 s, BGE 20 mM TES (pH 7.2).

4.3.2 Stability study

The EOF values of an uncoated, native TPE device were measured over 18 days (Figure 4.25) with the chips stored in water between experiments. No statistical decrease in EOF was observed over the first four days. Between days 4 and 18, however, a 55% decrease in EOF from 4.85 ± 0.57 to $2.16 \pm 0.53 \times 10^{-4} \text{ cm}^2/\text{V}\cdot\text{s}$ ($n = 5$) was observed. Similar trends in EOF values were measured for microchips stored in air. Next, EOF values were measured for plasma-oxidized microchips over a

period of 11 days. The EOF of plasma-treated TPE devices was higher and more stable over time than unmodified TPE (Figure 4.23).

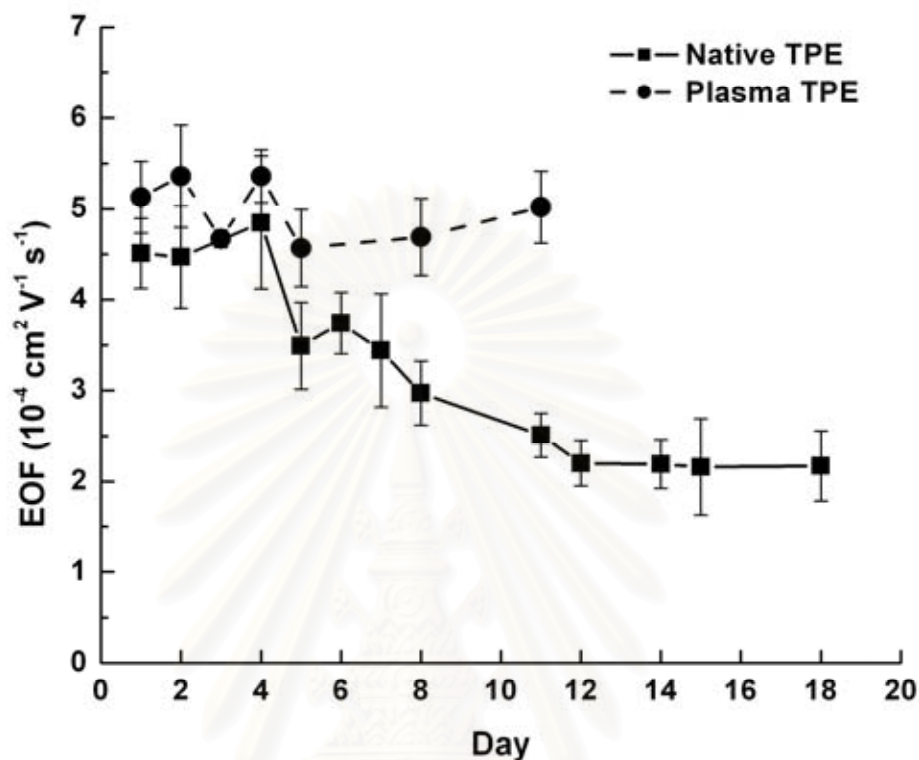


Figure 4.25 Day-to-day EOF stability of TPE microchips. EOF measurements are given for native TPE devices over an 18-day period (■) and for plasma-treated TPE devices over an 11 day period (●). EOF was determined using the current-monitoring method. Experimental conditions: applied field strength 200 V/cm, BGEs 20 mM phosphate (high ionic strength), and 18 mM phosphate (low ionic strength).

4.3.3 Effect of pH

The EOF values for MEC devices fabricated from untreated PDMS, untreated TPE, and plasma-oxidized TPE were measured as a function of pH and compared (Figure 4.26). Comparing untreated TPE and PDMS microchips, the EOF values corresponding to the TPE devices were on average 22% higher and were more stable across all pH values examined. The EOF values of the plasma oxidized TPE

devices were 5.13 ± 0.34 , 5.56 ± 0.22 , and $5.61 \pm 0.35 \times 10^{-4} \text{ cm}^2/\text{V}\cdot\text{s}$ ($n = 5$) for pH 4, 7, and 10, respectively, a 38% increase in EOF over PDMS and a 21% increase over native TPE, representing a 38% increase in EOF over PDMS and a 21% increase over untreated TPE. Chip-to-chip reproducibility of the TPE microchips was also established. The RSDs of EOF measurements from five chips were 2.7, 5.1, and 7.1% for pH 4, 7, and 10, respectively. Furthermore, small changes in the volume or mass of TPE components had little to no effect on the EOF. The stability of the EOF as a function of time for both untreated and plasma-oxidized TPE was much better than that of PDMS microchips and was similar to those of PMMA and PC [185]. The comparison with PDMS is more relevant, however, because TPE and PDMS devices are fabricated using similar methods. PDMS lacks stability, because hydrophobic, low-molecular weight oligomers diffuse to the surface over time [186-188]. TPE lacks this instability. It is denser, and its starting materials are less hydrophobic. Plasma treatment presumably modifies the TPE surface enough to separate reactive acids and alcohols. The exact chemical mechanisms by which stabilization is enhanced are currently under investigation.

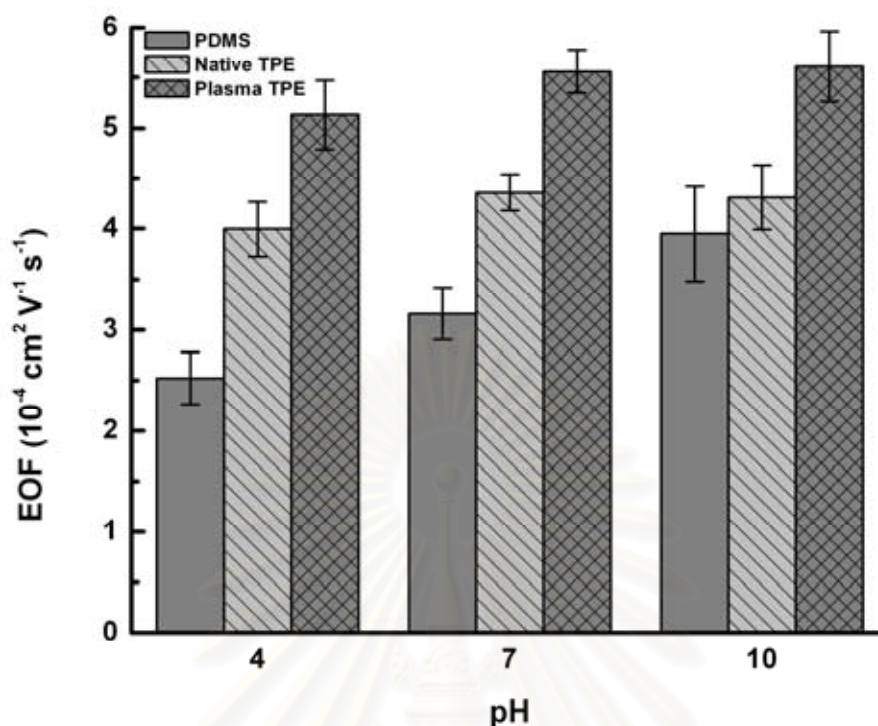


Figure 4.26 EOF measured for five microchips made at different times from different batches of TPE. Each chip was run multiple times at different pH values (4, 7, and 10) to determine the effect of pH effect on reproducibility. Other experimental parameters are identical to those described in Figure 4.22.

4.3.4 Effects of polymer coating

PEM coatings provide a method for controlling the surface chemistry of microchip devices [72, 189]. PEM coatings have been shown to be beneficial when working with PDMS microchips, because these coatings increase the EOF, surface stability, and hydrophilicity of the resulting devices. EOF values were measured for untreated TPE, TPE coated with PB, and TPE coated with a bilayer of PB and DS over a range of pH values from 3 to 10 (Figure 4.27). The EOF of the untreated TPE microchip was consistent across the entire pH range tested with a flow value of $(4.08 \pm 0.31) \times 10^{-4} \text{ cm}^2 \text{ V}^{-1} \cdot \text{s}^{-1}$ ($n = 10$). Addition of the PB cationic layer to the TPE surface not only reversed the flow as expected, but also significantly reduced the

magnitude of the EOF. Values for the EOF of the PB-treated TPE devices in phosphate buffer at the same pH values ranged from -2.69×10^{-4} to -1.51×10^{-4} $\text{cm}^2\text{V}^{-1}\cdot\text{s}^{-1}$ ($n = 3$). Addition of an anionic DS layer to the PB-coated surface resulted in EOF magnitudes similar to those of untreated TPE. EOF values between $(2.58 \pm 0.43) \times 10^{-4}$ and $(4.34 \pm 0.83) \times 10^{-4}$ $\text{cm}^2\text{V}^{-1}\cdot\text{s}^{-1}$ were observed for the pH 3 – 10 range.

Control of surface chemistry through application of a simple and effective PEM coating will allow TPE microchips to be used in a variety of ways. PEM coatings may be used to reverse, reduce, or even eliminate EOF. Reversal of EOF is useful in the separation of anionic species because the flow direction parallels anion migration, allowing for a shorter separation time and greater separation efficiency, which is the result of the narrower analyte peaks from reduced diffusion. Another benefit of adsorbed PEM coatings is that no additional PEs, such as surfactants, need to be added to the BGE as is the case with dynamic coatings. Instead, as expected, the polyelectrolytes are strongly bonded to the channel surfaces through electrostatic interactions.

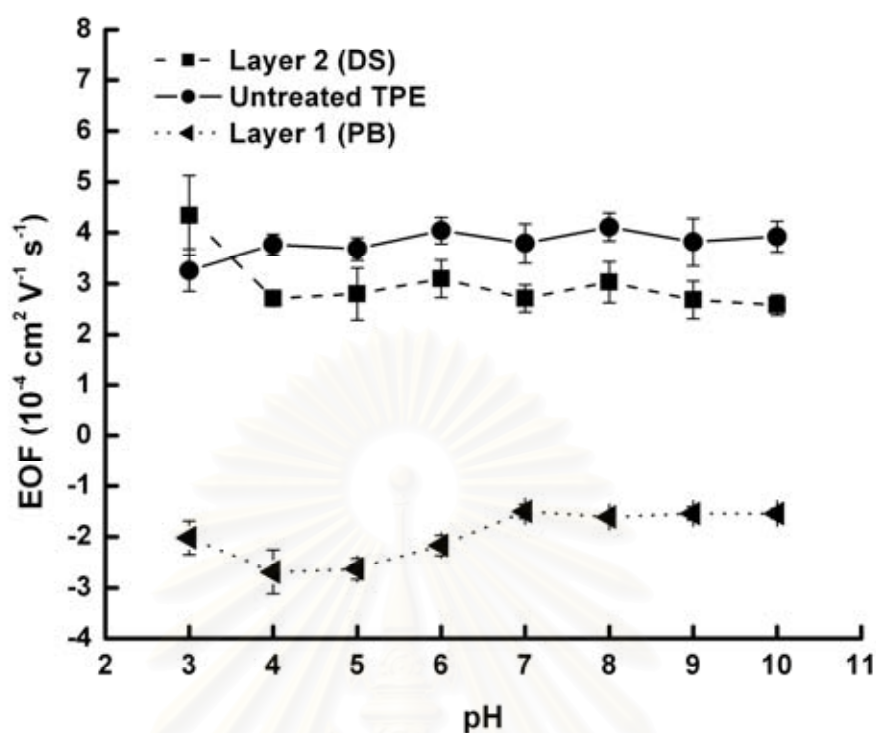


Figure 4.27 EOF values of untreated TPE (●) modified with a single layer of PB (anionic polyelectrolyte) (◄) or a double layer of DS (cationic polyelectrolyte) and PB (■) for pH values between 3 and 10. Other experiment parameters are identical to those described in Figure 4.22.

4.3.5 Microchip characterization and separation efficiency study

Dopamine, catechol, and ascorbic acid were chosen as model analytes for the characterization of TPE microfluidic devices. This choice of compounds allowed for a direct performance comparison with the PDMS microchips. Solutions of 1 μM dopamine, 1 μM catechol, and 1 μM ascorbic acid were separated using TPE and PDMS microchips (Figure 4.28). Peak tailing and peak width were dramatically decreased with TPE devices compared to PDMS devices. The dopamine and catechol peaks had skew values of 3.2 and 3.8, respectively, when separated with the PDMS microchip but had skew values of only 1.2 and 1.3, respectively, when separated with the TPE devices. The larger peak skew values might have been attributable to analyte adsorption onto the hydrophobic surface of the PDMS substrate and/or heterogeneous

EOF caused by inhomogeneous surface charge. The exact mechanism, however, could not be determined.

The separation efficiencies of the TPE devices are eight-fold higher than those of the PDMS devices (Figure 4.29). With TPE devices, separation efficiencies of $49,000 \pm 2,600$, $148,000 \pm 4500$, and $295,000 \pm 12,000$ N/m (corresponding to 2,940, 8,880, and 17,700 N, respectively) were observed for dopamine, catechol, and ascorbic acid separations, respectively. The respective values for separation with the PDMS devices were $18,000 \pm 1,200$, $24,000 \pm 1,400$, and $42,000 \pm 2,100$ N/m (corresponding to 1,040, 1,440, and 2,520 N, respectively). The higher separation efficiencies observed with the TPE devices can be attributed to the increased hydrophilicity of the TPE surface, the increased surface-charge stability, and the lack of hydrophobic recovery over time. The increased efficiency allows for a complete baseline-resolved separation of all three analytes with the TPE device. Furthermore, complete separation is achieved even before dopamine is isolated with the PDMS device. The higher separation efficiencies, better peak skews, and faster EOFs observed for the TPE microchips will allow for faster and better-resolved separation of complex samples.

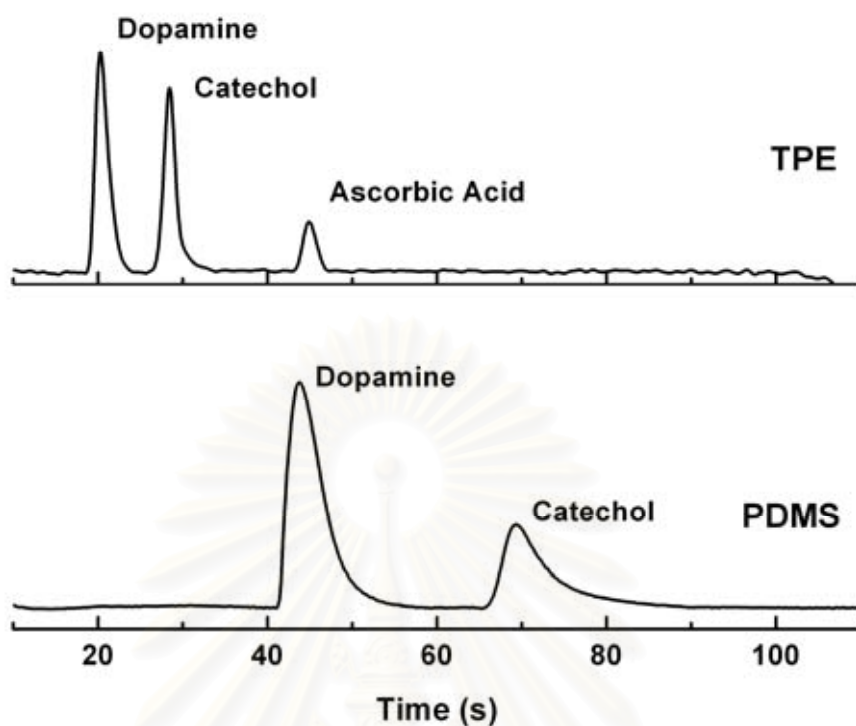


Figure 4.28 Example electropherograms of the separation of 1 μM dopamine, 1 μM catechol, and 1 μM ascorbic acid with a TPE microchip (top) and with a PDMS microchip (bottom). Experimental conditions: applied field strengths were 300 and 200 V/cm for the TPE and PDMS microchips, respectively, pinched injection time 15 s, BGE 20 mM TES pH (7.0).

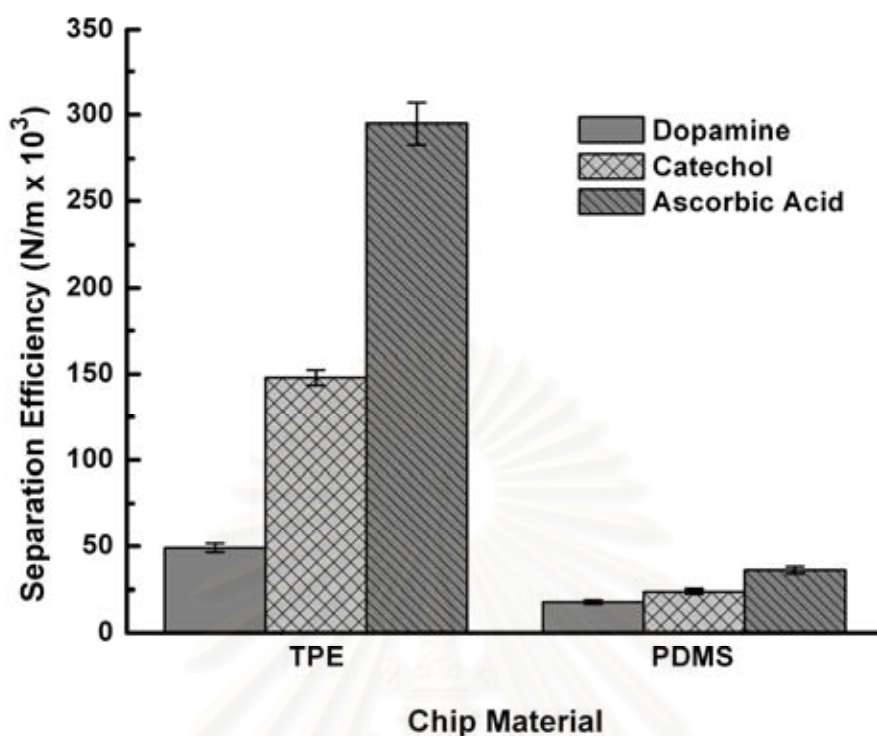


Figure 4.29 Efficiencies of separation of a solution containing 1 μM dopamine, 1 μM catechol, and 1 μM ascorbic acid with identical TPE (left) and PDMS (right) microchips.

4.3.6 Effect of field strength

The effects of applied field strength on migration time and peak shape were investigated. The separation of dopamine, catechol, and ascorbic acid with a TPE microchip using 20 mM TES (pH 7.0) running buffer was assessed as a function of separation potential (Figure 4.30). As expected, increasing the field strength decreased migration times. Comparing TPE and PDMS microchips, migration times were reduced by 31% with TPE microchips when tested at the same field strengths and were reduced by 58% when tested at the higher field strengths that are impermissible with the PDMS microchips. In our experiments, TPE was able to handle higher field strengths than PDMS without generating bubbles or destroying the microchip's bulk material. The maximum field strength used with the TPE devices before failure was 366 V/cm (2,200 V). The exact reason why TPE permits higher

applied fields was not determined, but this kind of property is generally attributable to improved heat transfer within the substrate material. The optimal separation potential was determined to be 266 V/cm (1,600 V), because it offered the fastest separation without sacrificing peak height.

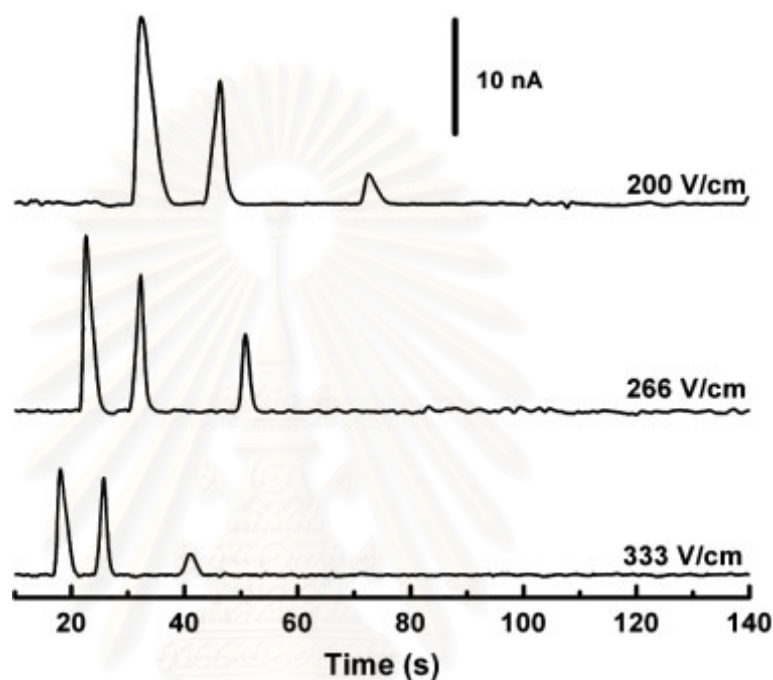


Figure 4.30 Separation of a solution of 1 μM dopamine, 1 μM catechol, and 1 μM ascorbic acid with a TPE microchip using a variety of separation potentials. The optimal separation potential was determined to be 266 V/cm (1600 V). Experimental conditions: pinched injection time 15 s, BGE 20 mM TES pH (7.0).

4.3.7 Compatibility of TPE for the detection of carbohydrates and thiols

As a final test of the compatibility of TPE with MCE-EC applications, PAD detection of carbohydrates and thiols was performed. A solution containing 50 μM homocysteine, 50 μM cysteine, and 50 μM glutathione was chosen as a model analyte. Direct detection has the potential to simplify the quantification of these biologically important compounds. A typical electropherogram from the separation of these three analytes is shown in Figure 4.31. The separation was performed using 20

mM boric acid (pH 9.4) with 2.5 mM TCEP as the BGE at an applied field strength of 233 V/cm and with a 15 s injection. TCEP was added to the buffer to ensure the thiol functionalities remained in their reduced state and were not autooxidized to form disulfides. Baseline resolution of all three analytes was observed. These results demonstrate the compatibility of the more general PAD mode with TPE microchips.

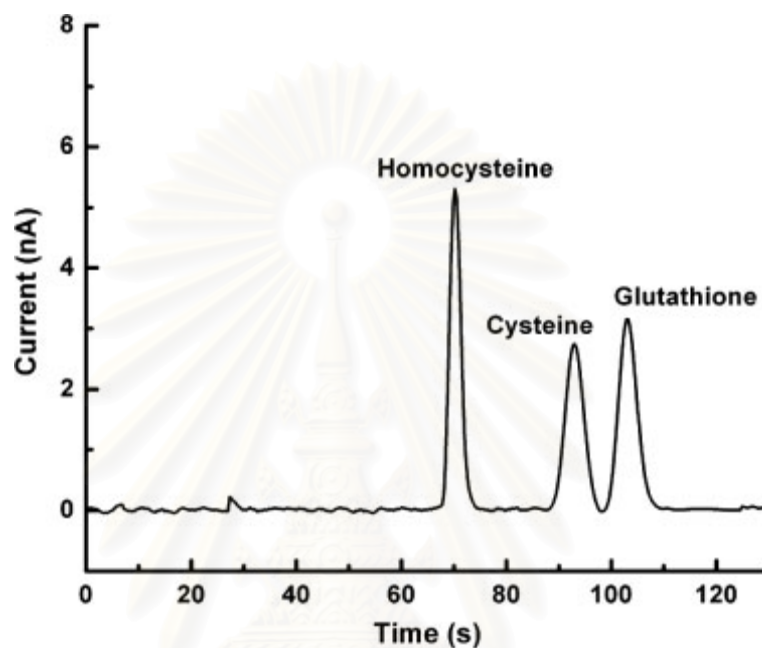


Figure 4.31 Electropherogram of the separation of 50 μ M homocysteine, 50 μ M glutathione, and 50 μ M cysteine with a TPE microchip. Experimental conditions: applied field strength 266 V/cm, pinched injection time 15 s, BGE 20 mM boric acid (pH 9.4) with 2.5 mM TCEP.

สถาบันวิทยบริการ
จุฬาลงกรณ์มหาวิทยาลัย

CHAPTER V

CONCLUSIONS AND FUTURE PERSPECTIVES

The primary aim of this dissertation was to develop an analytical device based on microchip CE with electrochemical detection for biomedical applications. First, a poly(dimethyl siloxane) (PDMS) MCE-EC device was constructed that was capable of separating carbohydrate and thiol compounds in human plasma samples. Second, PDMS MCE-EC devices were coated with several different cationic and anionic multilayer coatings, and the effects of these modifications on flow control and separation efficiency were also studied. Finally, TPE MCE-EC devices were fabricated and proven to be efficacious for the first time. Untreated and polymer-modified TPE were studied to compare these materials' surface stabilities and EOFs. Both amperometric detection and pulsed amperometric detection (PAD) were employed to demonstrate the compatibility of TPE with different electrochemical detection methods.

A new method for the simple, portable, rapid, and inexpensive analysis of carbohydrate and thiol compounds in human plasma using microchip capillary electrophoresis with electrochemical detection was developed. Electrochemical detection coupled with microchip CE enabled selective and sensitive detection of electroactive analytes and simplified the electropherograms. Analysis required very small samples, produced negligible waste, and was relatively rapid and simple. The devices' detection limits were very low, and the devices were sufficiently sensitive over the relevant concentration ranges for carbohydrate and thiol compounds in most biological samples. The precision of quantitative analysis was satisfactory. In addition, the whole procedure can be easily automated.

Surface modification of PDMS with layer-by-layer polyelectrolyte multilayer coatings stabilized EOF in these microchips and also enhanced separation efficiency. For all systems studied, a consistent EOF of $1.13 (\pm 0.45) \times 10^{-4} \text{ cm}^2 \text{V}^{-1} \text{s}^{-1}$ was observed for all devices coated with four or more polyelectrolyte layers, suggesting that it may be possible to vary the coating chemistry to affect separation without substantially altering EOF. In addition, PEMs significantly improved separation

efficiency in all systems tested. For PAH/PAA PEMs, the separation efficiency increased most rapidly and exhibited a maximum value after deposition of only four layers. The other two systems tested reached similar separation efficiencies, but only after six layers of coating had been deposited. In summary, PEMs provided a means to control EOF and enhance the separation efficiency of PDMS microchips.

Finally, the ability of TPE to serve as a substrate material for MCE-EC devices that perform the separation of several analytes was demonstrated. Compared to PDMS, the EOF values for TPE microchips were more stable over a wide range of pH values and over a longer period of time. Chip-to-chip reproducibility of these devices was also shown to be very good. The enhanced separation efficiencies of TPE-based microchips compared to those of other chips suggested that increasingly complex samples may be studied using chips made from this material.

Future work will focus on the development of microchip CE-EC-based methods for measuring other biologically important compounds *in vivo*.

REFERENCES

- [1] Manz, A.; Graber, N.; Widmer, H. M. Miniaturized Total Chemical-Analysis Systems - a Novel Concept for Chemical Sensing: Sens. Actuators, B 1 (1990): 244-248.
- [2] Duffy, D. C.; McDonald, J. C.; Schueller, O. J. A.; Whitesides, G. M. Rapid prototyping of microfluidic systems in poly(dimethylsiloxane): Anal.Chem. 70 (1998): 4974-4984.
- [3] Skoog, D. A.; Leary, J. J., Principles of Instrumental Analysis. New York: Harcourt Brace College Publishers, 1992.
- [4] Braun, R. D., Introduction to Instrumental Analysis. Singapore: McGraw-Hill Book 1987.
- [5] Skoog, D. A.; Holler, F. J.; Nieman, T. A., Principles of Instrumental Analysis. New York: Harcourt Brace College Publishers, 1998.
- [6] Christian, G. D., Analytical Chemistry. New York: John Wiley & Sons, 1986.
- [7] Eggins, B., Biosensors: An Introduction. New York: John Wiley & Sons, 1996.
- [8] Monk, S., Fundamentals of Electroanalytical Chemistry. New York: John Wiley & Sons, 2001.
- [9] Skoog, D. A.; West, D. M.; Holler, F., Fundamentals of Analytical Chemistry. New York: Saunders College Publishing, 1996.
- [10] Wang, J., Analytical Electrochemistry. New York: John Wiley & Sons, 1994.
- [11] Skoog, D. A. H., F. J. and Nieman, T. A., Principles of Instrumental Analysis. New York: Harcourt Brace College Publishers, 1998.
- [12] Sawyer, D. T., Experimental Electrochemistry for Chemists. New York.: John Wiley & Sons, 1974.
- [13] Lacourse, W. R., Pulse Electrochemical Detection in High-Performance Liquid Chromatography. New York: John Wiley & Sons, 1997.
- [14] LaCourse, W. R.; Johnson, D. C. Optimization of waveform for pulsed amperometric detection of carbohydrates based on pulsed voltammetry: Anal. Chem. 85 (1993): 50-55.
- [15] Kissinger, P. T.; Heineman, W. R., Laboratory Techniques in Electroanalytical Chemistry. New York: Marcel Dekker, 1996.
- [16] Rocklin, R. D.; Clarke, A. P.; Weitzhandler, M. Improved long-term reproducibility for pulsed amperometric detection of carbohydrates via a new quadruple-potential waveform: Anal. Chem. 70 (1998): 1496-1501.
- [17] http://www.chemsoc.org/ExemplarChem/entries/2003/leeds_chromatography/chromatography/Capillary Electrophoresis.
- [18] http://www.chemsoc.org/ExemplarChem/entries/2003/leeds_chromatography/chromatography/complete.htm Capillary Electrophoresis.
- [19] Weston, A.; Brown, P. R., HPLC and CE Principles and Practice. California: Academic Press, 1997.
- [20] Harrison, D. J.; Manz, A.; Fan, Z.; Luedi, H.; Widmer, H. M. Capillary electrophoresis and sample injection systems integrated on a planar glass chip: Anal. Chem. 64 (1992): 1926-1932.
- [21] Geschke, O., H. Klank, and P. Telleman, Microsystem Engineering of Lab-on-a-Chip Devices. 2004.

- [22] Huang, X.; Coleman, W. F.; Zare, R. N. Analysis of factors causing peak broadening in capillary zone electrophoresis: J. Chromatogr. A 480 (1989): 95-110.
- [23] Kurosu, Y.; Hibi, K.; Sasaki, T.; Saito, M. J. High. Resolut. Chromatogr. 14 (1991): 200.
- [24] Henry, C. S., Microchip Capillary Electrophoresis. New Jersey: Humana Press Inc., 2006.
- [25] Manz, A.; Graber, N.; Widmer, H. M. Miniaturized total chemical analysis systems: a novel concept for chemical sensing: Sens. Actuators, B: Chemical B1 (1990): 244-8.
- [26] Terry, S. C.; Jerman, J. H.; Angell, J. B. A gas chromatograph air analyzer fabricated on a silicon wafer: IEEE Trans. Electron Devices ED-26 (1979): 1880.
- [27] Manz, A.; Harrison, D. J.; Verpoorte, E. M. J.; Fettinger, J. C.; Paulus, A.; Luedi, H.; Widmer, H. M. Planar chips technology for miniaturization and integration of separation techniques into monitoring systems. Capillary electrophoresis on a chip: J. Chromatogr. 593 (1992): 253-8.
- [28] Jacobson, S. C.; Hergenroder, R.; Koutny, L. B.; Ramsey, J. M. High-Speed Separations on a Microchip: Anal. Chem. 66 (1994): 1114-18.
- [29] Fiorini, G. S.; Lorenz, R. M.; Kuo, J. S.; Chiu, D. T. Rapid prototyping of thermoset polyester microfluidic devices: Anal. Chem. 76 (2004): 4697-4704.
- [30] Fiorini, G. S.; Jeffries, G. D. M.; Lim, D. S. W.; Kuyper, C. L.; Chiu, D. T. using rapid prototyped polydimethylsiloxane molds: Lab Chip 3 (2003): 158-163.
- [31] Garcia, C. D.; Henry, C. S. Direct determination of carbohydrates, amino acids, and antibiotics by microchip electrophoresis with pulsed amperometric detection: Anal. Chem. 75 (2003): 4778-4783.
- [32] Vickers, J. A.; Henry, C. S. Simplified current decoupler for microchip capillary electrophoresis with electrochemical and pulsed amperometric detection: Electrophoresis 26 (2005): 4641-4647.
- [33] Harrison, D. J.; Fluri, K.; Seiler, K.; Fan, Z. H.; Effenhauser, C. S.; Manz, A. Micromachining a Miniaturized Capillary Electrophoresis - Based Chemical - Analysis System on a Chip: Science 261 (1993): 895-897.
- [34] Harrison, D. J.; Manz, A.; Fan, Z. H.; Ludi, H.; Widmer, H. M. Capillary Electrophoresis and Sample Injection Systems Integrated on a Planar Glass Chip: Anal. Chem. 64 (1992): 1926-1932.
- [35] Manz, A.; Harrison, D. J.; Verpoorte, E. M. J.; Fettinger, J. C.; Paulus, A.; Ludi, H.; Widmer, H. M. Planar Chips Technology for Miniaturization and Integration of Separation Techniques into Monitoring Systems – Capillary Electrophoresis on a Chip: J. Chromatogr. 593 (1992): 253-258.
- [36] Soper, S. A.; Ford, S. M.; Qi, S.; McCarley, R. L.; Kelly, K.; Murphy, M. C. Microelectromechanical Systems (MEMS) Fabricated in Polymeric Materials: Applications in Chemistry and Life Sciences: Anal. Chem. 72 (2000): 545A.
- [37] Xiao, D.; Le, T. V.; Wirth, M. J. Surface modification of the channels of poly(dimethylsiloxane) microfluidic chips with polyacrylamide for fast electrophoretic separations of proteins: Anal. Chem. 76 (2004): 2055-61.

- [38] Garcia, C. D.; Dressen, B. M.; Henderson, A.; Henry, C. S. Comparison of surfactants for dynamic surface modification of poly(dimethylsiloxane) microchips: Electrophoresis 26 (2005): 703-9.
- [39] Barbier, V.; Tatoulian, M.; Li, H.; Arefi-Khonsari, F.; Ajdari, A.; Tabeling, P. Stable modification of PDMS surface properties by plasma polymerization: Application to the formation of double emulsions in microfluidic systems: Langmuir 22 (2006): 5230-5232.
- [40] Makamba, H.; Kim, J. H.; Lim, K.; Park, N.; Hahn, J. H. Surface modification of poly(dimethylsiloxane) microchannels: Electrophoresis 24 (2003): 3607-19.
- [41] Wang, W.; Zhao, L.; Zhang, J. R.; Wang, X. M.; Zhu, J. J.; Chen, H. Y. Modification of poly(dimethylsiloxane) microfluidic channels with silica nanoparticles based on layer-by-layer assembly technique: J. Chromatogr. A 1136 (2006): 111-7.
- [42] Luo, Y.; Huang, B.; Wu, H.; Zare, R. N. Controlling electroosmotic flow in poly(dimethylsiloxane) separation channels by means of prepolymer additives: Anal. Chem. 78 (2006): 4588-92.
- [43] Belder, D.; Ludwig, M. Surface modification in microchip electrophoresis: Electrophoresis 24 (2003): 3595-606.
- [44] Pallandre, A.; de Lambert, B.; Attia, R.; Jonas, A. M.; Viovy, J. L. Surface treatment and characterization: perspectives to electrophoresis and lab-on-chips: Electrophoresis 27 (2006): 584-610.
- [45] Graul, T. W.; Schlenoff, J. B. Capillaries modified by polyelectrolyte multilayers for electrophoretic separations: Anal. Chem. 71 (1999): 4007-4013.
- [46] Jorgenson, J. W.; Lukacs, K. D. Zone Electrophoresis in Open-Tubular Glass-Capillaries: Anal. Chem. 53 (1981): 1298-1302.
- [47] Shariff, K.; Ghosal, S. Peak tailing in electrophoresis due to alteration of the wall charge by adsorbed analytes a Numerical simulations and asymptotic theory: Anal. Chim. Acta 507 (2004): 87-93.
- [48] Ghosal, S. Fluid mechanics of electroosmotic flow and its effect on band broadening in capillary electrophoresis: Electrophoresis 25 (2004): 214-28.
- [49] Hu, S.; Ren, X.; Bachman, M.; Sims, C. E.; Li, G. P.; Allbritton, N. Surface modification of poly(dimethylsiloxane) microfluidic devices by ultraviolet polymer grafting: Anal. Chem. 74 (2002): 4117-23.
- [50] Thorsen, T.; Maerkl, S. J.; Quake, S. R. Microfluidic large-scale integration: Science 298 (2002): 580-4.
- [51] Linder, V.; Verpoorte, E.; Thormann, W.; de Rooij, N. F.; Sigrist, H. Surface biopassivation of replicated poly(dimethylsiloxane) microfluidic channels and application to heterogeneous immunoreaction with on-chip fluorescence detection: Anal. Chem. 73 (2001): 4181-9.
- [52] Barker, S. L.; Tarlov, M. J.; Canavan, H.; Hickman, J. J.; Locascio, L. E. Plastic microfluidic devices modified with polyelectrolyte multilayers: Anal. Chem. 72 (2000): 4899-903.
- [53] Barker, S. L.; Ross, D.; Tarlov, M. J.; Gaitan, M.; Locascio, L. E. Control of flow direction in microfluidic devices with polyelectrolyte multilayers: Anal. Chem. 72 (2000): 5925-9.

- [54] Liu, Y.; Fanguy, J. C.; Bledsoe, J. M.; Henry, C. S. Dynamic coating using polyelectrolyte multilayers for chemical control of electroosmotic flow in capillary electrophoresis microchips: Anal. Chem. 72 (2000): 5939-5944.
- [55] Linder, V.; Verpoorte, E.; Thormann, W.; de Rooij, N. F.; Sigrist, M. Surface biopassivation of replicated poly(dimethylsiloxane) microfluidic channels and application to heterogeneous immunoreaction with on-chip fluorescence detection: Anal. Chem. 73 (2001): 4181-4189.
- [56] Katayama, H.; Ishihama, Y.; Asakawa, N. Stable capillary coating with successive multiple ionic polymer layers: Anal. Chem. 70 (1998): 2254-2260.
- [57] Katayama, H.; Ishihama, Y.; Asakawa, N. Stable cationic capillary coating with successive multiple ionic polymer layers for capillary electrophoresis: Anal. Chem. 70 (1998): 5272-5277.
- [58] Bai, X.; Roussel, C.; Jensen, H.; Girault, H. H. Polyelectrolyte-modified short microchannel for cation separation: Electrophoresis 25 (2004): 931-5.
- [59] Ro, K. W.; Chang, W. J.; Kim, H.; Koo, Y. M.; Hahn, J. H. Capillary electrochromatography and preconcentration of neutral compounds on poly(dimethylsiloxane) microchips: Electrophoresis 24 (2003): 3253-9.
- [60] Xiao, Y.; Wang, K.; Yu, X. D.; Xu, J. J.; Chen, H. Y. Separation of aminophenol isomers in polyelectrolyte multilayers modified PDMS microchip: Talanta 72 (2007): 1316-1321.
- [61] Decher, G.; Hong, J. D.; Schmitt, J. Buildup of Ultrathin Multilayer Films by a Self-Assembly Process .3. Consecutively Alternating Adsorption of Anionic and Cationic Polyelectrolytes on Charged Surfaces: Thin Solid Films 210 (1992): 831-835.
- [62] Decher, G. Fuzzy nanoassemblies: Toward layered polymeric multicomposites: Science 277 (1997): 1232-1237.
- [63] Schlenoff, J. B.; Dubas, S. T. Mechanism of polyelectrolyte multilayer growth: Charge overcompensation and distribution: Macromolecules 34 (2001): 592-598.
- [64] Schlenoff, J. B.; Ly, H.; Li, M. Charge and mass balance in polyelectrolyte multilayers: J. Am. Chem. Soc. 120 (1998): 7626-7634.
- [65] Gao, H.; Jiang, T.; Heineman, W. R.; Halsall, H. B.; Caruso, J. L. Capillary enzyme immunoassay with electrochemical detection for determining indole-3-acetic acid in tomato embryos: Fresenius J. Anal. Chem. 364 (1999): 170-174.
- [66] Maichel, B.; Gas, B.; Kenndler, E. Diffusion coefficient and capacity factor in capillary electrokinetic chromatography with replaceable charged polymeric pseudophase: Electrophoresis 21 (2000): 1505-12.
- [67] Potocek, B.; Chmela, E.; Maichel, B.; Tesarova, E.; Kenndler, E.; Gas, B. Capillary electrokinetic chromatography with charged linear polymers as a nonmicellar pseudostationary phase: Determination of capacity factors and characterization by solvation parameters: Anal. Chem. 72 (2000): 74-80.
- [68] Wang, Y.; Dubin, P. L. Capillary modification by noncovalent polycation adsorption: Effects of polymer molecular weight and adsorption ionic strength: Anal. Chem. 71 (1999): 3463-3468.
- [69] Chiu, R. W. Anal. Chim. Acta (1995): 193-201.

- [70] Cordova, E.; Gao, J. M.; Whitesides, G. M. Noncovalent polycationic coatings for capillaries in capillary electrophoresis of proteins: Anal. Chem. 69 (1997): 1370-1379.
- [71] Barker, S. L. R.; Ross, D.; Tarlov, M. J.; Gaitan, M.; Locascio, L. E. Control of flow direction in microfluidic devices with polyelectrolyte multilayers: Anal. Chem. 72 (2000): 5925-5929.
- [72] Barker, S. L. R.; Tarlov, M. J.; Canavan, H.; Hickman, J. J.; Locascio, L. E. Plastic microfluidic devices modified with polyelectrolyte multilayers: Anal. Chem. 72 (2000): 4899-4903.
- [73] Liang, Z.; Chiem, N.; Ocvirk, G.; Tang, T.; Fluri, K.; Harrison, D. J. Microfabrication of a Planar Absorbance and Fluorescence Cell for Integrated Capillary Electrophoresis Devices: Anal. Chem. 68 (1996): 1040-6.
- [74] Salimi-Moosavi, H.; Jiang, Y.; Lester, L.; McKinnon, G.; Harrison, D. J. A multireflection cell for enhanced absorbance detection in microchip-based capillary electrophoresis devices: Electrophoresis 21 (2000): 1291-9.
- [75] Ramsey, R. S.; McLuckey, S. A. Charge concentration in electrospray ionization: mass spectrometry for sensitive detection of proteins: J. Microcolumn Sep. 9 (1997): 523-528.
- [76] Ramsey, R. S.; Ramsey, J. M. Generating Electrospray from Microchip Devices Using Electroosmotic Pumping.: Anal. Chem. 69 (1997): 2617.
- [77] Jacobson, S. C.; Ramsey, J. M. Microchip electrophoresis with sample stacking: Electrophoresis 16 (1995): 481-6.
- [78] Jakeway, S. C.; de Mello, A. J.; Russell, E. L. Miniaturized total analysis systems for biological analysis: Fresenius J. Anal. Chem. 366 (2000): 525-539.
- [79] Jiang, G.; Attiya, S.; Ocvirk, G.; Lee, W. E.; Harrison, D. J. Red diode laser induced fluorescence detection with a confocal microscope on a microchip for capillary electrophoresis: Biosens. Bioelectron. 14 (2000): 861-9.
- [80] Mayrhofer, K.; Zemann, A. J.; Schnell, E.; Bonn, G. K. Capillary Electrophoresis and Contactless Conductivity Detection of Ions in Narrow Inner Diameter Capillaries: Anal. Chem. 71 (1999): 3828-3833.
- [81] Wang, J.; Polsky, R.; Tian, B.; Chatrathi, M. P. Voltammetry on microfluidic chip platforms: Anal. Chem. 72 (2000): 5285-9.
- [82] Ocvirk, G.; Tang, T.; Jed Harrison, D. Optimization of confocal epifluorescence microscopy for microchip-based miniaturized total analysis systems: Analyst 123 (1998): 1429-1434.
- [83] Walker, P. A., 3rd; Morris, M. D.; Burns, M. A.; Johnson, B. N. Isotachophoretic separations on a microchip. Normal Raman spectroscopy detection: Anal. Chem. 70 (1998): 3766-9.
- [84] Hashimoto, M.; Tsukagoshi, K.; Nakajima, R.; Kondo, K.; Arai, A. Microchip capillary electrophoresis using on-line chemiluminescence detection: J. Chromatogr. A 867 (2000): 271-9.
- [85] Jiang, G.; Attiya, S.; Ocvirk, G.; Lee, W. E.; Harrison, D. J. Red diode laser induced fluorescence detection with a confocal microscope on a microchip for capillary electrophoresis: Biosens. Bioelectron. 14 (2000): 861-869.
- [86] Liu, B.-F.; Hisamoto, H.; Terabe, S. Subsecond separation of cellular flavin coenzymes by microchip capillary electrophoresis with laser-induced fluorescence detection: J. Chromatogr. A 1021 (2003): 201-207.

- [87] Descroix, S.; Le Potier, I.; Niquet, C.; Minc, N.; Viovy, J. L.; Taverna, M. In-capillary non-covalent labeling of insulin and one gastrointestinal peptide for their analyses by capillary electrophoresis with laser-induced fluorescence detection: J. Chromatogr. A 1087 (2005): 203-209.
- [88] Wicks, D. A.; Li, P. C. H. Separation of fluorescent derivatives of hydroxyl-containing small molecules on a microfluidic chip: Anal. Chim. Acta. 507 (2004): 107-114.
- [89] Wu, Y. Y.; Lin, J. M.; Su, R. G.; Qu, F.; Cai, Z. W. An end-channel amperometric detector for microchip capillary electrophoresis: Talanta 64 (2004): 338-344.
- [90] Lee, H. L.; Chen, S. C. Microchip capillary electrophoresis with electrochemical detector for precolumn enzymatic analysis of glucose, creatinine, uric acid and ascorbic acid in urine and serum: Talanta 64 (2004): 750-757.
- [91] Lee, H. L.; Chen, S. C. Microchip capillary electrophoresis with amperometric detection for several carbohydrates: Talanta 64 (2004): 210-216.
- [92] Chailapakul, O.; Korsrisakul, S.; Siangproh, W.; Grudpan, K. Fast and simultaneous detection of heavy metals using a simple and reliable microchip-electrochemistry route: An alternative approach to food analysis: Talanta 74 (2008): 683-689.
- [93] Blasco, A. J.; Barrigas, I.; Gonzalez, M. C.; Escarpa, A. Fast and simultaneous detection of prominent natural antioxidants using analytical microsystems for capillary electrophoresis with a glassy carbon electrode: A new gateway to food environments: Electrophoresis 26 (2005): 4664-4673.
- [94] Castano-Alvarez, M.; Fernandez-Abedul, M. T.; Costa-Garcia, A. Poly(methylmethacrylate) and Topas capillary electrophoresis microchip performance with electrochemical detection: Electrophoresis 26 (2005): 3160-3168.
- [95] Castano-Alvarez, M.; Fernandez-Abedul, M. T.; Costa-Garcia, A. Amperometric PMMA-microchip with integrated gold working electrode for enzyme assays: Anal. Bioanal. Chem. 382 (2005): 303-310.
- [96] Garcia, C. D.; Henry, C. S. Coupling capillary electrophoresis and pulsed electrochemical detection: Electroanalysis 17 (2005): 1125-1131.
- [97] Garcia, C. D.; Henry, C. S. Comparison of pulsed electrochemical detection modes coupled with microchip capillary electrophoresis: Electroanalysis 17 (2005): 223-230.
- [98] Nyholm, L. Electrochemical techniques for lab-on-a-chip applications: Analyst 130 (2005): 599-605.
- [99] Yan, J. L.; Yang, X. R.; Wang, E. K. Electrochemical detection of anions on an electrophoresis microchip with integrated silver electrode: Electroanalysis 17 (2005): 1222-1226.
- [100] Chen, G.; Lin, Y. H.; Wang, J. Microchip capillary electrophoresis with electrochemical detection for monitoring environmental pollutants: Current Anal. Chem. 2 (2006): 43-50.
- [101] Dawoud, A. A.; Kawaguchi, T.; Jankowiak, R. In-channel modification of electrochemical detector for the detection of bio-targets on microchip: Electrochem. Commun. 9 (2007): 1536-1541.

- [102] Coltro, W. K.; da Silva, J. A.; da Silva, H. D.; Richter, E. M.; Furlan, R.; Angnes, L.; do Lago, C. L.; Mazo, L. H.; Carrilho, E. Electrophoresis microchip fabricated by a direct-printing process with end-channel amperometric detection: Electrophoresis 25 (2004): 3832-9.
- [103] Kuban, P.; Hauser, P. C. Application of an external contactless conductivity detector for the analysis of beverages by microchip capillary electrophoresis: Electrophoresis 26 (2005): 3169-78.
- [104] Vandaveer, W. R. I. V.; Pasas-Farmer, S. A.; Fischer, D. J.; Frankenfeld, C. N.; Lunte, S. M. Recent developments in electrochemical detection for microchip capillary electrophoresis: Electrophoresis 25 (2004): 3528-3549.
- [105] Wang, J.; Chatrathi, M. P. Microfabricated electrophoresis chip for bioassay of renal markers: Anal. Chem. 75 (2003): 525-9.
- [106] Wang, J. Electrochemical detection for microscale analytical systems: a review: Talanta 56 (2002): 223-231.
- [107] Vandaveer, W. R. I. V.; Pasas, S. A.; Martin, R. S.; Lunte, S. M. Recent developments in amperometric detection for microchip capillary electrophoresis: Electrophoresis 23 (2002): 3667-3677.
- [108] Backofen, U.; Matysik, F. M.; Lunte, C. E. A chip-based electrophoresis system with electrochemical detection and hydrodynamic injection: Anal. Chem. 74 (2002): 4054-9.
- [109] Dolnik, V.; Liu, S.; Jovanovich, S. Capillary electrophoresis on microchip: Electrophoresis 21 (2000): 41-54.
- [110] Liu, Y.; Ganser, D.; Schneider, A.; Liu, R.; Grodzinski, P.; Kroutchinina, N. Microfabricated polycarbonate CE devices for DNA analysis: Anal. Chem. 73 (2001): 4196-201.
- [111] Reyes, D. R.; Iossifidis, D.; Auroux, P. A.; Manz, A. Micro total analysis systems. 1. Introduction, theory, and technology: Anal. Chem. 74 (2002): 2623-36.
- [112] McDonald, J. C.; Duffy, D. C.; Anderson, J. R.; Chiu, D. T.; Wu, H.; Schueller, O. J.; Whitesides, G. M. Fabrication of microfluidic systems in poly(dimethylsiloxane): Electrophoresis 21 (2000): 27-40.
- [113] Effenhauser, C. S.; Bruin, G. J. M.; Paulus, A.; Ehrat, M. Integrated Capillary Electrophoresis on Flexible Silicone Microdevices: Analysis of DNA Restriction Fragments and Detection of Single DNA Molecules on Microchips: Anal. Chem. 69 (1997): 3451-3457.
- [114] Roberts, M. A.; Rossier, J. S.; Bercier, P.; Girault, H. UV laser machined polymer substrates for the development of microdiagnostic systems: Anal. Chem. 69 (1997): 2035-2042.
- [115] McCormick, R. M.; Nelson, R. J.; AlonsoAmigo, M. G.; Benvegnu, J.; Hooper, H. H. Microchannel electrophoretic separations of DNA in injection-molded plastic substrates: Anal. Chem. 69 (1997): 2626-2630.
- [116] Martynova, L.; Locascio, L. E.; Gaitan, M.; Kramer, G. W.; Christensen, R. G.; MacCrehan, W. A. Fabrication of plastic microfluid channels by imprinting methods: Anal. Chem. 69 (1997): 4783-4789.
- [117] Jikun Liu, T. P., Adam T. Woolley, and Milton L, Lee. Surface-Modified poly(methyl methacrylate) Capillary Electrophoresis Microchips for Protein and Peptide Analysis: Anal. Chem. 76 (2004): 6948-6955.
- [118] Kelly, R. T.; Woolley, A. T. Thermal Bonding of Polymeric Capillary Electrophoresis Microdevices in Water: Anal. Chem. 75 (2003): 1941-1945.

- [119] Roman, G. T.; Culbertson, C. T. Surface engineering of poly(dimethylsiloxane) microfluidic devices using transition metal sol-gel chemistry: Langmuir 22 (2006): 4445-4451.
- [120] Liu, Y.; Fanguy, J. C.; Bledsoe, J. M.; Henry, C. S. Dynamic coating using polyelectrolyte multilayers for chemical control of electroosmotic flow in capillary electrophoresis microchips: Anal. Chem. 72 (2000): 5939-5944.
- [121] McDonald, J. C.; Whitesides, G. M. Poly(dimethylsiloxane) as a material for fabricating microfluidic devices: Acc. Chem. Res. 35 (2002): 491-9.
- [122] Gonzalez, N.; Elvira, C.; San Roman, J.; Cifuentes, A. New physically adsorbed polymer coating for reproducible separations of basic and acidic proteins by capillary electrophoresis: J. Chromatogr. A 1012 (2003): 95-101.
- [123] Garcia Carlos, D. Comparison of surfactants for dynamic surface modification of poly(dimethylsiloxane) microchips: Electrophoresis 26 (2005): 703-709.
- [124] Henry, A. C.; Tutt, T. J.; Galloway, M.; Davidson, Y. Y.; McWhorter, C. S.; Soper, S. A.; McCarley, R. L. Surface modification of poly(methyl methacrylate) used in the fabrication of microanalytical devices: Anal. Chem. 72 (2000): 5331-5337.
- [125] Garcia, C. D.; Henry, C. S. Enhanced determination of glucose by microchip electrophoresis with pulsed amperometric detection: Anal. Chim. Acta 508 (2004): 1-9.
- [126] Liu, Y.; Vickers, J. A.; Henry, C. S. Simple and sensitive electrode design for microchip electrophoresis/electrochemistry: Anal. Chem. 76 (2004): 1513-7.
- [127] Chen, D. C.; Hsu, F. L.; Zhan, D. Z.; Chen, C. H. Palladium film decoupler for amperometric detection in electrophoresis chips: Anal. Chem. 73 (2001): 758-762.
- [128] Lai, C. C.; Chen, C. H.; Ko, F. H. In-channel dual-electrode amperometric detection in electrophoretic chips with a palladium film decoupler: J. Chromatogr. A 1023 (2004): 143-50.
- [129] Wu, C. C.; Wu, R. G.; Huang, J. G.; Lin, Y. C.; Hsien-Chang, C. Three-electrode electrochemical detector and platinum film decoupler integrated with a capillary electrophoresis microchip for amperometric detection: Anal. Chem. 75 (2003): 947-52.
- [130] Lacher, N. A.; Lunte, S. M.; Martin, R. S. Development of a microfabricated palladium decoupler/electrochemical detector for microchip capillary electrophoresis using a hybrid glass/poly(dimethylsiloxane) device: Anal. Chem. 76 (2004): 2482-2491.
- [131] Osbourn, D. M.; Lunte, C. E. Cellulose Acetate Decoupler for On-Column Electrochemical Detection in Capillary Electrophoresis: Anal. Chem. 73 (2001): 5961-5964.
- [132] Rossier, J. S.; Ferrigno, R.; Girault, H. H. Electrophoresis with electrochemical detection in a polymer microdevice: J. Electroanal. Chem. 492 (2000): 15-22.
- [133] Osbourn, D. M.; Lunte, C. E. On-column electrochemical detection for microchip capillary electrophoresis: Anal. Chem. 75 (2003): 2710-2714.
- [134] Kok, W. T., Sahin, Yuksel. Solid-state Field Decoupler for Off-Column Detection in Capillary Electrophoresis: Anal. Chem. 65 (1993): 2497.

- [135] Kovarik, M. L.; Li, M. W.; Martin, R. S. Integration of a carbon microelectrode with a microfabricated palladium decoupler for use in microchip capillary electrophoresis/electrochemistry: Electrophoresis 26 (2005): 202-210.
- [136] Joseph Lai, C.-C.; Chen, C.-h.; Ko, F.-H. In-channel dual-electrode amperometric detection in electrophoretic chips with a palladium film decoupler: J. Chromatogr. A 1023 (2004): 143-150.
- [137] Chen, G.; Lin, Y.; Wang, J. Monitoring environmental pollutants by microchip capillary electrophoresis with electrochemical detection: Talanta 68 (2006): 497-503.
- [138] Siangproh, W.; Chailapakul, O.; Laocharoensuk, R.; Wang, J. Microchip capillary electrophoresis/electrochemical detection of hydrazine compounds at a cobalt phthalocyanine modified electrochemical detector: Talanta 67 (2005): 903-907.
- [139] Kim, J.-H.; Kang, C. J.; Kim, Y.-S. Development of a microfabricated disposable microchip with a capillary electrophoresis and integrated three-electrode electrochemical detection: Biosens. Bioelectron. 20 (2005): 2314-2317.
- [140] Kim, J.-H.; Kang, C. J.; Jeon, D.; Kim, Y.-S. A disposable capillary electrophoresis microchip with an indium tin oxide decoupler / amperometric detector: Microelectron. Eng. Proceedings of the 30th International Conference on Micro- and Nano-Engineering 78-79 (2005): 563-570.
- [141] Lee, H.-L.; Chen, S.-C. Microchip capillary electrophoresis with electrochemical detector for precolumn enzymatic analysis of glucose, creatinine, uric acid and ascorbic acid in urine and serum: Talanta 64 (2004): 750-757.
- [142] Bao, N.; Xu, J.-J.; Dou, Y.-H.; Cai, Y.; Chen, H.-Y.; Xia, X.-H. Electrochemical detector for microchip electrophoresis of poly(dimethylsiloxane) with a three-dimensional adjustor: J Chromatogra. A 1041 (2004): 245-248.
- [143] Dill, K.; Montgomery, D. D.; Ghindilis, A. L.; Schwarzkopf, K. R. Immunoassays and sequence-specific DNA detection on a microchip using enzyme amplified electrochemical detection: J. Biochem. Bioph. Methods 59 (2004): 181-187.
- [144] Garcia, C. D.; Henry, C. S. Enhanced determination of glucose by microchip electrophoresis with pulsed amperometric detection: Anal. Chim. Acta 508 (2004): 1-9.
- [145] Amatore, C.; Belotti, M.; Chen, Y.; Roy, E.; Sella, C.; Thouin, L. Using electrochemical coupling between parallel microbands for in situ monitoring of flow rates in microfluidic channels: J. Electroanal. Chem. 573 (2004): 333-343.
- [146] Wang, J.; Tian, B.; Sahlin, E. Micromachined Electrophoresis Chips with Thick-Film Electrochemical Detectors: Anal. Chem. 71 (1999): 5436-5440.
- [147] Lu, W.; Cassidy, R. M.; Baranski, A. S. End-column electrochemical detection for inorganic and organic species in high-voltage capillary electrophoresis: J. Chromatogr. A 640 (1993): 433-440.

- [148] Hilmi, A.; Luong, J. H. T. Electrochemical Detectors Prepared by Electroless Deposition for Microfabricated Electrophoresis Chips: Anal. Chem. 72 (2000): 4677-4682.
- [149] Srinivas, P. R.; Kramer, B. S.; Srivastava, S. Trends in biomarker research for cancer detection: Lancet Oncology 2 (2001): 698-704.
- [150] Bischoff, R.; Luider, T. M. Methodological advances in the discovery of protein and peptide disease markers: J. Chromatogra. B 803 (2004): 27-40.
- [151] Pang, J. X.; Ginanni, N.; Dongre, A. R.; Hefta, S. A.; Opiteck, G. J. Biomarker discovery in urine by proteomics: Journal of Proteome Research 1 (2002): 161-169.
- [152] Gao, J.; Garulacan, L. A.; Storm, S. M.; Opiteck, G. J.; Dubaquié, Y.; Hefta, S. A.; Dambach, D. M.; Dongre, A. R. Biomarker discovery in biological fluids: Methods 35 (2005): 291-302.
- [153] Agarwal, D. P. Cardioprotective effects of light-moderate consumption of alcohol: A review of putative mechanisms: Alcohol and Alcoholism 37 (2002): 409-415.
- [154] Ebbesen, L. S.; Olesen, S. H.; Kruhoffer, M.; Ingerslev, J.; Orntoft, T. F. Folate deficiency induced hyperhomocysteinemia changes the expression of thrombosis-related genes: Blood Coagulation & Fibrinolysis 17 (2006): 293-301.
- [155] St Remy, R. R. D.; Montes-Bayon, M.; Sanz-Medel, A. Determination of total homocysteine in human serum by capillary gas chromatography with sulfur-specific detection by double focusing ICP-MS: Analytical and Bioanalytical Chemistry 377 (2003): 299-305.
- [156] Nelson, B. C.; Pfeiffer, C. M.; Sniegowski, L. T.; Satterfield, M. B. Development and evaluation of an isotope dilution LC/MS method for the determination of total homocysteine in human plasma: Anal. Chem. 75 (2003): 775-784.
- [157] Chwatko, G.; Bald, E. Determination of different species of homocysteine in human plasma by high-performance liquid chromatography with ultraviolet detection: J. Chromatogra. A 949 (2002): 141-151.
- [158] Sigit, J. I.; Hages, M.; Brensing, K. A.; Frotscher, U.; Pietrzik, K.; von Bergmann, K.; Lutjohann, D. Total plasma homocysteine and related amino acids in end-stage renal disease (ESRD) patients measured by gas chromatography-mass spectrometry - Comparison with the Abbott IMx homocysteine assay and the HPLC method: Clin. Chem. 39 (2001): 681-690.
- [159] Doncheva, N.; Penkov, A.; Velcheva, A.; Boev, M.; Popov, B.; Niagolov, Y. Study of homocysteine concentration in coronary heart disease patients and comparison of two determination methods: Ann. Nutri. Meta. 51 (2007): 82-87.
- [160] Moller, J.; Ahola, L.; Abrahamsson, L. Evaluation of the DPC IMMULITE 2000 assay for total homocysteine in plasma: Scand. J. Clin. Lab. 62 (2002): 369-373.
- [161] Zinellu, A.; Pinna, A.; Zinellu, E.; Sotgia, S.; Deiana, L.; Carru, C. High-throughput capillary electrophoresis method for plasma cysteinylglycine measurement: evidences for a clinical application: Amino Acids 34 (2008): 69-74.

- [162] Zinellu, A.; Sotgia, S.; Posadino, A. M.; Pasciu, V.; Perino, M. G.; Tadolini, B.; Deiana, L.; Carru, C. Highly sensitive simultaneous detection of cultured cellular thiols by laser induced fluorescence-capillary electrophoresis: Electrophoresis 26 (2005): 1063-1070.
- [163] Lochman, P.; Adam, T.; Friedecky, D.; Hlidkova, E.; Skopkova, Z. High-throughput capillary electrophoretic method for determination of total aminothiols in plasma and urine: Electrophoresis 24 (2003): 1200-1207.
- [164] Ducros, V.; Demuth, K.; Sauvart, M. P.; Quillard, M.; Causse, E.; Candito, M.; Read, M. H.; Draï, J.; Garcia, I.; Gerhardt, M. F.; Homocysteine, S. W. G. Methods for homocysteine analysis and biological relevance of the results: J. Chromatogr. B 781 (2002): 207-226.
- [165] Bayle, C.; Issac, C.; Salvayre, R.; Couderc, F.; Causse, E. Assay of total homocysteine and other thiols by capillary electrophoresis and laser-induced fluorescence detection II. Pre-analytical and analytical conditions: J. Chromatogr. A 979 (2002): 255-260.
- [166] Ducros, V.; Candito, M.; Causse, E.; Couderc, R.; Demuth, K.; Diop, M. E.; Draï, J.; Gerhardt, M. F.; Quillard, M.; Read, M. H.; Sauvart, M. P. Comparison of plasma total homocysteine determinations in 9 french hospital laboratories by using 6 different methods: Annales De Biologie Clinique 60 (2002): 421-428.
- [167] R., W., Practical Capillary Electrophoresis. Boston: Academic Press, 1993. p 17-43.
- [168] Wagner, L. D.; Vandaveer, W. R.; Padas-Farmer, S. A.; Lunte, S. Analytical determination of homocysteine by microchip capillary electrophoresis with electrochemical detection.: Abstracts of Papers of the American Chemical Society 229 (2005): U384-U384.
- [169] Chen, G.; Zhang, L. Y.; Wang, J. Miniaturized capillary electrophoresis system with a carbon nanotube microelectrode for rapid separation and detection of thiols: Talanta 64 (2004): 1018-1023.
- [170] White, P. C.; Lawrence, N. S.; Davis, J.; Compton, R. G. Electrochemical determination of thiols: A perspective: Electroanalysis 14 (2002): 89-98.
- [171] Lawrence, N. S.; Davis, J.; Compton, R. G. Electrochemical detection of thiols in biological media: Talanta 53 (2001): 1089-1094.
- [172] Padas, S. A.; Lacher, N. A.; Davies, M. I.; Lunte, S. M. Detection of homocysteine by conventional and microchip capillary electrophoresis/electrochemistry: Electrophoresis 23 (2002): 759-766.
- [173] Garcia, C. D.; Liu, Y.; Anderson, P.; Henry, C. S. Versatile 3-channel high-voltage power supply for microchip capillary electrophoresis: Lab on a Chip 3 (2003): 324-328.
- [174] Liu, Y.; Vickers, J. A.; Henry, C. S. Simple and sensitive electrode design for microchip electrophoresis/electrochemistry: Anal. Chem. 76 (2004): 1513-1517.
- [175] Liu, Y.; Wipf, D. O.; Henry, C. S. Conductivity detection for monitoring mixing reactions in microfluidic devices: Analyst 126 (2001): 1248-1251.
- [176] McDonald, J. C.; Whitesides, G. M. Poly(dimethylsiloxane) as a material for fabricating microfluidic devices: Acc. Chem. Res. 35 (2002): 491-499.

- [177] Dai, J. H.; Baker, G. L.; Bruening, M. L. Use of porous membranes modified with polyelectrolyte multilayers as substrates for protein arrays with low nonspecific adsorption: Anal. Chem. 78 (2006): 135-140.
- [178] Huang, X. H.; Gordon, M. J.; Zare, R. N. Current-Monitoring Method for Measuring the Electroosmotic Flow-Rate in Capillary Zone Electrophoresis: Anal. Chem. 60 (1988): 1837-1838.
- [179] Locascio, L. E.; Perso, C. E.; Lee, C. S. Measurement of electroosmotic flow in plastic imprinted microfluid devices and the effect of protein adsorption on flow rate: J. Chromatogr. A 857 (1999): 275-284.
- [180] Shultz-Lockyear, L. L.; Colyer, C. L.; Fan, Z. H.; Roy, K. I.; Harrison, D. J. Effects of injector geometry and sample matrix on injection and sample loading in integrated capillary electrophoresis devices: Electrophoresis 20 (1999): 529-38.
- [181] Jacobson, S. C.; Koutny, L. B.; Hergenroeder, R.; Moore, A. W., Jr.; Ramsey, J. M. Microchip Capillary Electrophoresis with an Integrated Postcolumn Reactor: Anal. Chem. 66 (1994): 3472-6.
- [182] Andersson, A.; Lindgren, A.; Hultberg, B. Effect of Thiol Oxidation and Thiol Export from Erythrocytes on Determination of Redox Status of Homocysteine and Other Thiols in Plasma from Healthy-Subjects and Patients with Cerebral Infarction: Clin. Chem. 41 (1995): 361-366.
- [183] Schlenoff, J. B.; Dubas, S. T.; Farhat, T. Sprayed polyelectrolyte multilayers: Langmuir 16 (2000): 9968-9969.
- [184] Dubas, S. T.; Schlenoff, J. B. Factors controlling the growth of polyelectrolyte multilayers: Macromolecules 32 (1999): 8153-8160.
- [185] Kirby, B. J.; Hasselbrink, E. F., Jr. Zeta potential of microfluidic substrates: 2. Data for polymers: Electrophoresis 25 (2004): 203-13.
- [186] Kim, J.; Chaudhury, M. K.; Owen, M. J. Hydrophobic recovery of polydimethylsiloxane elastomer exposed to partial electrical discharge: J. Colloid Interface Sci. 226 (2000): 231-236.
- [187] Kim, J.; Chaudhury, M. K.; Owen, M. J. Modeling hydrophobic recovery of electrically discharged polydimethylsiloxane elastomers: J. Colloid Interface Sci. 293 (2006): 364-375.
- [188] Fritz, J. L.; Owen, M. J. Hydrophobic recovery of plasma-treated polydimethylsiloxane: J. Adhesion. 54 (1995): 33-45.
- [189] Liu, Y.; Foote, R. S.; Jacobson, S. C.; Ramsey, R. S.; Ramsey, J. M. Electrophoretic separation of proteins on a microchip with noncovalent, postcolumn labeling: Anal. Chem. 72 (2000): 4608-13.

VITAE

Miss Kanokporn Boonsong was born on May, 31 1976 in Samut Songkhram, Thailand. She graduated with high school degree from Satthasamut School, Samut Songkhram in 1992. She received her Bachelor's degree of Science (Analytical Chemistry) with the second honor in 1999 from Rajamangala University of Technology Krungthep. Since then she has been appointed as an instructor at Rajamangala University of Technology Krungthep. In 2002, she has become a graduate student in the analytical field and a member of Electrochemical Research Group under the direction of Associate Professor Dr. Orawon Chailapakul. Then in 2005, she received the scholarship from the Thailand Research to do the research in the general area of microchip capillary electrophoresis with Associate Professor Dr. Charles S. Henry at Colorado State University, United States for 1 year. She graduated with a Ph.D degree in Chemistry of academic year 2007 from Chulalongkorn University.

Award:

- 2006 Presentation award of TJSE 2006
- 2007 Poster Award of International Symposium on Flow-Based Analysis
VII

List of Publications

1. Vickers, J. A., Dressen, B. M., Weston, M. C., **Boonsong, K.**, Chailapakul, O., Cropek, D. M., Henry, C. S.: Thermoset polyester as an alternative material for microchip electrophoresis/electrochemistry, Electrophoresis, **2007**, 28, 1123-1129.
2. **Boonsong K.**, Caulum, M. M., Dressen, B. M., Chailapakul, O., Cropek, D. M., Henry, C. S.: Influence of Polymer Structure on Electroosmotic Flow and Separation Efficiency in Successive Multiple Layer Coatings for Microchip Electrophoresis, Electrophoresis, accepted.